

AFFINE FUSION TADPOLES

ANDREW URICHUK

Bachelor of Science, University of Regina, 2012

A Thesis

Submitted to the School of Graduate Studies
of the University of Lethbridge
in Partial Fulfillment of the
Requirements for the Degree

MASTER OF SCIENCE

Department of Physics and Astronomy
University of Lethbridge
LETHBRIDGE, ALBERTA, CANADA

© Andrew Urichuk, 2015

AFFINE FUSION TADPOLES
ANDREW URICHUK

Date of Defence: August 31, 2015

Dr. M. Walton Supervisor	Professor	Ph.D.
-----------------------------	-----------	-------

Dr. S. Das Thesis Examination Committee	Professor	Ph.D.
--	-----------	-------

Dr. K. Peacock Thesis Examination Committee	Professor	Ph.D.
--	-----------	-------

Dr. L. Spencer Chair, Thesis Examination Committee	Assistant Professor	Ph.D.
---	---------------------	-------

Affine Fusion Tadpoles

Andrew Urichuk

Abstract

Fusion dimensions are integer-valued quantities equal to the dimensions of the spaces of conformal blocks, which describe the interactions of a conformal field theory (CFT). Our focus was on the Wess-Zumino-Witten models, a particularly interesting type of CFT, whose primary fields correspond to representations of affine Lie groups. Arguably, affine fusion tadpoles are the simplest $g \geq 1$ fusion dimension, having only a single incoming field and $g = 1$. We study the symmetries of the $SU(N)$ tadpole and Verlinde formula with the intention of finding a non-negative-integer decomposition. Such a decomposition might be indicative of a combinatorial atom for fusion, which could suggest a new combinatorial account of fusion dimensions. From produced tables we found that tadpole values appeared to be polynomial in the level k . Several conjectures were made and we sketch a method obtaining general forms of $SU(N)$ tadpoles via dominant weight sums.

Acknowledgements

I would like to express my gratitude to my supervisor Professor Mark Walton for his seemingly endless patience and assistance with the writing of this thesis, and his various insights into interesting aspects of the project.

And I would like to express thanks to my fiancée, whose unconditional support through this process was invaluable.

Contents

1	Introduction	1
2	Groups, Algebras, and Symmetries	22
2.1	Groups	24
2.1.1	Finite Groups	25
2.1.2	Lie Groups	28
2.1.3	The Lie Group $SU(2)$	31
2.2	Highest-Weight Representations	34
2.2.1	$SU(3)$ Weight Representation	38
2.2.2	Weyl Group	40
3	Tensor Products	43
3.1	Combining Representations	45
3.1.1	Utility of the Tensor Product	46
3.2	Young Tableaux for $SU(N)$	49
3.2.1	The Hook Formula	53
3.2.2	SSYT and Tensor Products	55
3.2.3	Littlewood-Richardson Coefficients	59
4	Fusion Products	62
4.1	Conformal Symmetry	64
4.1.1	The Conformal Group	64
4.1.2	Witt and Virasoro Algebras	65
4.1.3	Affine Lie Groups	68
4.1.4	Affine Weyl Group	71
4.2	Conformal Field Theory	72
4.2.1	Operator Product Expansion	75
4.2.2	Fusion Dimensions	79
4.3	Moore-Seiberg Duality	80
4.3.1	Kac-Peterson Formula	84
4.3.2	Verlinde Formula	85
4.3.3	Ising Model Fusion Example	87
4.3.4	Higher Genus Fusion and the Tadpole	91

5	Finding Affine Tadpoles	94
5.1	Kac-Walton Algorithm	96
5.2	Berenstein-Zelevinsky Triangles	98
5.2.1	Partial Proof of Equation (5.37)	111
5.3	Verlinde Formula and Symmetric Polynomials	120
6	Experimental Investigations of the Affine Tadpole	125
6.1	Breaking Up the Sums	127
6.1.1	No Sum Taken in (6.4)	128
6.1.2	Sum Over the Weyl Alcove	128
6.1.3	Sum Over the Projected Highest-Weight Representation . . .	128
6.1.4	Simple Currents of the Group	129
6.1.5	Galois Symmetries	129
6.1.6	Dominant Weight Sums	131
6.1.7	Dominant Weights and Simple Current Symmetries	132
6.1.8	Dominant Weights and Galois Symmetries	132
6.2	Observed Properties of the Dominant Weight Sums	133
6.3	Formulas and Conjectures for the Affine Tadpole	136
7	Conclusion and Conjectures	141
A	Exploring the Dominant Weight Sums	154
A.1	Working with the Dominant Weight Sums	155
A.1.1	General Dominant Weight Sums	159
A.2	Dominant Weight Sums and Tadpole Calculations	162
B	Tables of Tadpoles	166
B.1	Computed Values for Tadpoles \mathcal{T}_λ of Equation (5.56)	167
B.2	Dominant Weight Sums \mathcal{E}_λ of Equation (6.13)	170
B.3	Galois Orbit Sums $\mathcal{G}_\lambda(\sigma)$ of Equation (6.11)	178

List of Figures

2.1	Weight diagram for $SU(3)$ of the highest-weight representation $[1, 1]$, along with the Weyl group reflections marked on the relevant weights.	41
4.1	Two possible decompositions of the 4-point functions, where the inner edges are summed over and so left unlabelled.	78
4.2	A genus-1 surface, in this case the torus, with 3 marked points, corresponding to three external conformal fields, chosen to be λ, μ, ν	82
4.3	Torus complex parameterization in terms of modular parameter τ	82
4.4	The torus and its decomposition into cycles, which are related by the modular transformation S	84
4.5	A gluing process to obtain the 2-point, genus-1 fusion dimension, where the gluing occurs along the dotted lines.	92
4.6	The gluing process used to obtain the 1-point genus-1 fusion dimension, or tadpole, where the gluing occurs along the dotted lines.	93

List of Tables

2.1	Multiplication table for S_3	27
6.1	Root rank seems to indicate the degree of the polynomial of the dominant weight sum and whether it is increasing or decreasing.	135
7.1	Results of the various methods of partial sums used to break up the Verlinde formula.	146
B.1	$SU(3)$ Tadpole Values \mathcal{T}_λ	167
B.2	$SU(4)$ Tadpole Values \mathcal{T}_λ	168
B.3	$SU(5)$ Tadpole Values \mathcal{T}_λ	169
B.4	$SU(3)$ Dominant Weight Sums \mathcal{E}_λ	170
B.5	$SU(4)$ Dominant Weight Sums \mathcal{E}_λ	171
B.6	$SU(4)$ Dominant Weight Sums \mathcal{E}_λ Cont'd	172
B.7	$SU(5)$ Dominant Weight Sums \mathcal{E}_λ	172
B.8	$SU(5)$ Dominant Weight Sums \mathcal{E}_λ Cont'd	173
B.9	$SU(6)$ Dominant Weight Sums \mathcal{E}_λ	174
B.10	$SU(7)$ Dominant Weight Sums \mathcal{E}_λ 1/4	175
B.11	$SU(7)$ Dominant Weight Sums \mathcal{E}_λ 2/4	176
B.12	$SU(7)$ Dominant Weight Sums \mathcal{E}_λ 3/4	176
B.13	$SU(7)$ Dominant Weight Sums \mathcal{E}_λ 4/4	177
B.14	$SU(4)$ Galois orbit sums $\mathcal{G}_{[1,0,1]}(\sigma)$ of the tadpole $\mathcal{T}_{[1,0,1]}$	178
B.15	$SU(4)$ Galois orbit sums $\mathcal{G}_{[0,2,0]}(\sigma)$ of the tadpole $\mathcal{T}_{[0,2,0]}$	179
B.16	$SU(4)$ Galois orbit sums $\mathcal{G}_{[2,1,0]}(\sigma)$ of the tadpole $\mathcal{T}_{[2,1,0]}$	179

Chapter 1

Introduction

Conformal field theory (CFT) encompasses a class of highly symmetric theories with broad applications throughout physics. The application of CFTs to the study of a system involves identifying fields within the CFT framework with allowable physical states. For Wess-Zumino-Witten (WZW) models, which this thesis is concerned with, the fields can be put into correspondence with representations of affine Lie groups. These representations can be used to build up the rules for how conformal fields interact within a theory, via the fusion product. Fusion products combine two conformal fields into a third, which can be decomposed into constituent fields and written as a direct product (\oplus) of irreducible representations (irreps) of the affine Lie group underpinning the theory. The decomposition process lets us write interactions in terms of irreps, which themselves give an account of physical properties within the system, along with the ‘fusion dimensions.’ Fusion dimensions are non-negative integers, interpreted as the multiplicity of an irrep resulting from a fusion product.¹

Insight into fusion dimensions is useful for understanding the fusion product, which are themselves encode data about the interactions within a CFT. CFTs are defined on an arbitrary Riemann surface and so an account of the interactions takes this surface into account. Correlation functions of fields within a CFT are defined on these Riemann surfaces, which can be degenerated into trivalent graphs. Those trivalent graphs that follow from this degeneration procedure have their vertices labelled by a fusion dimension. Trivalent graphs, along with their labelled fusion dimensions, give a simplified account of interactions in a CFT relative to the correlation function, but are much easier to work with. This thesis is focused on a special case of the fusion dimension called the tadpole, which occurs when considering the interaction of a single field with itself.

General fusion dimensions can be calculated by using the Verlinde formula (4.31). The Verlinde formula is consistent with a gluing procedure between 3-point fusion

¹Fusion dimensions have several names such as fusion numbers, Verlinde dimensions, and Verlinde numbers. In this thesis we stick to the fusion dimension terminology.

dimensions, more commonly known as fusion coefficients, to find the form of arbitrary point fusion dimensions. By connecting the edges of two trivalent vertices one finds that a fewer-point fusion dimension can appear, although it will have a loop. There are two significant cases: the 2-point fusion dimension at genus-1, and the 1-point fusion dimension at genus-1, which we call the tadpole. This follows the standard terminology for Feynman diagrams that originated in [4].

Tadpoles are highly simplified when compared to more general fusion dimensions, although their calculation is still quite involved. In the WZW models tadpoles can be written as sums over a character of a simple Lie group, suggesting that there may be a way to account for them by Lie theoretic properties. Such a Lie theoretic description might give us insight into a possible combinatorial atom of the fusion dimensions. We sought a symmetry based explanation of the non-negativity of fusion dimensions by looking at partial sums of the Verlinde formula.

Symmetries, exact and approximate, play a central role in any description of the universe. Lie groups provide the mathematical rules for continuous symmetries, which are central to many modern formulations of physical theories. Equally important to physicists is the ability to take a group, which is an abstract entity, and convert it into something useful. Representation theory can be used to represent a group as a set: of operators, of matrices, and many other types of mathematical objects.

Continuous transformation laws in physics are an important example of the utility of groups and representation theory to physics. These culminate in Noether's theorem, which relates continuous transformations of a theory's action to its conservation laws. These transformations can be understood as a representation of a Lie group, whose group structure tells us how the transformations combine. Treatment of a theory's transformations as being representations of a group that encodes its symmetry is an elegant perspective, since it conveys symmetries of the problem very naturally.

Groups accounting for the symmetries of a theory can be used to find that the-

ory's conserved quantities by analyzing its action's behaviour under transformation. Symmetries on their own do not completely fix the form of the action, however—a particularly important example of which is the ability to add gauge terms to an action without affecting the physics. Gauge fields are extremely important to modern physics and are the basis of gauge theory. Group theory and representation theory provide physicists with powerful theoretical tools necessary to understand the universe around us in terms of symmetries.

Groups, at their most basic, encode symmetry in a system-independent manner. Much like coordinate independence allows us to solve a variety of systems at once, codifying the symmetries in an abstract way makes accounting for them much more straightforward. The representation of a group involves identifying the group elements with more physical ideas. For example: a water molecule has molecular bonds that satisfy a reflective symmetry. The reflection group, consisting of a reflection element and the identity, can be defined to act on the coordinates of the water molecule. Applications of the reflection operator on the water molecule will result in no observable geometric change. The classical magnetic field is pseudo-vector, whose transformation rule requires that there be a sign change induced by reflections. Since the geometry of the water molecule is unchanged under reflection any effects arising from the geometry must also be unchanged. A magnetic moment of the molecule emerges based on geometry, and so the molecule's invariance under reflection is indicative of there being no magnetic moment.

Mathematically, groups are defined as a set of objects along with a composition rule, which tells us how group elements combine. Importantly, the composition rule must map group elements onto other group elements, a condition known as closure. Furthermore, the composition rule of a group must be associative, and the group must contain the identity, along with an inverse element for every group element. There is a subset of group elements that can be used to form any other element of the group

under the composition rule, and we say that the subset ‘generates’ the full group. The elements in this special subset are called the generators. The set of generators and the composition rule are enough to uniquely specify a group.

We work with finite, simple Lie, and affine Lie groups in this thesis. Finite groups are, in many senses, the easiest to work with and define. As their name suggests, they consist of a finite number of elements. This finiteness makes it possible to write down a multiplication table and exhaust all possible combinations of elements within the group. Generally, finite groups can be broken up into so-called finite simple groups, which can be used to ‘build up’ any other finite group. After a lengthy research program, these simple finite groups were completely classified by mathematicians, a celebrated accomplishment in mathematics.² Our work does not need the full strength of the theory of finite groups; however, the profound accomplishments in this field are notable. Use of finite groups in this thesis will be limited to applications of the symmetric group, which accounts for permutations of a finite list of elements.

Finite-dimensional Lie groups are the second type of group we consider and play a far more central role for our study. Arguably the most important type of group in physics, Lie groups have an infinite number of elements, which are in correspondence with points of an underlying finite-dimensional manifold. These finite-dimensional manifolds are called Lie manifolds and have the important property of smoothness, which can be exploited to obtain the generators of the Lie group. Generators of a Lie group obey a so-called Lie algebra, which are bijective to the infinitesimal group action. These small transformations near the identity can be used to construct the global action of the group, although it is worth noting that the Lie algebra does not uniquely specify the global group.³ Representations of the Lie group will share this property, which allows us to represent a Lie algebra as infinitesimal linear

²This classification is fairly recent, with the final proof published in 2004, although it is often considered completed by 1984. There is an ongoing effort to simplify the original proof, which is notoriously complicated.

³The most notable example of this being the rotation group $SO(3)$ and $SU(2)$.

transformations. In the same way that one can build up the group elements, the infinitesimal linear transformations can be used to construct finite transformations.

Ubiquity of continuous transformations in physics makes the Lie group/Lie algebra correspondence an extremely useful property. Like other groups, the Lie groups can be studied in a representation-independent way and consequently, so can their Lie algebras. By looking at the commutation of the Lie algebra elements a set of constants called the structure constants can be defined. Structure constants define the Lie algebra and can be used to build up the full Lie group. These structure constants have representation independent behaviour and so are very useful to consider when identifying the proper symmetry to apply. Due to the connection between continuous transformations and Noether's theorem it is common to conflate symmetry with the Lie groups and refer to the former as responsible for the conserved quantities of a theory.

Gauge symmetry is a particularly successful and modern application of groups to physics. The study of phenomenon in terms of their fundamental symmetry is the underlying idea of gauge theory. Gauge theories are used to account for the non-uniqueness of potentials, which can be used to describe the same physics. The simplest gauge theory is given by Maxwell's equations and describe electromagnetic interactions. Gauge freedom is in this case based on the choice of a gradient field $\partial^\mu f$ added to the electromagnetic vector potential.⁴ Specifically $A^\mu \rightarrow A^\mu + \partial^\mu f$, where we require that f is a smooth function in order for the gauge tensor $F_{\mu,\nu}$ to be invariant. The gauge tensor is the electromagnetic stress tensor defined as $F_{\mu,\nu} = \partial_\mu A_\nu - \partial_\nu A_\mu$. We can apply the gauge transformation and see that: $F_{\mu,\nu} \rightarrow F'_{\mu,\nu} = \partial_\mu(A_\nu + \partial_\nu f) - \partial_\nu(A_\mu + \partial_\mu f) = F_{\mu,\nu} + \partial_\mu \partial_\nu f - \partial_\nu \partial_\mu f = F_{\mu,\nu}$. With the final step following when $\partial_\mu \partial_\nu f = \partial_\nu \partial_\mu f$, which is valid if f is smooth.

Most famous among gauge theories is the standard model, which describes the be-

⁴Electro-magnetic vector potential refers to the standard electric potential V combined with the magnetic vector potential \vec{A} to make a 4-potential.

haviour of three of the four fundamental forces, with the exclusion of gravity. Gauge freedom of the standard model is given by combining the gauge symmetries of each of the forces that fit within its framework. Electromagnetism is described by the gauge group $U(1)_{EM}$, which can be geometrically imagined as the rotations around a circle. The electroweak force is described by the $SU(2) \times U(1)$ gauge group, which is spontaneously broken to the $U(1)_{EM}$ gauge symmetry. Finally, the strong force gauge group is $SU(3)$. Based on this the total gauge group of the standard model is $U(1) \times SU(2) \times SU(3)$, the direct product of the gauge groups of all three theories. Taking this perspective recasts physics in the language of symmetries and restricts the possible forms that a theory can take. This perspective also provides a mathematical justification for the emergence of additive quantum numbers and indicates why they are conserved. Additive quantum numbers are identified with numbers characteristic of representations of a group, known mathematically as the weights of a representation.⁵

There are a special class of weights that can be used to define a representation; these weights are called the highest-weights. Highest weight representations of a group are constructed by specifying a ‘highest weight vector.’ As an example, we consider quantum angular momentum, which is described by the Lie group of $SU(2)$. Possible angular momentum states of a system are equatable to those fixed-weight vectors appearing in the weight system of a highest-weight representation. Weights in a highest-weight representation $[2J]$ can be labelled with the eigenvalues of the \hat{J}_z operator, which is the projection of the angular momentum on the z -axis. Angular momentum states are arranged in terms of these projected values of the angular momentum measured along the z -axis. Somewhat familiar examples of an angular system are those provided by spin 1 and spin $\frac{1}{2}$ particles, which have the respective states: $|1, 1\rangle, |1, 0\rangle, |1, -1\rangle$ and $|\frac{1}{2}, \frac{1}{2}\rangle, |\frac{1}{2}, -\frac{1}{2}\rangle$. The notation $|J, m\rangle$ indicates

⁵In reality it’s not quite so clean, but within a division or multiplication of a constant the two are equivalent.

the highest-weight $2J$ and the weight label $2m$ in the highest-weight representation. These objects and the angular momentum operators are discussed with more detail in Section 2.1.3.

Standard treatment of the quantum angular momentum system involves defining ladder operators \hat{J}_+ and \hat{J}_- , which raise and lower the states.⁶ These raising and lowering operators change the \hat{J}_z eigenvalues in integral values of ± 1 . Ladder operators can be accounted for in the highest-weight representation picture as being the results of ‘simple roots’ acting on the highest-weight vector. Simple roots can be used to find all possible weights in the weight system of the highest-weight representation. These possible weight states can be identified with possible angular momentum states of a system.

Two angular momentum vectors \vec{J}_1 and \vec{J}_2 can be taken as the constituent vectors of a total angular momentum $\vec{J}_3 = \vec{J}_1 + \vec{J}_2$. An account of \vec{J}_3 requires that we determine all possible angular momentum states. The two particle system can be found to yield a maximum total angular momentum, defined by equation (2.10), and using ladder operators on J_3 we find: $(J_1 + J_2), (J_1 + J_2 - 1), \dots, |J_1 - J_2|$. More general group representations will require more than a single integer to prescribe a weight. These integer coefficients that label the weights are called the ‘Dynkin labels.’ This addition process is not quite what one would expect from a naive calculation. These results can be naturally explained by the introduction of the tensor product decomposition operation. Tensor products provide a method for taking two representations and combining them into a third. This third representation can, in general, be decomposed into irreps. Tensor products and their decompositions tell us about the interactions of the system based on knowledge of the constituent pieces.

Tensor products appear in a variety of circumstances in physics, they give us a method for combining two representations and obtaining a third. The representation

⁶Raising operators annihilate the state when it is a highest-weight and the lowering operator annihilates the state when it acts on the lowest-weight state.

that results from a tensor product can be decomposed into a direct sum of irreducible representations, or irreps, a process that has been studied in great detail. These studies have resulted in a number of algorithms, although for our purposes we will take a relatively limited perspective and only consider the Berenstein-Zelevinsky (BZ) triangles (see Section 5.2) and the Littlewood-Richardson (LR) rule (see Section 3.2.3). These tools can be used to compute the tensor product multiplicities, which are non-negative integers that count the number of times an irrep appears in a tensor product decomposition. These multiplicities are non-trivial to compute and often require the use of a computer algorithm, particularly for larger groups. Many of the algorithms used for computing the tensor products multiplicities are combinatorial, meaning that they use counting arguments that make use of non-negative integers. Conceptually, combinatorial explanations are extremely important since they provide a fundamental description through the use of an underlying combinatorial atom.

Affine Lie groups can be considered a generalization of the simple Lie groups; they emerge in the study of symmetries of WZW models, which are a class of CFT. Symmetries present in CFT are: the Poincaré symmetries, present in special relativity, an additional scale transformation, and the special conformal transformation. The group that encodes these symmetries is called the conformal group. Local behaviour of the conformal group leads to a conformal algebra. For 2-dimensions the conformal algebra becomes the ∞ -dimensional Witt algebra. In order to satisfy the unitarity condition of quantum theory the Witt algebra must be centrally extended, forming the Virasoro algebra. Studying CFTs can, in a certain sense, be understood as studying the consequences of the Virasoro algebra. As shown by Sugawara [44], this Virasoro algebra can be embedded in the enveloping algebra of an affine Lie algebra. States in WZW models can be put in correspondence with representations of the affine Lie groups, with the ∞ -dimensional algebra behaving like a set of local constraints. WZW models are the main focus of this thesis due to their relative simplicity and

the identification of their states as vectors in representations of the affine Lie groups.

On its own, CFT is a fascinating and rich topic of study⁷ with extensive mathematical machinery that underpins the theory. WZW models [20] form a special class of CFT that, as mentioned, have states, indicated by primary fields, that can be identified with representations of an affine Lie group. Primary fields are one of two types of fundamental conformal fields, the second being secondary fields. Secondary fields are, in general, infinite in number, but they can be generated from the possibly finite number of primary fields via the application of operators. Operations on the primary fields to obtain secondary fields work in an analogous way as the ladder operators from quantum mechanics. Families of fields can be built up in this way and are labelled by primary fields. These families of fields are related to highest-weight representations of an affine Lie group.

The main distinction between the simple Lie groups and the affine Lie groups is the addition of a central charge. Physically, the Virasoro central charge in the Virasoro algebra can be interpreted as the coefficient of the Wess-Zumino (WZ) term in its action $c = \frac{k \dim(\mathfrak{g})}{k+h^\vee}$ [20]. The dimension $\dim(\mathfrak{g})$ is simply the dimensions of the Lie algebra \mathfrak{g} and h^\vee is the dual Coxeter number. The level k is the central charge of the affine Lie algebra, which can be thought of as a centrally extended loop algebra. The level imposes an additional property on the WZW models and must be specified along with a highest-weight vector to obtain a unique representation. Specification of the level imposes a restriction on the number of possible secondary fields, truncating them after a certain number of operator applications on the primary fields.

Imposition of the level brings with it the consequence that there will be a finite number of possible highest-weight states. There is a minimum level at which a highest-weight first appears, called its threshold level. Drawing the weight space of the Lie group $SU(3)$ provides a useful picture. With a set of axes corresponding to the

⁷The downside of this is that most objects have at least two or three names.

roots of the simple Lie group, for the affine case there is an additional ‘affine wall’ $\{\lambda \mid (\lambda + \rho) \cdot \theta = N + k\}$ that truncates the set of possible highest-weights. The weight ρ is the Weyl vector, and θ is the highest root. For $SU(N)$ the Weyl vector and highest root are $\rho = [1, 1, \dots, 1, 1]$ and $\theta = [1, 0, \dots, 0, 1]$, respectively. We say that a simplex⁸ contains all possible highest-weights and is called the (affine) Weyl alcove.

Weight systems of the highest-weight representation of a Lie group can be geometrically organized by using the simple roots to move between the weights. The weight system itself has a number of symmetries, such as the Weyl symmetry that relates weight to one another via primitive reflections. For $SU(N)$, the Weyl group is isomorphic to the symmetric group S_N , which is the set of permutations of an N element list. The Weyl group maps a weight system of a highest-weight representation back onto itself. Weyl groups can be used to write the weight system in terms of a union of unique and disjoint Weyl orbits. Weight multiplicities will be equal for all weights in a given Weyl orbit.

The affine wall present in the affine Lie group introduces an additional primitive reflection element to the Weyl group, called the affine reflection ω_0 . The primitive affine reflection corresponds to reflections across the affine wall, and so its action has a level dependence. Combining the affine Weyl reflection with the other Weyl reflections turn the finite-dimensional Weyl group⁹ into the ∞ -dimensional affine Weyl group. Affine reflections move the weights up and down in energy levels, which are eigenvalues of the Virasoro generator L_0 . We can take advantage of the ∞ -dimensional affine Weyl group to shrink the possible highest-weights to those contained in the Weyl alcove. Affine and horizontal Weyl groups map weights from the highest-weight representation of an affine Lie group back into the same highest-weight representation.

⁸In the case of $SU(3)$, the simplex reduces to the familiar triangle.

⁹When dealing with the affine Lie groups, we refer to the horizontal Weyl group as the subgroup the affine Weyl group generated by its generators minus the affine reflection element ω_0 .

We can introduce another transformation, that of the simple currents. Simple currents are defined as transformations on the Weyl alcove. They relate the weights in a given Weyl alcove to one another by cycling through their Dynkin labels. Notably, simple currents are most naturally a property of the affine Lie groups and are difficult to adapt to the non-affine Lie group case.

Galois transformations are another symmetry that can be defined between weights in an affine highest-weight representation [15]. At their most basic Galois transformations relate distinct primitive M -th roots of unity to other distinct primitive M -th roots of unity. The origins of the Galois group are in the study of rational polynomials, where it relates the roots (or zeroes) that split a polynomial to one another. For our purposes we consider the Galois action as relating weights, although it is more fundamentally understood as transforming the root of unity corresponding to a weight. Similar to the simple currents, the Galois action breaks up the Weyl alcove into distinct orbits and is a naturally affine symmetry. Galois orbits are complicated to calculate and must be recalculated at every level. As transformations, they can be used to group the weights appearing in the Weyl alcove into distinct Galois orbits at a level k .

Interactions between conformal fields in a WZW model are encoded in an operation called the operator product expansion (OPE). The OPE is a product of local fields that is expanded out in terms of the position difference of the fields; the results are written in terms of the fields in the theory. For the WZW models, defined as they are at fixed level, OPEs require that the level of the fields be unchanged throughout the operation.

OPEs are used in order to obtain fundamental objects in CFT called conformal blocks. Conformal blocks are the building blocks of correlation functions and live on a Riemann surface with a number of holes, the genus, and marked points. Marked points on the Riemann surface are related to incoming and outgoing fields and the

genus indicating a self-interaction-like interaction. Conformal blocks prescribe the interactions for fields in a CFT and can be used to construct general correlation functions.

We can consider the OPE of a family of fields, then the number of times a family appears in an interaction between two fields is accounted for by the fusion dimension. These fusion dimensions correspond to the dimension of the space of conformal blocks, and can be thought of as analogous to the tensor product multiplicities for the tensor products. Necessarily, fusion dimensions are non-negative integers and provide similar data as the OPE, albeit less detailed.

Affine tensor products can be defined, where the operation will add the levels of the initial representations together to give the level of the resulting representation. Any change in the level will alter the WZW model we are considering, which indicates that the affine tensor product cannot be used to reproduce the results of the OPE. An adapted tensor product that leaves the level unchanged, the fusion product, can be introduced a natural way that preserved many of its useful properties. In particular, the fusion product is: commutative, associative, distributive, and conjugation invariant. The emergence of the fusion product occurs by imposing a truncation on the tensor product of the related simple Lie algebra irreps, based on the level ' k .' Simple tensor products are equivalent to fusion products when the level is taken to infinity. The field that results from the affine fusion of two fields can itself be decomposed as a direct sum of irreps with their fusion dimensions indicating how often each irrep appears. Future references to the fusion product will presume the decomposition procedure.

Fusion products can be understood as close analogs of the tensor products. An interesting relation is that as the level $k \rightarrow \infty$ the fusion product converges to the (simple Lie) tensor product, which can be restated as fusion dimensions at infinite level being equal to tensor product multiplicities. Curiously, despite the close rela-

relationship between the fusion and tensor products a combinatorial description of fusion dimensions is not yet known.

Fusion dimensions can be utilized in order to understand certain properties of a CFT correlation function more simply. We will see that the Riemann surface that a correlation function lives on can be degenerated into trivalent graphs. These trivalent graphs can be labelled on their vertices with fusion coefficients, which are 3-point fusion dimensions, and their external edges labelled with the interacting fields. These graphs are extremely useful and allow us to encode a conjectured equivalence of the s - and t -channels of the combination of four primary fields for an OPE. This equivalence is known as the crossing symmetry and is a requirement for the consistency of a given CFT.

Fusion products, like the OPE, prescribe how to combine primary fields, though they do so in a simpler way. Fusion products of n -primary fields can be accounted for with an n -point fusion dimension that consists of n -external edges of a graph. Degenerations of the Riemann surfaces are not unique, but the resulting graphs will be related to one another by unitary transformation. Relations between the non-unique degenerations of the Riemann surfaces are described by Moore Seiberg duality [33].

Moore-Seiberg duality tells us that we are able to look at a Riemann surface with marked points representing the conformal block and degenerate it into trivalent graphs. Although multiple graphs corresponding to different sets of conformal blocks can appear in the construction, Moore-Seiberg tell us that they must all result in the same correlation function. This relationship requires the existence of unitary transformations between all graphs obtained from the degeneration of a surface. These trivalent graphs will represent an n -point fusion dimension and be topologically related to the original Riemann surface. A special case of Moore-Seiberg duality is the crossing symmetry, which emerges when considering a 4-point correlation function. The reproduction of the crossing symmetry is not shocking, since the Moore-Seiberg

duality was motivated by that very property.

A second very important case to consider from the perspective of Moore-Seiberg is in the degeneration of the conformal block on the torus $S^1 \times S^1$. Conformal blocks of the torus can be identified as being equal to the affine character. There are several decompositions, corresponding to the different ways of representing cycles of the torus. Based on the required unitary transformations that we know that the cycles will be related in a unitary way. The transformations between the possible independent cycles on the torus are known to be the modular group. Hence, the affine characters will transform covariantly under modular transformations. We can interpret this result and say that from the perspective of Moore-Seiberg duality the modular symmetry of a CFT is tied to the consistency of the model.

S -modular matrices are one of the two generating modular matrices that transform the affine character. Computation of these matrices outright is a difficult procedure for general models. Luckily, for the WZW models we can take advantage of the Kac-Peterson equation [23], which relates the S -modular matrices with the simple Lie group characters.

Looking back to the Moore-Seiberg duality we remind ourselves that we can also relate compositions of fusion products to one another, so long as they're topologically equivalent. What this lets us do is to write down the general Verlinde formula, using only that the internal edges are summed over and that $\sum_{\sigma \in P_+^k} S_{\mu,\sigma} S_{\bar{\mu},\lambda} = \delta_\lambda^\sigma$:

$${}^{(N,g,k)}\mathcal{N}_{\lambda_1,\dots,\lambda_M} = \sum_{\sigma \in P_+^k} (S_{0,\sigma})^{2(1-g)} \prod_{i=1}^M \left(\frac{S_{\lambda_i,\sigma}}{S_{0,\sigma}} \right). \quad (1.1)$$

The genus g increases whenever a sum over internal edges results in an internal loop in the graph. This process of combining fusion coefficients and summing over their inner edges is a procedure we refer to as gluing. This result is the same irrespective how the gluing procedure was performed. The basic Verlinde formula, which computes

the fusion coefficient, is retrieved when $g = 0$ and $M = 3$.

S -modular matrices can be used to diagonalize the fusion matrices, whose components consist of the fusion dimensions, which leads to a set of eigenvalues 4.3.2. This procedure ends with the extremely important Verlinde formula, which relates the S -modular matrices to the fusion dimensions. The Verlinde formula gives us a fundamentally affine method for computing the fusion dimension:

$$\mathcal{N}_{\lambda,\mu}^{\nu} = \sum_{\sigma \in P_+^k} S_{\lambda,\sigma} \left(\frac{S_{\mu,\sigma}}{S_{0,\sigma}} \right) S_{\bar{\nu},\sigma}. \quad (1.2)$$

The 2-point fusion dimension with genus-1 looks like a handle operator, consisting of a loop along a straight line. It is obtained by gluing two 3-point fusion graphs together along their legs such that one of the 3-point fusion graphs has 2 outgoing fields corresponding to the 2 incoming fields of the second. Despite being a smaller point function and having a higher genus it is fairly clear that the 2-point fusion dimension at genus-1 plays a less fundamental role than the fusion coefficient.¹⁰

Tadpoles, named due to their shape, do not appear to share this same type of gluing property. Instead the only way to generate a tadpole from the 3-point fusion graph is to self-glue two legs of the 3-point fusion graph. Unlike the other fusion dimensions we are still technically working with a single fusion coefficient. Due to the gluing action requiring that the two fields glued be conjugate to each other the tadpole can be thought of as the trace of the fusion coefficient. From this procedure it is arguable that the tadpole is the simplest example of higher-genus fusion.

Diagrammatically, tadpoles have a single incoming field and a loop. They can be thought of as being the resulting trace of a fusion coefficient. This equivalence lets us identify the tadpole as the dimension of the space of the conformal blocks along their diagonal. The tadpole's simplified properties mean it can be computed

¹⁰Fusion coefficient being defined as the 3-point fusion and so corresponding to the 3-point fusion graphs.

far more easily than the standard fusion coefficient. This simplification is very useful in searching for underlying structures in the Verlinde formula.

Our study of the tadpoles was motivated by the absence of a manifestly combinatorial account of the fusion dimensions. Within the Verlinde formula it is not at all clear that fusion dimensions are non-negative integers. All values appear to be complex valued up until the final sum in the Verlinde formula is evaluated. When using the Kac-Walton formula, the result is manifestly an integer, although it is not immediately obvious that it must be positive. The depth rule and its variations clearly compute positive integers, but they are difficult to implement in calculations. With the exception of the Verlinde formula, these computational methods are adapted from computing tensor product multiplicities. Our study was concerned with finding a deeper affine understanding of fusion that might lead to the identification of a combinatorial atom. To that end we had hoped to rewrite the Verlinde formula in terms of a sum of non-negative-integers that could have led to candidate combinatorial arguments. Such a technique, particularly if motivated by symmetry considerations, might provide a finer resolution description for more general fusion dimensions as well.

The simplicity of affine fusion tadpoles, compared to the other fusion dimensions, made them an ideal candidate for looking for an underlying structure in the fusion dimensions. Combinations of known symmetries of the weight system and Weyl alcove of a highest-weight representation were used to break up and reorder the sums in the Verlinde formula. Breaking up the sums was based on the idea that by choosing the correct symmetry a sum over non-negative integers would yield the affine tadpole. Partial sums were broken up into those affecting the Weyl alcove and those relevant to the weight system of the representation. Our treatment of them involved working through all possible summation methods in both cases and combinations of them.

Other methods to compute the fusion dimensions, adapted from tensor product

multiplicity calculations, were also applied to the tadpole question. These methods are not manifestly affine, but they still provide some useful insights. Several methods of computing fusion were used and attempts were made to adapt them to the special case of tadpole calculation. The methods tried were: the Kac-Walton formula, Racah-Speiser algorithm, the generalized Berenstein-Zelevinsky triangles (generalized BZ triangles), and note the recent success of an adapted Littlewood–Richardson (LR) algorithm method from Morse et al. [34].¹¹

The generalized BZ triangles interpret the fusion dimension as being equal to the volume of a discrete polytope [8]. These polytope volumes are obtained by considering the number of valid generalized BZ triangles, whose constraints are based on the rank of the group. While interesting, this method becomes too complicated to use for higher rank groups due to the number of constraints on the polytope volume that must be imposed. With this method we were able to prove cases of a conjectured formula at ranks 2, 3, and 4 for particular classes of tadpoles.

Semi-standard Young tableaux (SSYT) can be used in conjunction with the Littlewood–Richardson (LR) algorithm to great effect for calculating tensor multiplicities of the $SU(N)$ groups. Applications to fusion are not so straightforward, even for the case of $\widehat{SU}(N)$.¹² Recent results from Morse et al. [34] were investigated and found to be unsuitable for the calculation of the tadpoles.

Tadpoles can be written as a sum of Schur polynomials, which are a basis for the symmetric polynomials. This relation utilizes Schur–Weyl duality, which is a very powerful result that relates the symmetric group, of which the symmetric polynomials form a representation, with the special unitary group $S_N \leftrightarrow SU(N)$. We take advantage of this correspondence with a conjectured method that was used to find several explicit expressions for certain classes of tadpoles in terms of $N - 1$ degree

¹¹Use of the LR algorithm is only valid for $SU(N)$ groups, although there exist generalizations for other groups [25].

¹²The hat denotes an affine Lie group instead of the non-affine $SU(N)$.

polynomials in the level k . Our search for these polynomials was due to results noticed when summing over the Weyl alcove and Weyl orbits and called the dominant weight sums. These dominant weight sums were labelled by a dominant weight and appeared to contribute values to the tadpole that were matched by a polynomial in the level k . We conjectured polynomials in the level k who appear to reproduce the values of the dominant weight sums (defined in equation (6.13)).

Application of the Kac-Walton algorithm [22, 46] to the problem of fusion dimension greatly simplifies calculation by connecting it to the multiplicity of weights in highest-weights irreps. One need only replace the affine Weyl group with the simple Weyl group to have a formula for the tensor product multiplicities. This makes it clear that the fusion product is a truncation of the tensor product:

$$\mathcal{N}_{\lambda,\mu}^{\nu} = \sum_{w \in \widehat{W}} (-1)^{\ell(w)} \text{mult}_{\lambda}((\mu + \rho) - w(\nu + \rho)). \quad (1.3)$$

Unlike the other methods here the Kac-Walton algorithm is manifestly geometric, where the affine Weyl group \widehat{W} is used to transform multiplicities so that they either add or subtract. Whether a multiplicity adds or subtracts is based on the minimum length of the affine Weyl element needed to reflect a weight into the dominant Weyl alcove, which is the set of valid highest-weights. The minimum length of an affine or non-affine Weyl element is defined as the minimum number of primitive reflections needed to form the element. The Kac-Walton algorithm, when applied to the tadpole, resulted in some simplification, but the additional required sum over the Weyl alcove made using this method difficult. The sum over the Weyl alcove makes it necessary to repeat the procedure of adding and subtracting multiplicities for every weight in the Weyl alcove. Further, the affine Weyl group contains a level dependence and so everything must be recalculated at every level. In the end these two factors leave the algorithm somewhat unsuitable for application to the tadpole.

Analysis of the tadpole formula was done by partially summing over symmetries and transformations in the weight system of the highest-weight representations, the Weyl alcove, and combinations of the two of them. Sums in the Verlinde formula were rearranged and the results checked against a brute force calculation, to ensure that errors did not occur. These experimental investigations resulted in several interesting observations, although they remain unexplained.

From these experiments we found two types of partial sums with integer values. Those sums indexed by the Galois orbits and carried out over weights in the weight system (6.11), and those that were indexed by the Weyl orbits and summed over the Weyl alcove (6.13), called the dominant weight sums. Though these partial sum methods were integer-valued, they were sometimes negative. Patterns were not obvious in the Galois orbit sums, but the dominant weight sum had a number of interesting patterns. Most notably, the dominant weight sums agreed with values produced by polynomials in the level k . Dominant weight sums appeared to be closely related to the simple root structure of the dominant weight element, specifically the number of unique integers that specify the dual Dynkin labels. These observations are reported in Section 6.2 and an explanation for the polynomials is attempted in Appendix A.1.

Investigations of the dominant weight sums resulted in several formulas. Conjectural forms of the dominant weight are recorded in Appendix A.1, and conjectures about polynomials in k equalling tadpoles are reported in Section 6.3. These formulas are suggestive of a set of more general relations. Our conjectures are very general, and account for both arbitrary level and dimension. They were found to agree with the results calculated by other means and listed in our tables (see Section B.1). They also coincided with computed values for the tadpole from the generalized BZ triangles. Generalized BZ triangles were used to prove conjectured formulas for the cases of $N = 2, 3$, and 4 . The hypothesized formulas are suggestive of polytope volumes, possibly paving the way for a combinatorial interpretation of the tadpole.

Experimental investigations into the tadpole suggested curious properties at work behind the scenes. It would be interesting if there was an explanation of the properties that have been experimentally observed from a Lie-theoretic perspective.

Chapter 2

Groups, Algebras, and Symmetries

Symmetries are the cornerstone upon which modern physics has been built. A theory's symmetries can be used to identify conserved quantities, restrict the forms that the action can take, and informs us about the possible states and interactions that can occur in its framework. Groups, and the group theory describing them, are a mathematically formulated method of accounting for symmetries that can be applied to physical as well as mathematical systems.

Groups encode symmetries in an abstract way and can be applied to concrete systems via representations. Representing a group can be done in many ways: as a transformation, as the states of a system, as a set of operators, among many other possibilities. Choosing a representation is based on how one wants to interpret the symmetry of the system of interest.

The most famous symmetry group is, arguably, the circle group $U(1)$. The elements of $U(1)$ form a set isomorphic to the points on the unit circle. The transformations induced by $U(1)$ can be imagined as rotations around a point. This isomorphism is realized by defining a group parameter θ , which is used to denote group elements as in terms of $e^{i\theta}$. A group of $U(1)$ transformations leaves the Quantum-Electro-Dynamics (QED) Lagrangian unchanged.

In quantum mechanics representations of the $SU(2)$ group can be used in order to describe angular momentum states of a system. Angular momentum states are defined in terms of their maximum total angular momentum and a projection of the angular momentum along the z -axis. A set of operators are introduced that act on these states such that every axis has its angular momentum accounted for. Since the operators on the x, y, z axis cannot have simultaneously diagonalized eigenvalues they are used to construct raising and lowering operators. The full set of states can be constructed using the raising and lowering operators. A maximum angular momentum value is used to define a representation. This is an example of a highest-weight representation, where the maximum angular momentum plays the role of highest-weight.

Those states resulting from a physical analysis of quantum angular momentum are isomorphic to those states found by considering a corresponding highest-weight representation of $SU(2)$. Physical states of a system can be identified with the states of a highest-weight representation, which recasts the problem of angular momentum as a question of symmetries. Interpretation of a physical problem in terms of groups and group theoretic language is mathematically helpful, since it provides access to powerful group theoretic techniques. Philosophically, a successful group theoretic approach is satisfying since they can be related back to symmetries of the system.

2.1 Groups

The connection of groups to symmetries, and the powerful mathematical machinery that underpins group theory, makes them a potent tool for physicists. In order to facilitate their use it is helpful to understand how a group is defined and how they encode symmetry.

A group codifies symmetry in an abstract sense, which makes it applicable to many disparate systems. Mathematically, groups are defined as sets of objects along with a composition law satisfying specific properties.¹ This composition law prescribes how elements in the set will combine with one another. A group has a composition law along with a set of group elements that must obey the four group axioms: closure, identity, associativity, and inverse.

Definition 1. *A group is a set of elements G with a composition law between elements denoted ‘ \cdot ’ such that the four ‘group axioms’ are satisfied.*

- *Closure: for all $a, b \in G$ the operation $a \cdot b \in G$.*
- *Identity: there is some unique element $e \in G$ such that $e \cdot a = a \cdot e = a$.*

¹When groups are realized by transformations, group multiplication is understood as being the composition of these transformations.

- *Associativity: for all $a, b, c \in G$ we have that $(a \cdot b) \cdot c = a \cdot (b \cdot c)$.*
- *Inverse: for every $a \in G$ there is an element $b \in G$ such that $a \cdot b = b \cdot a = e$.*

These axioms are applicable to a broad class of objects. For this thesis we use the symmetric group (an example of a finite group), the simple Lie groups, and affine Lie groups. Finite groups are the most basic type of group, due to having a finite number of elements, and permit straightforward analysis. Simple Lie groups and affine Lie groups have an infinite number of elements, which are in 1–1 correspondence with points of a manifold. The Lie group manifold allows us to define a local algebra called the Lie algebra,² which accounts for ‘local’ group behaviour near the identity element.

2.1.1 Finite Groups

As an exercise, it is instructive to go through how a group satisfies the group axioms. Finite groups make for particularly straightforward examples, since we can choose a group small enough that an exhaustive treatment is possible. Doing so usually involves building a multiplication table for the elements and lets us observe how the group axioms are satisfied. A particularly important example for us is the symmetric group S_N , which is the permutation group of an N -element list.

The symmetric group consists of $N!$ unique elements and can be generated completely by transpositions, which are a switch of any two elements in a list. These transpositions are said to generate the group since every element can be written in terms of a composition of transpositions. When a subset of the group can be used to obtain the whole group, a role played by the transpositions for S_N , we call that subset the generators. Studying the generators allows us to discuss a group in terms of a relatively small number of its elements.³ For a group G with generating elements

²When considering the affine Lie groups the situation is largely unchanged, although in that case we will be dealing with an affine Lie algebra instead.

³For the study of the simple Lie groups the presence of the generators, which are finite in number, are central to using their representations.

$g_1, g_2 \in G$ we can write $\langle g_1, g_2 \rangle = G$, to mean that G is generated by the set contained in the angled brackets.

The generating transpositions for S_N can be reinterpreted as simple reflections about $N - 1$ hyperplanes, along with a required identity element. Given that the transpositions are isomorphic to reflections we can identify the Weyl group W_N of $SU(N)$, which are generated by primitive reflections, as isomorphic to the symmetric group S_N . As with the transpositions, combinations of these primitive reflections can be used to recreate every other element of the Weyl group.⁴

We consider the example of S_3 in order to demonstrate the group axioms. S_3 is the symmetric group for $N = 3$ and is isomorphic to the Weyl group W_3 of $SU(3)$.

Example 1. *Taking our group S_3 , we have 2 generating transpositions $(12), (23)$, which we denote as: ω_1, ω_2 . The transpositions act on a list (a, b, c) , with (i, j) exchanging the positions of the i^{th} and j^{th} components. We know that applying the same transposition twice on a list*

$$(1, 2) \cdot (1, 2) \cdot (a, b, d) = (1, 2) \cdot (b, a, c) = (a, b, c),$$

so the identity element $\omega_i^2 = I \in S_3$. We note that $(1, 2)(2, 3)(1, 2) \simeq (2, 3)(1, 2)(2, 3)$ by checking:

$$(1, 2)(2, 3)(1, 2) \cdot (a, b, c) = (1, 2)(2, 3) \cdot (b, a, c) = (1, 2) \cdot (b, c, a) = (c, b, a),$$

$$(2, 3)(1, 2)(2, 3) \cdot (a, b, c) = (2, 3)(1, 2) \cdot (a, c, b) = (2, 3) \cdot (c, a, b) = (c, b, a).$$

We introduce the slight simplification of the notation to $\omega_{1,2} := \omega_1\omega_2 = (1, 2)(2, 3)$ and note that $\omega_{1,2} = (1, 2)(2, 3) \neq (2, 3)(1, 2) = \omega_{2,1}$. We can define the longest elements as $\omega_{1,2,1} = \omega_{2,1,2}$, which we saw by considering the transpositions action on the list.

⁴These $N - 1$ elements that correspond to the reflections about a unique axis are called generators.

	I	ω_1	ω_2	$\omega_{1,2}$	$\omega_{2,1}$	$\omega_{1,2,1}$
I	I	ω_1	ω_2	$\omega_{1,2}$	$\omega_{2,1}$	$\omega_{1,2,1}$
ω_1	ω_1	I	$\omega_{1,2}$	ω_2	$\omega_{1,2,1}$	$\omega_{2,1}$
ω_2	ω_2	$\omega_{2,1}$	I	$\omega_{1,2,1}$	ω_1	$\omega_{1,2}$
$\omega_{2,1}$	$\omega_{2,1}$	ω_2	$\omega_{1,2,1}$	I	$\omega_{1,2}$	ω_1
$\omega_{1,2}$	$\omega_{1,2}$	$\omega_{1,2,1}$	ω_1	$\omega_{2,1}$	I	ω_2
$\omega_{1,2,1}$	$\omega_{1,2,1}$	$\omega_{1,2}$	$\omega_{2,1}$	ω_1	ω_2	I

Table 2.1: Multiplication table for S_3 .

We choose to write only $\omega_{1,2,1}$ in order to avoid confusion on the multiplication table. Writing down the multiplication table of the group we can check the group axioms by brute force.

We can read off the properties of S_3 from Table 2.1 in order to find that it satisfies the axioms.

- The identity element is identified as the element that does not reflect.
- The inverse condition is satisfied since every element has the identity appearing along its row and column.
- Closure is found by exhaustion here, since the table includes all possible combinations of the elements.
- Similarly to closure, we can look at the table and conclude that associativity is satisfied by exhaustion.

For more general applications it is often not practical, or even possible, to draw a full multiplication table. Even for finite groups, the larger groups quickly become too large for this to be an efficient method of analysis. Finite groups can be treated instead in terms of constituent simple finite groups [42], which are classified into a finite number of types.

Simple finite groups are called simple because they contain within them no normal subgroups, defined below. Both the reflection and cyclic groups are simple groups

since they contain no normal subgroups other than the identity⁵ and the groups themselves.

Definition 2. *Given two non-trivial groups G and H with $H \subset G$, if for every $g \in G$ the two sets⁶ $g \cdot H = H \cdot g$ then H is said to be a normal subgroup of G .*

Simple finite groups can be used to reconstruct any other finite group, although the group decomposition is not necessarily unique as there are many composition methods.⁷ The complete classification of the finite simple groups is a very complicated and celebrated result in mathematics.

2.1.2 Lie Groups

Lie groups are somewhat more complicated to analyze than the finite groups, but are extremely important for their physical applications. Arguably the most common use of Lie groups are their application to continuous transformations. Connecting the Lie groups with continuous transformations lets us apply Noether's theorem to find the conserved quantities of a theory, effectively relating conserved values to the symmetries of a theory. As complicated as the Lie groups are, this example should make it clear that it is well worth the effort to understand them.

Understanding the Lie groups is greatly assisted by taking advantage of their underlying manifold, often referred to as a Lie manifold. Lie manifolds are smooth, which tells us that the Lie group elements, and their representations, are infinitely differentiable and continuous everywhere. This makes it possible to account for continuous symmetries of a system with a Lie group.

Lie manifolds allow us to consider the local behaviour of the Lie group about a

⁵A group that contains the identity element as its only element is called the trivial group.

⁶The notation $g \cdot H$ means using the composition law to combine g with every element $h_i \in H$, that is $g \cdot H = \{g \cdot h_1, g \cdot h_2, \dots\}$.

⁷Such composition methods include the direct and semi direct products to name a two of the most common.

point on that manifold. Often the point is taken to be the identity, whose representation is often straightforward to identify. Consideration of the behaviour of points very close to⁸ the identity element is used to identify the generators of the Lie group. These generators and their relations to one another can then be codified with the Lie algebra, which accounts for local behaviour of the group.

Due to smoothness the small scale behaviour of the Lie algebra can be used to build up general Lie group elements. This building up process allows us to identify the smallest movements away from the identity element as being the generating elements of the Lie group. Continuity, implied by smoothness, is essential here and it requires that when two group elements are ‘close together’ on the manifold, the parameters defining these elements are also ‘close together.’⁹ These variations around the identity correspond to the Lie Group generators and this process can be used to find a representation of the generators given a form for the identity.

We can write the elements of a Lie group G in terms of group parameters τ^a , where $a = \{1, \dots, \dim(G)\}$, with $g(\tau) \in G$. Commonly, the Lie group can be represented as a set of linear operators $D(\tau)$, which confers the advantage of linear operators being particularly simple to work with. Constructing a general transformation is done by repeatedly applying the linear operators to themselves. The identity is identified as being the linear representation equal to 1:

$$G(\tau)|_{\tau=0} = Id, \quad D(\tau)|_{\tau=0} = 1. \quad (2.1)$$

Considering a small change in the group parameter τ around the identity element we only keep the first order variations. Variations $d\tau$ are given by the transformed

⁸‘Close to ...’ can be more rigorously understood as being ‘in the neighborhood of ...’

⁹This definition of continuity is analogous to the definition from calculus.

linear operator and can be written:

$$D(\tau + d\tau)|_{\tau=0} \approx 1 + id\tau_a X^a, \quad (2.2)$$

with the X^a being the generators of the group. Considering the action of many $D(d\tau)$'s we can write general Lie group elements as

$$D(\tau) = \lim_{k \rightarrow \infty} (D(d\tau))^k = \lim_{k \rightarrow \infty} (1 + id\tau_a X^a)^k, \quad (2.3)$$

$$= e^{i\tau_a X^a}, \quad (2.4)$$

where the final step is motivated by the definition of exponential.

In general the generators, X^a , do not necessarily commute and consequently their exponential representation will not generally commute either. Non-commuting elements have their behaviour accounted for by the Lie brackets,¹⁰ which can be used to study the Lie algebra in a representation independent way.

Using the Lie brackets to perform representation independent analysis is extremely useful. Lie algebra can be accounted for in terms of structure constants $f_c^{a,b}$, which are defined in terms of commutators of Lie generators:

$$[X^a, X^b] = X^c f_c^{a,b}. \quad (2.5)$$

Being representation independent these structure constants $f_c^{a,b}$ specify the algebra and point to a corresponding group.

Lie groups have an analogous notion of a finite simple group, which, for a finite group, means that they contain no normal subgroups other than the trivial group and the whole group. For Lie groups there is an analogous structure, the semi-simple Lie groups, that act as their building blocks. By this we mean that general Lie groups

¹⁰Physicists may recognize these as being the commutation relations.

can be written in terms of compositions of semi-simple Lie groups. In order to define this we need to introduce the notion of an invariant subalgebra and include both definitions below.

Definition 3. *Given a Lie algebra \mathfrak{g} corresponding to a Lie group G we can choose two elements $h, g \in \mathfrak{g}$ and determine another element $h' = g^{-1}hg$. Whenever the h' can be used to generate an algebra that is neither the trivial algebra nor the whole algebra \mathfrak{g} then we say that $\langle h' \rangle$ is an invariant subalgebra of \mathfrak{g} .*

Definition 4. *When a Lie algebra \mathfrak{g} has no Abelian¹¹ invariant subalgebras then \mathfrak{g} is said to be semi-simple. Equivalently, when a Lie group can be written in terms of a direct product of simple Lie groups, the Lie group is said to be semi-simple.*

Semi-simple Lie groups are completely classified and very important to keep in mind. They are compiled below with an identification of some different notations.

- Unitary Group $U(N)$
- Special Unitary Group $SU(N) \simeq A_{N-1}$
- Special Orthogonal Group $SO(2N + 1) \simeq B_N$
- Symplectic Group $Sp(2N) \simeq C_N$
- Special Orthogonal Group $SO(2N) \simeq D_N$
- The exceptional groups: $G_2, F_4, E_6, E_7,$ and E_8

2.1.3 The Lie Group $SU(2)$

As an example of a Lie group manifesting itself in a physical way, we consider the relationship between quantum angular momentum and an $SU(2)$ representation. Treating the problem of quantum angular momentum can be done by introducing a set of

¹¹Abelian means that all elements of the group commute with every other element.

operators $\hat{J}_x, \hat{J}_y, \hat{J}_z$, each accounting for a component of angular momentum. These operators obey the commutation relations:

$$[\hat{J}_x, \hat{J}_y] = i\hat{J}_z, \quad [\hat{J}_y, \hat{J}_z] = i\hat{J}_x, \quad [\hat{J}_z, \hat{J}_x] = i\hat{J}_y. \quad (2.6)$$

We note that none of these operators commute with one another.

Since the operators in equation (2.6) do not commute, this indicates that it is not possible to simultaneously diagonalize all three operators. What we can do is to note that the operator \hat{J}_z commutes with $\vec{J}^2 = \hat{J}_x^2 + \hat{J}_y^2 + \hat{J}_z^2$. That these two operators commute means that they can be diagonalized simultaneously. Their eigenvalues are m for \hat{J}_z and $J(J+1)$ for \vec{J}^2 , collected in equation (2.10). The eigenvalue m is the projection of the total angular momentum along the z -axis and J is defined as the total angular momentum eigenvalue.

J and m are used together to label quantum mechanical angular momentum states as $|J, m\rangle$. For a given angular momentum the z -axis projection of the angular momentum has a number of possible values. A set of angular momentum states $P(J)$ is specified by the total angular momentum J by possible z -axis projections: $P(J) = \{J, J-1, \dots, -J+1, -J\}$. In the $|J, m\rangle$ notation we equivalently have:

$$P(J) = \{|J, J\rangle, |J, J-1\rangle, \dots, |J, -J\rangle\}. \quad (2.7)$$

We can introduce raising and lowering operators by rewriting \vec{J}^2 as:

$$\begin{aligned} \vec{J}^2 &= \frac{1}{2} \left((\hat{J}_x + i\hat{J}_y)(\hat{J}_x - i\hat{J}_y) + (\hat{J}_x - i\hat{J}_y)(\hat{J}_x + i\hat{J}_y) \right), \\ &= \hat{J}_+ \hat{J}_- + \hat{J}_- \hat{J}_+. \end{aligned} \quad (2.8)$$

The commutation relations of these operators are then given by:

$$[\hat{J}_+, \hat{J}_-] = 2\hat{J}_z, \quad [\hat{J}_\pm, \hat{J}_z] = \pm\hat{J}_\pm. \quad (2.9)$$

The raising operator $\hat{J}_+ = \hat{J}_x + i\hat{J}_y$ and lowering operator $\hat{J}_- = \hat{J}_x - i\hat{J}_y$ affect the state of the system, increasing or decreasing the quantum number m . So we have the following operator behaviours, subject to the condition that $m + 1 \leq J$ and $m - 1 \geq -J$ to avoid accidental annihilation:

$$\hat{J}_+ |J, m\rangle = \sqrt{J(J+1)} |J, m+1\rangle, \quad \hat{J}_- |J, m\rangle = \sqrt{J(J-1)} |J, m-1\rangle, \quad (2.10)$$

$$\hat{J}_z |J, m\rangle = m |J, m\rangle, \quad \vec{J}^2 |J, m\rangle = J(J+1) |J, m\rangle. \quad (2.11)$$

These raising and lowering operators are important in that they can be used to build angular momentum representations given a highest angular momentum J . So by specifying a total angular momentum J , or highest-weight $2J$, the system of angular momentum is uniquely determined.

Raising and lowering operators can be interpreted as playing the role of the roots in a highest-weight representation. Weights are twice the value of eigenvalues m and the roots are twice ± 1 , which let us account for the ladder operators as roots. Roots are used to move up and down along the possible weights contained in a highest-weight representation, which for $SU(2)$ are simply integer valued increments along a number line between $\pm J$. In general, the simple roots will be vectors and build up the highest-weight representation by acting on the highest-weight. Using roots to build up a highest-weight representation of $SU(2)$ results in the same kind of angular momentum representation one expects in physics.

Treating angular momentum as a special example of a highest-weight representation makes it explicit clear that there is an important distinction between spin 1 and spin $\frac{1}{2}$ particles despite their similar underlying symmetries. These two repre-

representations share no states in their highest-weight representations, with $J = \frac{1}{2}$ consisting of states $P([\frac{1}{2}]) = \{|\frac{1}{2}, \frac{1}{2}\rangle, |\frac{1}{2}, -\frac{1}{2}\rangle\}$ and $J = 1$ having the weight system $P([1]) = \{|1, 1\rangle, |1, 0\rangle, |1, -1\rangle\}$.

Example 2. *Given a highest weight element of $J = 2$, which corresponds to a angular spin 2 system, we will have the weight system:*

$$P([2]) = \{|2, 2\rangle, |2, 1\rangle, |2, 0\rangle, |2, -1\rangle, |2, -2\rangle\}. \quad (2.12)$$

2.2 Highest-Weight Representations

Having identified the raising and lowering operators in addition to the z -axis projection operator $\{\hat{J}_-, \hat{J}_+, \hat{J}_z\}$ we can use $SU(2)$ as a guide for what to do with more general algebras.

Taking a highest weight state given by $|h\rangle$ and acting on them with Virasoro raising operators (defined formally in Section 4.1.2). For the purposes of this section we will consider their action as being analogous to the $SU(2)$ operators. Taking a highest-weight state and acting on it with a raising operator we require that $L_1\phi(0)|0\rangle = L_1|h\rangle = 0$, meaning there is no higher than highest weight in the representation. On the other end an analogous situation occurs, where an application of L_{-1} on the minimum-weight state annihilates the state. Taking a generic weight h' the operators have the following action on the state:¹²

$$\begin{aligned} L_0|h'\rangle &= h'|h'\rangle, \\ L_0(L_{-1}|h'\rangle) &= L_0|h' - 1\rangle = (h' - 1)|h' - 1\rangle, \\ L_0(L_1|h'\rangle) &= L_0|h' + 1\rangle = (h' + 1)|h' + 1\rangle. \end{aligned}$$

¹²We assume that h' is not the highest or lowest weight when acting with the raising and lowering operators respectively.

These operators obey a similar algebra as the quantum operators in equation (2.9); however, they have a sign change:

$$[L_+, L_-] = 2L_0, \quad [L_z, L_{\pm}] = \pm L_{\pm}.$$

Highest-weights in $SU(2)$ can be thought of as just a number, but more generally highest-weights are vectors [20]. These highest weight vectors are specified by $N - 1$ integer coefficients called the Dynkin labels. The eigenvalues of L_0 are used to label a basis of the highest-weight system. We can reuse what we know about $SU(2)$ in order to build more general weight representations by ‘combining’ $SU(2)$ groups, along with an additional couplings between labels [3].

This process is achieved by considering the algebra of the $SU(2)$ group, denoted $su(2)$, as building up more general algebras. We begin by defining the Abelian sub-algebra $g_{\alpha} = su(2) \subset g$ of g , where g is the total Abelian algebra written as a direct sum of these g_{α} along with a coupling. That g is Abelian sub-algebra follows from the direct sums being abelian operators, meaning that they can be reordered without conflict. We join these with the Cartan space \mathcal{A} :

$$g = \mathcal{A} \oplus \left(\bigoplus g_{\pm\alpha} \right). \quad (2.13)$$

The Cartan space defines couplings between the subalgebras and we note that \mathcal{A} commutes with the sub-algebras.

Root spaces $g_{\pm\alpha}$ are one dimensional and generated by the root vectors $e_{\alpha} \in g_{+\alpha}$ and $f_{\alpha} \in g_{-\alpha}$. From these two root vectors we can introduce the co-roots $h_{\alpha} = [e_{\alpha}, f_{\alpha}]$, which span \mathcal{A} . Simple roots are root vectors that cannot be written as sums of other root vectors and we identify them as α_i . Co-roots are defined in terms of these simple

roots as:

$$\alpha^\vee = h_\alpha = \frac{2}{(\alpha, \alpha)} \alpha. \quad (2.14)$$

The action of \mathcal{A} leaves the roots spaces $g_\alpha := g_{+\alpha} \oplus g_{-\alpha}$ unaffected and so taking an element $X \in g_\alpha$ and $A \in \mathcal{A}$ the weights can then be written in terms of an adjoint representation $[A, X] = \alpha(A) \cdot X$ [14], which we saw when considering $SU(2)$ as $[\hat{J}_z, \hat{J}_\pm] = (\pm 1) \hat{J}_\pm$. This analogy with $SU(2)$ should clarify that these $\alpha(A)$ are eigenvalues corresponding to the weight that labels the state. A representation of the root space g_α , denoted V_α can be taken and summed into a single space:

$$V = \bigoplus V_\alpha. \quad (2.15)$$

The number of V_α will be equal to the number of g_α .

We can now formally introduce the notion of a ‘highest weight vector’ $v \in V_\alpha$ with the condition that for any $A \in \mathcal{A}$ and element in the dual space $\alpha \in \mathcal{A}^*$ then we have the following:

$$H(v) = \alpha(H) \cdot v \quad (2.16)$$

These $\alpha(A)$ are the resulting eigenvalues from a diagonalized set of elements $A \in \mathcal{A}$, which we identify as being the weight. Root spaces allow us to move down the weight space specified by the highest-weight vector v . A simple root $\alpha_\beta \in g_\beta$ has the following action $g_\beta : V_\alpha \rightarrow V_{\alpha+\beta}$.

Consideration of a space \mathcal{A}^* , dual to the co-root space \mathcal{A} , we can introduce the fundamental weights Λ^i . Due to the dual nature of these two spaces there will be an equal number of fundamental weights as co-roots. Stated another way, we require that for every simple co-root α_j^\vee and fundamental weight Λ^i then the bilinear product

$\alpha_j^\vee \cdot \Lambda^i = \delta_j^i$. For the simple Lie group $SU(N)$ the simple co-roots α_j^\vee are identical to the simple roots α_j . This identification motivates our abuse of terminology and we refer to the simple co-roots as simple roots, unless otherwise indicated.

An important class of weights λ can be identified as those weights that can be written as a non-negative linear combination of fundamental weights, and are called the dominant weights. The total set of dominant weights is called the Weyl chamber or the fundamental Weyl chamber, which will later be turned into the Weyl alcove by a truncation (see Section 4.1.3). Notably, all valid highest-weights will be also be dominant weights.

Weights λ are usually notated with the Dynkin labels, which are coefficients that indicate the number of fundamental weights that compose λ . For $SU(N)$ the fundamental weights in terms of Dynkin labels are written $[1, 0, 0 \dots 0] = \Lambda^1$, which can be transformed into co-root or dual Dynkin label notation as: $\frac{1}{N-1}\{N-1, N-2, \dots, 1\} = \Lambda^1$. Cartan matrices can be used to transform between these two notations and have their horizontal entries given as simple roots written in Dynkin label notation, see for example equation (2.18).

The dual relation between fundamental weights and simple roots can be utilized in computing bilinear products, by switching between Dynkin and dual Dynkin label notations. General bilinear products can be defined in terms of the dual Dynkin labels μ^i , noting the upper index, and the Dynkin labels λ_i , noting the lowered indices, as:

$$\{\mu^1, \dots, \mu^{N-1}\} \cdot [\lambda_1, \dots, \lambda_{N-1}] = \mu^1 \lambda_1 + \dots + \mu^{N-1} \lambda_{N-1} = (\mu, \lambda). \quad (2.17)$$

Though the Dynkin label notation is often used both Dynkin and dual Dynkin labels can be used to denote equivalent weights.

Highest-weight representations are an example of a particularly important type of representation called irreducible representations, or irreps.

Definition 5. *An irrep is a representation that cannot be written in terms of a direct sum of other representations. Alternatively an irrep is a representation that contains within it no non-trivial representations closed under the action.*

Irreps can often be used to identify physical classifications or properties based on symmetry. A particularly notable example of this is from Gell–Mann’s treatment of baryonic particles forming a representation of $SU(3)$, where the irreps resulted in classes of hadronic particles. With this treatment one can identify the irreps emerging from the combination of quark states with classes of baryonic particles.

2.2.1 $SU(3)$ Weight Representation

In order to clarify the role of roots and Dynkin labels in a highest-weight representation it is useful to go through an example that exhibits more general properties. To this end we consider representations of $SU(3)$, which is the next simplest group after $SU(2)$ and is, similarly, an important Lie group for physics. Historically, $SU(3)$ was used as an approximate symmetry for hadronic nuclear physics and in modern physics it is used as the gauge group for quantum chromodynamics (QCD).

Example 3. *Take $SU(3)$ as our group and $v = [1, 1]$ as our highest-weight vector. $SU(3)$ has a more complicated structure than $SU(2)$, whose weights could be constructed by adding and subtracting integer values. For $SU(3)$ the gaps between weights in a highest-weight representation are accounted for by the simple roots, given by $\alpha_1 = [2, -1]$ and $\alpha_2 = [-1, 2]$ in the Dynkin label notation. Additionally the Cartan matrix A , which can be used to transform between the dual Dynkin labels, which are equal to the number of roots required to form a weight, and the Dynkin label notation.*

$$A = \begin{pmatrix} 2 & -1 \\ -1 & 2 \end{pmatrix} \quad (2.18)$$

Simple roots act on the highest-weight state in order to decrease it and in so doing we construct the weight system of the highest-weight representation. Noting that $[0, 0]$ actually appears twice in the highest weight system; we say that it has a weight multiplicity of 2. The Dynkin and dual Dynkin label notations are distinguished by their brackets $[\dots]$ and $\{\dots\}$, respectively. Drawing the highest weight system and using the Cartan matrix to transform between the two notations, we find:

$$\begin{array}{cccc}
 & [1, 1] & & \{1, 1\} \\
 [2, -1] & & [-1, 2] & \{1, 0\} & & \{0, 1\} \\
 & 2 \times [0, 0] & \simeq & 2 \times \{0, 0\} & & \\
 [1, -2] & & [-2, 1] & \{-1, 0\} & & \{0, -1\} \\
 & [-1, -1] & & \{-1, -1\} & &
 \end{array}$$

Example 4. As a second example, we can consider the highest-weight representation specified by $[3, 0]$. Looking at the resulting weight system and the action of the simple roots on the weights there are a couple of notable characteristics. First, the simple roots can be imagined as discrete shifts in a direction and second, not all combinations of roots are valid elements of the highest weight system. We draw out the highest-weight representation below (all weight multiplicities are 1 in this case):

$$\begin{array}{cccc}
 [3, 0] & & & \\
 & [1, 1] & & \\
 [2, -1] & & [-1, 2] & \\
 & [0, 0] & & [-3, 3] \\
 [1, -2] & & [-2, 1] & \\
 & [-1, -1] & & \\
 [0, -3] & & &
 \end{array}$$

Similarly, and expectedly, the representations containing the possible states are uniquely specified by the highest weight element.

There are symmetries present between weight elements of the highest-weight representation, among these the Weyl reflections are the most basic. In our example if we draw lines crossing through the $[0, 0]$ weight and normal to the simple root vectors, then weights on either side might be noted as related by reflection. By combining reflection elements we can relate group elements with one another, which can be used to break the group in ‘Weyl orbits.’ We consider the Weyl orbits of the adjoint highest-weight representation ($R([1, 1])$) in Figure 2.1.

2.2.2 Weyl Group

In the examples of highest-weight representations of the $SU(3)$ Lie groups we saw that there was a great deal of structure in the diagrams. This structure permits us to define a symmetry between weights, where are related to the other by a series of reflections. Graphing the weights of the Lie group on a diagram, the simple root vectors will be normal to hyperplanes, around which the reflections occur. Those primitive reflections that relate weights to one another generate the Weyl group.

Interpreting the Weyl group as being generated by a series of primitive reflections lets us identify the Weyl group with the symmetric group. $SU(3)$ has 2 simple roots, so the Weyl group W_3 of $SU(3)$ is generated by two reflections $W_3 = \langle \omega_1, \omega_2 \rangle$.¹³ From our discrete group example it is not difficult find that: $S_3 \simeq W_3 = \langle \omega_1, \omega_2 \rangle$.

More important to us is the way that the Weyl elements act on the weights of the highest-weight representation. By treating the Weyl group explicitly as a set of reflections we can write them down in a straightforwardly geometric fashion. With the only remaining subtlety being the appropriate normalization of the simple roots in order to properly reflect the weight element. A simple Weyl group element’s action

¹³The notation $\langle a_1, a_2 \dots a_m \rangle$, we remind ourselves, is used to indicate the group generated by the elements a_i .

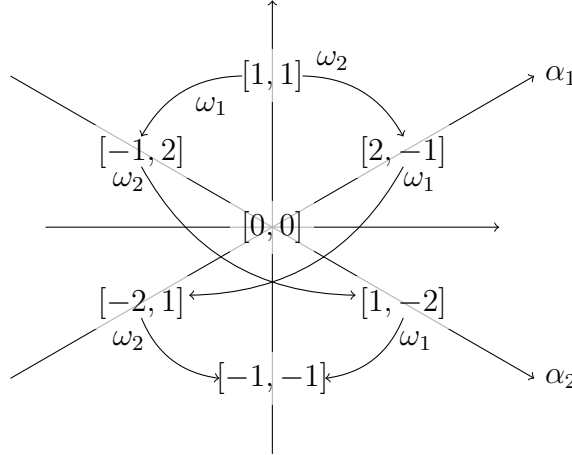


Figure 2.1: Weight diagram for $SU(3)$ of the highest-weight representation $[1, 1]$, along with the Weyl group reflections marked on the relevant weights.

on an arbitrary weight is written below:

$$\omega_i(\lambda) = \lambda - 2 \frac{(\alpha_i \cdot \lambda)}{(\alpha_i \cdot \alpha_i)} \alpha_i, \quad (2.19)$$

where the notation $(\lambda \cdot \alpha_i)$ is the bilinear product.

So there are $|W_N| = |S_N| = N!$ Weyl elements, which are written in terms of primitive reflections. As in the S_3 example it is possible for the same Weyl element to be expressible more than one way in terms of simple reflections. For example, the Weyl group for $SU(3)$ has a single longest reflection that corresponds to a negative conjugate transform $-C = \omega_1\omega_2\omega_1 = \omega_2\omega_1\omega_2$. The conjugate transform has the action $C[\lambda_1, \lambda_2] \rightarrow [\lambda_2, \lambda_1]$ on a general weight in $SU(3)$. More generally, one can write the conjugation of a weight λ in $SU(N)$ as being: $[\lambda_1, \dots, \lambda_{N-1}] \rightarrow [\lambda_{N-1}, \dots, \lambda_1]$.

Considering the action of the Weyl group on the highest-weight representation we can construct a set of orbits, which are the weights that transform into one another under the Weyl action. For example we can take Weyl orbit of the adjoint

representation of $SU(3)$ from Figure 2.1. We see there are two distinct Weyl orbits:

$$W[1, 1] = \{[1, 1], [2, -1], [-1, 2], [-2, 1], [1, -2], [-1, -1]\}, W[0, 0] = \{[0, 0]\}. \quad (2.20)$$

That the zero weight is the only element in its Weyl orbit should not come as a surprise. These Weyl orbits let us decompose the weight system of a highest-weight representation into non-intersecting sets. We can then consider the weight system as being the union of the resulting sets:

$$P([1, 1]) = W[1, 1] \cup W[0, 0], \quad (2.21)$$

$$P([1, 1])/W := \{[1, 1], [0, 0]\}. \quad (2.22)$$

$P(\lambda)/W$ being defined to mean those dominant weights of a highest-weight representation that label unique Weyl orbits. That is for an element $\mu \in P(\lambda)$ then we say that every $\sigma \in W\mu$ is labelled by μ in $P(\lambda)/W$.

Weyl orbits of distinct dominant weight are disjoint with respect to one another. Multiplicities of the dominant weights labelling the various Weyl orbits, will be the same as the multiplicities of each weight within the respective Weyl orbit. This follows based on the Weyl orbit completely decomposing the weight system, which requires that all weights be accounted for in the decomposition process.

Thus far we have only consider how to represent groups and have treated these representations as static objects. In physics, however, we are interested in systems that are dynamic and changing. Utilization of groups and representations for more dynamic scenarios requires an additional piece, which we introduce in the next chapter. This is done by determining an operation that will combine group representations, called the tensor product.

Chapter 3

Tensor Products

Tensor products are ubiquitous in physics and are important in this thesis due to their connection with the fusion product. Acting on group representations, the tensor product operation takes two or more representations and produces a third resultant representation.¹ Physical systems that correspond to some representation of a group can be combined via the tensor product to build up more complicated systems. A concrete example of this is the case of quantum angular momentum, described by representations of $SU(2)$. Tensor products account for the mathematical rules of quantum angular momentum addition.

In general, the representation resulting from a tensor product is a reducible one, meaning that it can be written as a direct sum of irreps. Decomposition of a reducible representation is, in general, non-trivial. One obtains a direct sum of irreps and a set of multiplicities that count how often an irrep appears. Those multiplicities that appear in the decomposition of a tensor product are called the tensor product multiplicities. For any decomposition the multiplicities are non-zero only for finitely many irreps, meaning that any reducible representation can be written as a direct sum of a finite number of irreps.

Our primary interest is in giving an account of the tensor product multiplicities that emerge after the decomposition of the tensor products resultant reducible representation. These descriptions can then later be adapted to the case of the fusion product. Tensor product multiplicities are uniquely specified by the two original representations and the resultant irrep. Often the terminology ‘tensor product’ is abused so that a reference to the tensor product assumes that a decomposition is also being performed. Assumption of the decomposition process when referring to the tensor product will be standard throughout this thesis, unless otherwise specified.

¹This third representation resulting from the tensor product will be a representation of the same Lie group, but generally not an irrep.

3.1 Combining Representations

A highest-weight representation of a Lie group G can be written, based on Section 2.2, by specifying a highest-weight. For $SU(2)$, the maximum value of J determined the highest weight and the \hat{J}_z operators corresponded to the possible projections onto the z -axis. These two sets of diagonalized eigenvalues, the z -axis projection of the angular momentum and the maximum angular momentum, were used to furnish a set of states. $SU(2)$ is the simplest possible example of a highest-weight representation.

Two highest-weight representations of a simple Lie group can be combined by use of the tensor product, which can be understood as accounting for how two or more subsystems interact. Tensor product multiplicities are non-negative integers—being zero only when the irrep is not present in the decomposition. Take the arbitrary weights λ, λ' , and λ'' as highest-weights identifying a representation of some Lie group G . Introducing coefficients C , which denote the tensor-product multiplicities, a formula for the tensor product is:

$$R(\lambda) \otimes R(\lambda') \hookrightarrow \bigoplus_{\lambda''} C_{\lambda, \lambda'}^{\lambda''} R(\lambda''). \quad (3.1)$$

From this formula we can deduce the following properties of the tensor product multiplicities, based on the behaviour of the direct sums and how representations combine.

- Direct sums, and as a result the tensor products, are distributive, associative, and commutative. From these properties it must follow that the indices in the tensor product multiplicities can be reordered: $C_{\lambda, \lambda'}^{\lambda''} = C_{\lambda', \lambda}^{\lambda''}$.
- There are infinitely many possible highest-weight representations $R(\lambda)$, but the coefficient is non-zero in equation (3.1) only for a finite number of irreps $R(\lambda'')$.
- $R(0)$ acts like the identity for the tensor product, such that $C_{\lambda, 0}^{\lambda''} = \delta_{\lambda}^{\lambda''}$.

- For every representation $R(\lambda)$ there is a unique conjugate representation $R(\lambda)^\dagger = R(\lambda^\dagger)$. Combining this with the identity condition we have $C_{\lambda,0}^{\lambda^\dagger} = \delta_\lambda^{\lambda^\dagger} = 1$. The zero highest-weight representation $R(0)$, which is its own conjugate, will always appear in a tensor product of a highest-weight representation and its conjugate.
- When the conjugate of every weight is taken then the tensor product multiplicity is unchanged $C_{\lambda,\lambda'}^{\lambda''} = C_{\lambda^\dagger,\lambda'^\dagger}^{\lambda''^\dagger}$.

Finding where the tensor product multiplicities $C_{\lambda,\lambda'}^{\lambda''} \neq 0$ is an easier task than calculating all possible $C_{\lambda,\lambda'}^{\lambda''}$ outright. Computing $C_{\lambda,\lambda'}^{\lambda''}$ can be done by hand for suitably simple cases,² where the dimension and number of weight states in a representation is fairly small. For representations containing many states, computing tensor product multiplicities by hand is substantially more difficult, although algorithms exist to do so allowing the value to be obtained from computer calculation. Several general methods for computing the tensor product multiplicities exist and can be written in terms of combinatorial arguments. Combinatorial arguments are important in that they count fundamental objects and so provide a great deal of insight into the multiplicities that they compute.

3.1.1 Utility of the Tensor Product

Taking the tensor product of two representations, labelled by the highest weights λ and μ , we obtain a third representation. This resulting representation is then decomposed into a direct sum over a set of irreps with their highest-weights denoted ν . Each individual irrep comes with a corresponding tensor product multiplicity, written as $C_{\lambda,\mu}^\nu$. Two of these indices are fixed by the representations being combined, and the ν index specifies the irrep that is part of the tensor product. Irreps can be used to account for possible substates within a larger system and have physical consequences.

²These calculations for $SU(2)$ are a rite of passage in most introductory quantum mechanics classes.

We will note several examples of these subsystems, particularly in Section 3.2.2, where they can be used to account for classes of baryons. Physical consequences of these irreps makes it clear that the tensor product and its decomposition are more than just mathematical abstractions.

The simplest case of the tensor product is in its application to quantum angular momentum, where we are considering representations of $SU(2)$. Taking a particle with some angular momentum \vec{J} we can consider the physical states. Based on the raising and lowering operators defined in Section 2.1.3 we note that J plays the role of a highest weight. We record the angular momentum states in the form $|2J, 2m\rangle$, which are twice the value of the eigenvalues of the simultaneously diagonalized operators as in equation (3.2) in order to avoid $\frac{1}{2}$ -integers. When notating a representation of $SU(2)$ with Dynkin labels, $[2J]$ denotes the highest-weight and $2m$ are the constituent weights within the highest-weight representation.³

$$\vec{J}^2 |2J, 2m\rangle = 2J(2J + 2) |2J, 2m\rangle \quad \hat{J}_z |2J, 2m\rangle = 2m |2J, 2m\rangle \quad (3.2)$$

Interpreting the $2J$ physically, they are simply twice value of the labels in the physics notation, so are again just the projection along the z -axis and the maximum angular momentum of an irrep. So we can write a highest weight representation in terms of the Dynkin labels as $P([2J]) = \{|2J, 2J\rangle, |2J, 2(J - 1)\rangle, \dots, |2J, 0\rangle, \dots |2J, -2J\rangle\}$. The states in $P([2J])$ are obtained via repeated application of the lowering operators on the highest-weight state $|2J, 2J\rangle$.

Raising and lowering operators can be used to great effect in determining the behaviour of quantum angular momentum addition. We will consider such a case and later demonstrate that the tensor product reproduces the result. As an example we consider the case of two spin- $\frac{1}{2}$ particles.

³Using the natural unit convention of $\bar{h} = 1$ so that the eigenvalues are integer valued.

Example 5. Each $\text{spin}-\frac{1}{2}$ particle is described by the highest-weight representation $P([1]) = \{|1, 1\rangle, |1, -1\rangle\}$. Combining two such $\text{spin}-\frac{1}{2}$ particles requires that we account for all the ways that the two angular momentum states might add together. We introduce a basis of $R([1]) \otimes R([1])$:

$$\{|1, 1\rangle \otimes |1, 1\rangle, |1, -1\rangle \otimes |1, 1\rangle, |1, 1\rangle \otimes |1, -1\rangle, |1, -1\rangle \otimes |1, -1\rangle\}.$$

This can be decomposed as basis of $SU(2)_{\text{Diag}} \supset SU(2) \otimes SU(2)$ invariant subspace:

$$\begin{aligned} & \{|1, 1\rangle \otimes |1, 1\rangle, \frac{1}{\sqrt{2}}(|1, 1\rangle \otimes |1, -1\rangle + |1, -1\rangle \otimes |1, 1\rangle), \\ & \frac{1}{\sqrt{2}}(|1, 1\rangle \otimes |1, -1\rangle - |1, -1\rangle \otimes |1, 1\rangle), |1, -1\rangle \otimes |1, -1\rangle\}. \end{aligned}$$

One can find that the individual products result in the following states:

$$|1, 1\rangle \otimes |1, 1\rangle \hookrightarrow |2, 2\rangle, \quad (3.3)$$

$$|1, -1\rangle \otimes |1, 1\rangle \hookrightarrow |2, 0\rangle + |0, 0\rangle, \quad (3.4)$$

$$|1, -1\rangle \otimes |1, -1\rangle \hookrightarrow |2, -2\rangle. \quad (3.5)$$

Equation (3.4) is noted as accounting for the two equivalent possibilities of $|1, -1\rangle \otimes |1, 1\rangle$ and $|1, 1\rangle \otimes |1, -1\rangle$. Combining these individual results we can then write the tensor product decomposition of a state as:

$$\begin{aligned} & \frac{1}{\sqrt{2}}(|1, 1\rangle + |1, -1\rangle) \otimes \frac{1}{\sqrt{2}}(|1, 1\rangle + |1, -1\rangle) = \{|1, 1\rangle \otimes |1, 1\rangle + (|1, 1\rangle \otimes |1, -1\rangle) + \\ & + \frac{1}{2}(|1, 1\rangle \otimes |1, -1\rangle - |1, -1\rangle \otimes |1, 1\rangle) + |1, -1\rangle \otimes |1, -1\rangle\} \\ & \hookrightarrow \frac{1}{2}(|2, 2\rangle + |2, 0\rangle + |2, -2\rangle) + \frac{1}{2}(|0, 0\rangle) \end{aligned} \quad (3.6)$$

This result can be written more succinctly by writing the states in terms of highest-

weight representations ($[H]$). Combining the first set of weights as $P([2]) = \{ | 2, 2 \rangle, | 2, 0 \rangle, | 2, -2 \rangle \}$ and the second as $P([0]) = \{ | 0, 0 \rangle \}$ we obtain:

$$R([1]) \otimes R([1]) \hookrightarrow R([2]) \oplus R([0]).$$

For this example we note that the tensor product multiplicities are $C_{[1],[1]}^{[2]} = C_{[1],[1]}^{[0]} = 1$, with all other multiplicities being zero. These two new irreps on the RHS can be interpreted as possible subsystems. In particular the total system can be thought of as being composed of: $R([0])$, a zero angular momentum state, and $R([2])$ being an angular momentum $J = 1$ state. Interpreting constituent irreps as being physical sub-systems is useful for understanding a variety of phenomena.

Tensor product multiplicities of $SU(2)$ are sometimes called the Clebsch-Gordan series coefficients [18], for which there are general series solutions. Tensor products are applicable not only to $SU(2)$, but to more general groups as well.

Tensor product multiplicities can be calculated on their own and matched up with their relevant irreps, which is useful when we want information about a specific sub-state. Even in the $SU(2)$ case the computation can be quite difficult. There are many methods that can be used to account for the tensor product multiplicities, among them are the algorithm involving Berenstein-Zelevinsky triangles (BZ triangles) [2], and the Littlewood-Richardson (LR) rule [28].

3.2 Young Tableaux for $SU(N)$

In order to talk about the LR rule we first introduce Young tableaux.⁴ This will give us an opportunity to introduce the partition notation for weights, which will be used again in Appendix A.1. Semi-standard Young tableaux (SSYT), are of primary interest since they are a generalization of the standard Young tableaux. Specifically,

⁴‘Tableaux’ is the plural for the singular ‘tableau.’

a Young tableau specifies the highest weight of an $SU(N)$ irrep and the corresponding SSYT label its states. The LR rule and Young tableaux provide a reasonably straightforward method for computing tensor products of $SU(N)$ representations.⁵

SSYT provide us with a simple way to look at tensor product multiplicity calculations and neatly tie them to combinatorial arguments [14]. Originally the Young tableaux were created to study the symmetric groups S_N [49], but Schur-Weyl duality allows us to apply them to representations of $SU(N)$. Schur-Weyl duality is a powerful result from representation theory that provides an isomorphism between representations of $S_N \leftrightarrow SU(N)$.

Before we can use the Young tableaux a connection between them and highest-weights must be established. This is achieved with the introduction of partitions and their correspondence with the Young tableaux.

Definition 6. *A partition of a positive integer n is denoted $(\lambda) = (\lambda_{(1)}, \dots, \lambda_{(L)})$ with $\lambda_{(i)} \in \mathbb{N}_0$. The partition (λ) must satisfy both $\lambda_{(1)} \geq \lambda_{(2)} \geq \dots \geq \lambda_{(L)}$ and $\sum \lambda_{(i)} = n$. When these conditions hold we say that (λ) is a partition of n and write $(\lambda) \vdash n$ with $|(\lambda)| = (\lambda_{(1)} + \dots + \lambda_{(L)}) = n$.*

For a partition $(\lambda) = (\lambda_{(1)}, \dots, \lambda_{(L)})$ then $\lambda_{(i)}$ is said to be the i^{th} ‘part’ of the partition and L is the length of the partition.

Comparing two or more partitions cannot always be done, since it requires that $|(\lambda)| = |(\mu)|$. A partial ordering called the dominance ordering can be imposed in the case that the two partitions are comparable.

Definition 7. *We say a partition (μ) dominates a partition (λ) when the parts satisfy:*

$$\mu_{(1)} + \dots + \mu_{(L')} \geq \lambda_{(1)} + \dots + \lambda_{(L')},$$

⁵We are primarily considered with their applications to $SU(N)$, but it is possible to general the Young tableaux further in order to account for representations of other simple Lie groups [25].

for all L' less than or equal to the length L of the partition.

We write $(\lambda) \trianglelefteq (\mu)$ when (λ) is dominated by (μ) . $|(\lambda)| = \sum \lambda_{(i)} = n$ is taken to be shorthand for the sum of all parts of the partition (λ) , n being the integer that the partition is built from. Having established notation for partitions we can connect them with the Young tableaux.

Definition 8. *Writing a partition $(\lambda) \vdash n$, it can be identified with the ‘shape’ of a Young tableau, where the tableau will have a number of boxes in its i^{th} row equal the i^{th} part $\lambda_{(i)} \in (\lambda)$.*

For example the tableau resulting from a shape $(\lambda) = (3, 2, 1, 1) \vdash 7$ is:⁶

$$T(3, 2, 1, 1) = \begin{array}{|c|c|c|} \hline \square & \square & \square \\ \hline \square & \square & \\ \hline \square & & \\ \hline \square & & \\ \hline \end{array} \quad (3.7)$$

In order to make clear the distinction between a tableau and the partition giving its shape, the tableaux are denoted by $T(\lambda)$.

There is a one-to-one map from the partitions of n to Young tableaux with n boxes. Dominance ordering on the partitions imposes a partial ordering on the Young tableaux, which results in a Hasse diagram [49] involving every possible partition of a positive integer.

Partitions can be used to account for a second property of the Young tableaux called the content. Content tells us about the integers that are used to fill the boxes of a Young tableaux, subject to certain rules, and distinguish SSYT from the filling of a standard Young tableaux. A valid filling for SSYT has integers increasing weakly along the rows, from left to right; and strictly increasing as one descends a column from top to bottom.

⁶We are using the English notion as our convention, which has the boxes descending, but could just as easily use the French notation, the difference being that the boxes would instead ascend.

Definition 9. A partition $(\mu) \vdash n$ is called the content of an n -box Young tableau when the part $\mu_{(i)}$ is the number of times that the integer ‘ i ’ appears in the filling of the Young tableau.

Unlike the shape of a tableaux the content is not unique. Furthermore, there can be multiple fillings of a SSYT permitted by a given content. We can associate a multiplicity, called the Kostka number, to these fillings when given a specific shape and a content. Kostka numbers count the possible SSYT fillings permitted by the content and shape. Due to the Schur-Weyl duality these are in fact the weight multiplicities as they appear in the highest-weight representation; this equality is recorded in equation (3.9).

Example 6. Taking the partition $(3, 1, 1)$ as content this defines any filling consisting of three 1’s, one 2, and one 3. For tableau $T(4, 1)$ we find that there are two possible ways to fill the tableau with the content $(3, 1, 1)$. The two valid SSYT are:

$$\begin{array}{|c|c|c|c|} \hline 1 & 1 & 1 & 2 \\ \hline 3 & & & \\ \hline \end{array}, \quad \begin{array}{|c|c|c|c|} \hline 1 & 1 & 1 & 3 \\ \hline 2 & & & \\ \hline \end{array}.$$

When computing a Kostka number we know immediately that a tableau $T(\lambda)$ with a content λ will have a Kostka number $K_{(\lambda),(\lambda)} = 1$. From the filling definition of the Kostka number we know that any content μ that is not dominated by λ will result in $K_{(\lambda),(\mu)} = 0$.

Definition 10. Given two partitions $(\lambda), (\mu)$ of the same integer n , then the Kostka number $K_{(\lambda),(\mu)}$ gives the number of SSYT of shape (λ) with content (μ) . Kostka numbers $K_{(\lambda),(\mu)}$ are zero unless $(\mu) \trianglelefteq (\lambda)$.

Kostka numbers are equal to the weight multiplicities in an $SU(N)$ highest-weight representation. This equivalence indicates that the weights in the highest-weight representation can be identified with partitions and vice-versa. For weights in a

highest-weight representation of $SU(N)$ the weights and partitions are related by:

$$\lambda = [\lambda_1, \lambda_2, \dots, \lambda_{N-1}] := \left(\sum_{i=1}^{N-1} \lambda_i, \sum_{i=2}^{N-1} \lambda_i, \dots, \lambda_{N-1} \right) = (\lambda). \quad (3.8)$$

This equivalence is a consequence of the Schur-Weyl duality, which relates irreps of the general linear group to irreps of the symmetric group. This duality underpins the use of SSYT as irreps of $SU(N)$ and other simple Lie groups [25]. For weight multiplicities of some highest-weight representation $R(\lambda)$ of $SU(N)$ and weight system $P(\lambda)$ then for a weight $\mu \in P(\lambda)$ we have:

$$\text{mult}_\lambda(\mu) = K_{(\lambda),(\mu)}. \quad (3.9)$$

3.2.1 The Hook Formula

There are a number of notable properties of the Young tableau, a particularly interesting one being the hook formula. The hook formula computes the dimension of the irrep corresponding to a SSYT in a surprisingly simple way. The dimension of an irrep will be equal to the number valid SSYT, $|T(\lambda)|$:

$$|T(\lambda)| = \text{Dim}(R(\lambda)), \quad (3.10)$$

which is an identification that follows from Schur-Weyl duality

To get to the hook formula it is necessary to introduce the notion of a ‘hook.’ A hook is a straight line drawn through boxes in the Young tableau with a right turn in a ‘corner’ box, marked by x in (3.11). An example tableau $T(4, 3, 1)$ demonstrates

a single hook:⁷

$$\begin{array}{|c|c|c|c|} \hline & x & h & h \\ \hline & h & & \\ \hline & & & \\ \hline \end{array} . \tag{3.11}$$

The hook length $h_\lambda(x)$ is defined to be the number of boxes that a hook passes through with its corner in the box x . So for the example tableau (3.11), the hook length for the example corner box x is $h_\lambda(x) = 4$. Finding the hook length of each corner box we can write the following, with the relevant hook length inserted into the relevant boxes:

$$\begin{array}{|c|c|c|c|} \hline 6 & 4 & 3 & 1 \\ \hline 4 & 2 & 1 & \\ \hline 1 & & & \\ \hline \end{array} . \tag{3.12}$$

Now we introduce a second set of integers $F(u)$, which are associated with a box ‘ u ’ of the Young tableau. Labelling the top left hand box with an integer equal to the rank+1 of the group and increment +1 for a movement to the right and -1 for each movement down. Using the example tableau (3.11) again, and taking it to be a highest-weight representation for $SU(4)$:⁸

$$\begin{array}{|c|c|c|c|} \hline 4 & 5 & 6 & 7 \\ \hline 3 & 4 & 5 & \\ \hline 2 & & & \\ \hline \end{array} \tag{3.13}$$

Combining these two definitions we can write down the hook length formula [17] for the $SU(N)$ irreps:

$$|\mathbb{T}(\lambda)| = \frac{\prod_{u \in \mathbb{T}(\lambda)} F(u)}{\prod_{x \in \mathbb{T}(\lambda)} h_\lambda(x)}. \tag{3.14}$$

This useful formula is also called the factoring hooks rule [17].

⁷Using equation (3.8), the Dynkin label notation of this partition is $[1, 2, 1]$.

⁸We could also have written this tableau for a highest-weight element of a representation of $SU(8)$, although the values for $F(u)$ would begin at 8 instead of 4.

Making use of the formula with our example tableau we can make use of (3.14) to find the dimension of the irrep:

$$\text{Dim}(T(4, 3, 1)) = \frac{4 \cdot 5 \cdot 6 \cdot 7 \cdot 3 \cdot 4 \cdot 5 \cdot 2}{6 \cdot 4 \cdot 3 \cdot 1 \cdot 4 \cdot 2 \cdot 1 \cdot 1} = 175 \quad (3.15)$$

3.2.2 SSYT and Tensor Products

Our purpose in introducing the Young tableaux was for their application to computing tensor products. Schur-Weyl duality indicates that the SSYT should have their product whose behaviour reproduces the tensor product of irreps. Again, we note that we are primarily concerned with the tensor product in the case of $SU(N)$ and so make use of equation (3.8), rewritten below for convenience:

$$\lambda = [\lambda_1, \lambda_2, \dots, \lambda_{N-1}] := \left(\sum_{i=1}^{N-1} \lambda_i, \sum_{i=2}^{N-1} \lambda_i, \dots, \lambda_{N-1} \right) = (\lambda). \quad (3.16)$$

Noting that the round brackets denote a partition and that the square brackets denote Dynkin labels.

Dynkin label notation can be used to write the fundamental ‘quark and anti-quark’ $SU(3)$ representations, as introduced by Gell-Mann, as $[1, 0]$ and $[0, 1]$ respectively. Their tensor product is:

$$\begin{aligned} [1, 0] \otimes [0, 1] &= [1, 1] \oplus [0, 0], \\ 3 \times \bar{3} &= 8 + 1. \end{aligned} \quad (3.17)$$

The second line is the product written in terms of the dimension of the irreps of the SSYT. Recasting the problem in terms of SSYT from equation (3.16) we can rewrite the result as a product of Young tableaux. Using the transformation between the

weights and Young tableaux we find the following result:

$$\begin{array}{|c|} \hline \square \\ \hline \square \\ \hline \end{array} \otimes \begin{array}{|c|} \hline \square \\ \hline \square \\ \hline \end{array} = \begin{array}{|c|c|} \hline \square & \square \\ \hline \square & \square \\ \hline \end{array} \oplus \begin{array}{|c|} \hline \square \\ \hline \square \\ \hline \square \\ \hline \end{array}. \tag{3.18}$$

A tableaux with N stacked rows will be equivalent to the zero highest-weight irrep.⁹ This example gives us an indication of how the product of two Young tableaux behaves.

Products of Young tableaux are based on the ways that we can stack the boxes according to a SSYT filling. Valid fillings must have box entries that strictly increase as we move down the column. Label the boxes of Young tableaux the resulting tensor product is done by placing the boxes in a pattern valid for SSYT. This procedure is demonstrated by a more complicated example below, where the unlabelled boxes stay in place.

$$\begin{array}{|c|c|} \hline \square & \square \\ \hline \square & \square \\ \hline \end{array} \otimes \begin{array}{|c|c|} \hline \square & \square \\ \hline \square & \square \\ \hline \end{array} = \begin{array}{|c|c|} \hline \square & \square \\ \hline \square & \square \\ \hline \end{array} \otimes \begin{array}{|c|c|} \hline 1 & 1 \\ \hline 2 & \\ \hline \end{array},$$

$$= \begin{array}{|c|c|c|c|} \hline \square & \square & 1 & 1 \\ \hline \square & 2 & & \\ \hline \end{array} \oplus \begin{array}{|c|c|c|c|} \hline \square & \square & 1 & 1 \\ \hline \square & & & \\ \hline 2 & & & \\ \hline \end{array} \oplus \begin{array}{|c|c|c|} \hline \square & \square & 1 \\ \hline \square & 1 & \\ \hline 2 & & \\ \hline \end{array} \oplus \begin{array}{|c|c|c|} \hline \square & \square & 1 \\ \hline \square & 2 & \\ \hline 1 & & \\ \hline \end{array} \oplus \begin{array}{|c|c|} \hline \square & \square \\ \hline \square & 1 \\ \hline 1 & 2 \\ \hline \end{array} \oplus \begin{array}{|c|c|c|} \hline \square & \square & 1 \\ \hline \square & 1 & 2 \\ \hline & & \\ \hline \end{array},$$

$$[1, 1] \otimes [1, 1] = [2, 2] \oplus [3, 0] \oplus 2[1, 1] \oplus [0, 0] \oplus [0, 3].$$

Alternatively, we can write down the result in terms of the dimension of each irrep. By finding the number of valid SSYT we can also write the result as:

$$8 \times 8 = 27 + 10 + \bar{10} + 8 + 8 + 1.$$

⁹This is a very useful simplifying procedure letting us eliminate any column with N stacked rows. As an example consider the following Young tableau of $SU(4)$:

$$T([0, 0, 1]) = \begin{array}{|c|c|c|} \hline \square & \square & \square \\ \hline \square & \square & \square \\ \hline \square & \square & \square \\ \hline \square & \square & \square \\ \hline \end{array} \simeq \begin{array}{|c|} \hline \square \\ \hline \square \\ \hline \square \\ \hline \end{array}.$$

A particularly famous application of $SU(3)$ was by Gell-Mann, who noticed a relation between baryon number and a combination of strangeness and isospin. To him this suggested that experimentally observed baryons were states of an $SU(3)$ representation. Knowing that we need only specify a highest weight vector, we write $\lambda = [\lambda_1, \lambda_2]$ with $\lambda_1, \lambda_2 \geq 0$ as highest-weight defining an $SU(3)$ representation. Analysing the weight states for a highest-weight representation is more difficult than in the $SU(2)$ case as we saw in Section 2.2.1, since states have spacing based on two simple roots:¹⁰ $\alpha_1 = [2, -1]$ and $\alpha_2 = [-1, 2]$.

A quark has 3 types, identified in the literature as ‘flavors,’ of quarks with relatively low mass, which is important for the validity of the symmetry. The $SU(3)$ weight system of a highest-weight representation defined by highest weight $[1, 0]$ is given by:

$$\begin{array}{cc} [-1, 1] & [1, 0] \\ & [0, -1]. \end{array}$$

These states correspond to, reading left to right and beginning at the top, the strange, up, and down quark states. If three quarks compose a baryon then it should follow that we need to combine three quark representations to obtain the possible baryon states. This is facilitated by taking the tensor product of three $R([1, 0])$ highest-weight representations.

Computing the tensor product of these three representations is not overly difficult, although it is useful to go through. The first step is the standard tensor product and is carried out in the brackets and decompose it:

$$\square \otimes (\square \otimes \square) = \square \otimes \left(\begin{array}{c} \square \\ \square \end{array} \oplus \square \square \right).$$

Then using the distributivity of the tensor product over the direct sum, we obtain a

¹⁰Looking back at the $SU(2)$ case there was only a single simple root that was used to build up the highest-weight representation.

direct sum of tensor products:

$$\square \otimes \left(\begin{array}{|c|} \hline \square \\ \hline \square \\ \hline \end{array} \oplus \begin{array}{|c|c|} \hline \square & \square \\ \hline \end{array} \right) = \left(\square \otimes \begin{array}{|c|} \hline \square \\ \hline \square \\ \hline \end{array} \right) \oplus \left(\begin{array}{|c|} \hline \square \\ \hline \square \\ \hline \end{array} \oplus \begin{array}{|c|c|} \hline \square & \square \\ \hline \end{array} \right).$$

Finding the decompositions of these tensor products leaves us with our final result:

$$\left(\square \otimes \begin{array}{|c|} \hline \square \\ \hline \square \\ \hline \end{array} \right) \oplus \left(\begin{array}{|c|} \hline \square \\ \hline \square \\ \hline \end{array} \oplus \begin{array}{|c|c|} \hline \square & \square \\ \hline \end{array} \right) = \begin{array}{|c|c|} \hline \square & \square \\ \hline \square & \square \\ \hline \end{array} \oplus \begin{array}{|c|} \hline \square \\ \hline \square \\ \hline \square \\ \hline \end{array} \oplus \begin{array}{|c|c|c|} \hline \square & \square & \square \\ \hline \end{array} \oplus \begin{array}{|c|c|} \hline \square & \square \\ \hline \square & \square \\ \hline \end{array}.$$

On reordering we find the final result:

$$\square \otimes \square \otimes \square = \begin{array}{|c|c|c|} \hline \square & \square & \square \\ \hline \end{array} \oplus 2 \begin{array}{|c|c|} \hline \square & \square \\ \hline \square & \square \\ \hline \end{array} \oplus \begin{array}{|c|} \hline \square \\ \hline \square \\ \hline \square \\ \hline \end{array}. \quad (3.19)$$

As a final step we calculate the hook length, observing that the dimension corresponds to the possible particles in each of the possible quark arrangements.

$$3 \otimes 3 \otimes 3 = 10 \oplus 8 \oplus \bar{8} \oplus 1.$$

Alternatively, in Dynkin label notation, the tensor product takes the following form:

$$R([1, 0]) \otimes R([1, 0]) \otimes R([1, 0]) = R([3, 0]) \oplus 2R([1, 1]) \oplus R([0, 0]). \quad (3.20)$$

Gell-Mann was able to use his, at the time, conjectured quarks to account for already observed particles and predict an additional resonance particle, which would be found shortly after publication of his paper [16].¹¹ Irreps resulting from the tensor products of the quarks group certain physical states together; these particles have comparable masses, which allows for the partial symmetry to emerge.

¹¹Notably, the experimenters who found this new hadronic resonance were not aware of his prediction before obtaining their result.

3.2.3 Littlewood-Richardson Coefficients

Having seen how the SSYT can be applied to the tensor product it is useful to introduce an alternative account for the tensor product multiplicities, the LR-coefficients. Equal to the tensor product multiplicities for $SU(N)$, the LR-coefficients give an explicitly combinatorial account of the multiplicities. Given two Young tableau with shapes (μ) and (ν) we have:

$$T(\mu) \otimes T(\nu) = \sum_{\gamma} \mathcal{L}_{\mu,\nu}^{\gamma} T(\gamma), \tag{3.21}$$

the LR-coefficients $\mathcal{L}_{\mu,\nu}^{\gamma}$ are equal to the tensor-product multiplicities $C_{\mu,\nu}^{\gamma}$ of equation (3.1). We consider the LR rule for the case of $SU(N)$, but like the SSYT it too can be generalized to other simple Lie groups [28].

We consider another example with $(\mu) = (1, 1)$, $(\nu) = (2, 2)$ as highest-weight representations of $SU(6)$. In the example we pay particular attention to the multiplicities in terms of the LR-coefficients \mathcal{L} :

Example 7.

$$T(\mu) \equiv \begin{array}{|c|} \hline \square \\ \hline \square \\ \hline \end{array} \qquad T(\nu) \equiv \begin{array}{|c|c|} \hline \square & \square \\ \hline \square & \square \\ \hline \end{array}.$$

Then the tensor product can be computed via SSYT techniques and we identify the coefficients with the multiplicity out the front:

$$\begin{aligned} & \begin{array}{|c|c|} \hline \square & \square \\ \hline \square & \square \\ \hline \end{array} \otimes \begin{array}{|c|} \hline \square \\ \hline \square \\ \hline \end{array} = \begin{array}{|c|c|c|} \hline \square & \square & \square \\ \hline \square & \square & \square \\ \hline \square & & \square \\ \hline \end{array} \oplus \begin{array}{|c|c|c|} \hline \square & \square & \square \\ \hline \square & \square & \square \\ \hline \square & \square & \square \\ \hline \end{array} \oplus \begin{array}{|c|c|} \hline \square & \square \\ \hline \square & \square \\ \hline \square & \square \\ \hline \square & \square \\ \hline \end{array}, \\ = & \mathcal{L}_{(2,2),(1,1)}^{(3,2,1)} \times \begin{array}{|c|c|c|} \hline \square & \square & \square \\ \hline \square & \square & \square \\ \hline \square & & \square \\ \hline \end{array} \oplus \mathcal{L}_{(2,2),(1,1)}^{(3,3)} \times \begin{array}{|c|c|c|} \hline \square & \square & \square \\ \hline \square & \square & \square \\ \hline \square & \square & \square \\ \hline \end{array} \oplus \mathcal{L}_{(2,2),(1,1)}^{(2,2,1,1)} \times \begin{array}{|c|c|} \hline \square & \square \\ \hline \square & \square \\ \hline \square & \square \\ \hline \square & \square \\ \hline \end{array}. \end{aligned}$$

In this case all included coefficients are equal to 1, but the intended illustration of the role played by the LR coefficients is clear.

The main advantage of these coefficients is that they have a number of natural combinatorial interpretations for tensor product multiplicities. One such argument among many [28] is presented here. Our preferred account of the LR-coefficients requires another modification to the Young tableaux, the skew-SSYT. This preference is motivated by aesthetic considerations and how the combinatorial account smoothly emerges.

Definition 11. *A skew-SSYT $T(\lambda/\mu)$ are defined for each (λ) , (μ) , with the requirement that $(\mu) \trianglelefteq (\lambda)$. Taking a tableaux of shape (λ) we remove a tableaux of shape (μ) such that both tableaux are centered at the top left corner and so obtain a skew-SSYT of shape $(\lambda)/(\mu)$. Skew-SSYT obey the same filling rules along its rows and columns as the SSYT, which we remind ourselves was weakly increasing to the right in its rows and strongly increasing down columns.*

As an example of a skew-tableau we can consider $T(\lambda) = \begin{array}{|c|c|c|} \hline \square & \square & \square \\ \hline \square & & \\ \hline \end{array}$ and $T(\mu) = \begin{array}{|c|c|} \hline \square & \square \\ \hline \square & \\ \hline \end{array}$ then $T(\lambda/\mu) = \begin{array}{|c|c|c|} \hline \square & \square & \square \\ \hline \square & & \\ \hline \square & \square & \\ \hline \end{array}$. With this definition we can return to defining the LR-coefficients by re-introducing the content.

Definition 12. *Littlewood-Richardson coefficients, $\mathcal{L}_{\mu,\lambda}^\nu$, are equal the number of possible fillings of a skew SSYT of shape $T(\nu/\mu)$ with content (λ) . The content must also be a valid partition [27].*

Alternatively, we can interpret the LR coefficients in terms of (μ) and (λ) . In particular we combine the two partition elements to form a skew-SSYT so that the missing boxes are present on the bottom left and the possible fillings of the tableau, given a content ν , yield the associated LR coefficient. Below we use the operation \star to indicate the gluing of the corner of one tableau to another, so as to obtain a skew-tableau.

Example 8.

$$\mu \star \lambda = \square \star \begin{array}{|c|} \hline \square \\ \hline \square \\ \hline \end{array} = \begin{array}{|c|} \hline \square \\ \hline \square \\ \hline \end{array} \begin{array}{|c|} \hline \square \\ \hline \square \\ \hline \end{array}$$

Now we can consider strictly those contents that yield possible fillings of the skew-SSYT. This provides us with a strong restriction of the types of irreps we need to consider and in the example the only two are given by:

$$\mathcal{L}_{(1),(1,1)}^{(2,1)} = 1 \qquad \mathcal{L}_{(1),(1,1)}^{(1,1,1)} = 1, \qquad (3.22)$$

agreeing with the previous calculation.

Clearly, the filling cannot have a partition size larger than the number of blocks in the skew-SSYT and so we can quickly remove any partition other than those partitions (ν) that satisfy $|\nu| = |\mu| + |\lambda|$. In the above example we need not consider any (ν) with the first part of the partition being 3 since there are no possible ways to fill the skew-SSYT in a way satisfying the increasing condition along the columns.

Interpreting the LR coefficients in terms of the possible fillings or skew-SSYT is a very useful method since it lets us ignore a large number of weights immediately. Additionally this process is particularly useful if we are interested in the tensor product multiplicity corresponding to a specific irrep resulting from a tensor product decomposition.

Tensor products afford us a method of accounting for how states isomorphic to group representations can be interact with one another. As we shall see, they are not the only such operation. In conformal field theory (CFT) a similar operation emerges, called the fusion product. This fusion product will minimally encode information about the interactions of the conformal fields and be much simpler to compute compared to other methods.

Chapter 4

Fusion Products

CFTs are widely used in physics, having found particularly useful applications in the fields of solid state and condensed matter physics. The Ising model at its critical point [11] is arguably the most famous example of a CFT. Cast in the role of an effective theory, CFTs have been successfully used to describe many phenomena. Since CFTs are utilized in so many areas of physics, a better understanding of these theories has potentially far-reaching consequences.

In this chapter, we briefly introduce CFTs and will touch on the mathematics that underpins them. For this thesis we are concerned with a specific class of CFT, called the Wess-Zumino-Witten (WZW) models. These WZW models have a number of useful properties, most notable for us is that the number of primary conformal fields is finite and they are isomorphic to representations of affine Lie groups. Determination of the dynamics of the theory can be done by combining these primary fields via the operator product expansion (OPE). OPEs are in general difficult to perform and so in practice the fusion product, which encodes similar data, is used instead.

An account of the affine fusion product as behaving like a truncated tensor product can be given. Multiplicities that appear in the fusion product are called the fusion dimensions, and can be understood as truncated tensor product multiplicities. Fusion dimensions can be calculated via adjusted tensor product multiplicity methods (see Section 5.1). A combinatorial and fundamentally affine description for the fusion dimensions is not currently known, although it has been long sought. In this thesis we attempt to find a way to write a particularly simple case of the fusion dimension, defined in Section 4.3.4, in terms of non-negative integers. Successfully doing so might indicate the presence of an object underlying the fusion dimensions, not only for the case considered, but potentially for all fusion dimensions.

4.1 Conformal Symmetry

As their name suggests, CFTs obey a conformal symmetry. As a particularly strong form of symmetry, the conformal symmetry is highly restrictive on the types of objects that can appear in the theory. Despite these restrictions, there are many different classes of CFT, from minimal models to logarithmic CFTs, some of which are listed in Section 4.2.

4.1.1 The Conformal Group

Conformal symmetries can be understood fairly easily classically. A conformal group consists of all angle-preserving transformations, which means that the conformal symmetry will contain Poincaré transforms. These symmetries are given by the conformal group $\text{Conf}(\mathbb{R}^{p,q})$, which is isomorphic to $\text{SO}(p+1, q+1)$ [41] when $D > 2$. It contains as subgroups: the translations, rotations, dilations, and the special conformal transformations.

Translations and rotations are in their standard Poincaré forms. Dilation transformations are also in their standard form, given by the scaling transformation of some value λ as $\vec{r} \rightarrow \lambda\vec{r}$. Special conformal transformations are the major addition to the possible transformations of the conformal group and for dimensions $D > 2$ the dimension of the conformal algebra is finite.

For $D = 2$, which is a special case, we can write down the well known special conformal transformation on the Riemann sphere given by:

$$z \rightarrow \frac{az + b}{cz + d}. \quad (4.1)$$

This finite conformal transformation with $a, b, c, d \in \mathbb{C}$ and $ad - bc = 1$ can be identified with the group $\text{SL}(2, \mathbb{C})/\mathbb{Z}$. Interestingly, this group is isomorphic to $\text{SO}(3, 1)$, which is $\text{SO}(p+1, q+1)$ with $p = 2$ and $q = 0$. Although the conformal group

dimension is finite for $D = 2$, an infinite dimensional conformal algebra, known as the Witt algebra, emerges. This ∞ -dimensional conformal algebra or Witt algebra that emerges accounts for all the angle preserving analytic functions $z \rightarrow f(z)$ in \mathbb{C} . The Witt algebra can be thought of as being a ‘classical’ conformal algebra.

The ∞ -dimensional Witt algebra can be used as a set of local constraints on the theory. For conformal groups with larger dimensions, $D > 2$, these infinite local constraints are no longer present since the Witt algebra does not appear. Absent the infinite number of local constraints CFT are much harder to work with, consequently most developments of the theory have occurred for the $D = 2$ case. Recently there has been some successful work in extending CFTs to higher dimensional cases [39]. For the remainder of this thesis we are strictly concerned with the case of conformal symmetry on $D = 2$ surfaces.

4.1.2 Witt and Virasoro Algebras

Dealing with the case of $D = 2$, we can account for the infinitesimal behaviour of the theory by considering the complex plane with complex coordinate z . As with any Lie group, we can write down an algebra describing the behaviour near the identity. Consider a holomorphic transformation:

$$z \rightarrow z - a_n z^{n+1} = z + a_n [\ell_n, z], \quad (4.2)$$

which motivates the operators $\ell_n = -z^{n+1} \partial_z$. As elements of the sequence $(\ell_n)_{n \in \mathbb{Z}}$ the ℓ_n form a basis for the vector fields and satisfy the following Lie bracket:

$$[\ell_n, \ell_m] = (n - m) \ell_{n+m}. \quad (4.3)$$

This defines Witt algebra $\text{Witt} = \{\ell_n : n \in \mathbb{Z}\}$. It appears for both Minkowski $\mathbb{R}^{(1,1)}$ and Euclidean $\mathbb{R}^{(2,0)}$, where both are $D = 2$ spaces. An anti-holomorphic trans-

formation can also be considered, and is the complex conjugate of the holomorphic transformation. Anti-holomorphic conformal transformations preserve angle, but reverse the orientation. Consequently, anti-holomorphic algebras are identical to the holomorphic algebra, the sole difference being a complex conjugation, and so have the brackets:

$$[\bar{\ell}_n, \bar{\ell}_m] = (n - m)\bar{\ell}_{n+m}, \quad [\ell_m, \bar{\ell}_n] = 0. \quad (4.4)$$

Separation of the holomorphic and anti-holomorphic pieces is a general and useful property of the 2D CFTs.

We can consider what happens when the Witt algebra is quantized, which moves us from the classical to the quantum regime. Quantization of the Witt algebra results in the appearance of non-unitary states for non-trivial CFTs [9].¹ This symmetry breaking that occurs is known as the conformal or Weyl anomaly, and leads to the appearance of a non-trivial central charge [31]. Symmetry breaking and the appearance of a non-trivial central charge indicates that for a unitary theory, with no non-positive norm states, we require more than a naive Witt quantization. This involves the introduction of a central extension. Witt algebras have only one non-trivial central extension, which results in the Virasoro algebra [41].

There are multiple methods for finding the central extension. One such method involves introducing holomorphic and anti-holomorphic operators, L_n, \bar{L}_n that belong to the new unitarity-restoring algebra. These operators can be used to write the CFT stress tensor:

$$T(z) = \sum_{n=-\infty}^{\infty} \frac{L_n}{z^{n+2}}, \quad \frac{1}{2\pi i} \oint z^{n+1} T(z) = L_n. \quad (4.5)$$

¹Trivial CFT is the theory that consists of only a vacuum, which can be written down for the Witt algebra, although it is not a particularly interesting case.

Inverting the sum in the second step leaves us with an expression for the L_n generators. This expression for L_n in terms of the stress tensor lets us evaluate the Lie brackets by contour integration. We find that the Lie brackets have the following form:

$$[L_n, L_m] = (n - m)L_{n+m} + \frac{c}{12}(n^3 - n)\delta_{n+m,0}, \quad (4.6)$$

which is identified with the Virasoro algebra [20]. The central extension of the Witt algebra leading to the Virasoro algebra has a unique form [41], so we can define the Virasoro algebra Vir as $\text{Vir} = \text{Witt} \oplus \mathbb{C}c$.

Like the Witt algebra, the holomorphic and anti-holomorphic parts of the Virasoro algebra can be separated. They satisfy the commutator

$$[L_n, \bar{L}_m] = 0, \quad (4.7)$$

L_n and \bar{L}_m can be written in terms of repeated commutation of the conformal generators L_1 and \bar{L}_1 , respectively. L_{-1} generates translations, L_0 generates the scaling and rotations, and L_1 generates the special conformal transformations. In the standard radial quantization [20] of CFT the scaling transformation is also the time translation. Eigenvalues of L_0 are interpreted as energies.

The anti-holomorphic Virasoro algebra is left implicit since it shares the same form, and the conformal blocks and fusion are holomorphic objects. The coefficient c is called the central charge and plays an important role in the classification of different conformal models (see Section 4.2). In string theory, non-zero central charge emerges as a consequence of a curved space-time background, where it is coupled to the Ricci tensor. The central charge is a measure of the size of the CFT. For example, for N free bosons, $c = N$; and for N free fermions $c = N/2$ [48].

Having obtained the Virasoro algebra it is interesting to wonder how it might be realized, since there is no ‘Virasoro group.’ However, its algebra can be realized by a

generalization of the Lie groups, the affine Lie groups [41]. Like the Virasoro algebra emerging from the Witt algebra the affine Lie groups emerge from a central extension process, but have many similarities with the simple Lie groups [12].

4.1.3 Affine Lie Groups

The Lie groups were found to be represented by highest-weight representations in Section 2.2. For affine Lie groups we can take a similar tact and once again define a highest-weight representation, although some additional considerations will be necessary.

Affine Lie groups emerge when considering a set of conformal fields $J^a(z)$, which can be written in terms of a mode expansion:

$$J^a(z) = \sum_{n \in \mathbb{Z}} J_n^a z^{-1-n}. \quad (4.8)$$

These J^a are distinct from the angular momentum operators \hat{J} . With a similar process as for the Virasoro commutators we find:

$$[J_n^a, J_m^b] = if^{abc} J_{m+n}^c + k\delta^{ab}\delta_{m+n,0}, \quad (4.9)$$

which can be connected with the Virasoro algebra in equation (4.6). The value k are called the levels and are related to the central extension $c = \frac{k \dim(\mathfrak{g})}{k+h^\vee}$, where h^\vee is the dual Coxeter number, which for simply laced algebras are the number of non-zero roots divided by the rank of the algebra. These operators J_{-1} act on highest-weight states and build up an irrep of the affine Lie algebra.

Highest-weight representations of the simple Lie groups are found by specifying a highest-weight and acting on the highest-weight state repeatedly with these lowering operators. Alternatively given a highest-weight the simple roots can be used to build up a highest-weight lattice that labelling the possible states. Like the simple Lie

group case, the simple roots are those elements of the root space that cannot be formed by the addition of other roots.

Simple roots reappear in the affine highest-weight representations of the affine Lie groups, where they play a similar role as they do in simple highest-weight representations. Affine highest-weight representations require additional information to the highest-weight in order to uniquely specify a representation, which is given by the level k . This level is identified as the central extension of the loop algebra imposed in order to obtain the affine Kac-Moody algebra, and from there the affine Lie algebras [10, 44].

Primary fields in the WZW models correspond to those centrally extended algebras appearing when the level is integer-valued. Primary fields are in 1–1 correspondence with highest weight states and representations of the affine Lie group. Affine weights, the weights of affine Lie groups, have an additional Dynkin label compared to the weights of the simple Lie groups, the zeroth Dynkin label. Appending the zeroth Dynkin label to a simple weight σ turns it into an affine weight $\hat{\sigma}$.²

This new zeroth Dynkin label is related to both the horizontal Dynkin labels and the level in the following way:

$$\lambda_0 = k - \lambda \cdot \theta = k - \sum_{i=1}^N \lambda_i m_i^\vee, \quad (4.10)$$

which results in the affine weights being written as:

$$\hat{\lambda} = [k - \sum_{i=1}^{N-1} \lambda_i m_i^\vee; \lambda_1, \dots, \lambda_{N-1}]. \quad (4.11)$$

The m_i^\vee are the co-marks and identical to the co-marks of the highest-weight representation of the simple Lie groups and k is the level. For the case of $\widehat{SU}(N)$ the

²In the literature the zeroth Dynkin label is sometimes also considered as being the N^{th} Dynkin label.

co-marks are $m_i^\vee = 1$ [3]. Notably, the zeroth Dynkin labels change depends on the level considered.

The affine operators J_0^a form a horizontal subalgebra of equation (4.9), which we note as yielding the simple Lie algebras. Affine highest-weight representations can be broken into these horizontal pieces, which are indexed by L_0 eigenvalues that are interpreted as the energy. These energy eigenvalues are also called conformal dimensions h_λ :

$$L_0 | \hat{\lambda} \rangle = h_\lambda | \hat{\lambda} \rangle = \frac{\lambda \cdot (\lambda + 2\rho)}{2(k + h^\vee)} | \hat{\lambda} \rangle \quad (4.12)$$

One can use the $J_{\pm 1}^a$ to move between horizontal representations, where each of these representations is the highest-weight representation of a corresponding simple Lie algebra.

Like the other Dynkin labels the zeroth Dynkin labels of a highest-weight must be non-negative in order for it to be a valid highest-weight. The behaviour of the zeroth Dynkin label in equation (4.10) indicates that the level has a truncative effect on possible highest-weights, due to the zeroth Dynkin label being required to be non-negative. Those highest-weights that satisfy the non-negativity condition exist in a subspace of horizontal weight space called the Weyl alcove. Every highest-weight has a special value of the level, called the threshold level k_0 , where its zeroth Dynkin label λ_0 is 0. A weight's threshold level indicates the minimum level at which that highest-weight first appears in the Weyl alcove.

Definition 13. *For every affine weight $\hat{\lambda}$ in a highest-weight representation of an affine Lie group \hat{G} we write $\hat{\lambda} \in R(\hat{G})$ in a Dynkin label notation as: $\hat{\lambda} = [k - \sum_i \lambda_i m_i^\vee; \lambda_1, \dots, \lambda_{N-1}]$. The zeroth Dynkin label is separated from the simple Dynkin labels by the semi-colon.*

Definition 14. *For every possible highest-weight element $\hat{\lambda}$ of some affine Lie group*

\widehat{G} there will be a minimum level that the highest-weight first appears at in the Weyl alcove, called the threshold level k_0 . At its threshold level $\widehat{\lambda}$ has $\lambda_0 := k_0 - \sum_i \lambda_i m_i^\vee = 0$.

We have described how the highest-weight representation procedure can be altered to suit the affine Lie groups. We now consider new symmetries introduced by the additional structure of the affine Lie groups. Affine highest-weight representations will have all the symmetries the simple highest-weight representations, along with new uniquely affine symmetries. Among these new symmetries is the Galois symmetry [15] (see Section 6.1.5), the simple current symmetry (see Section 6.1.4), and the affine Weyl symmetry.

4.1.4 Affine Weyl Group

Horizontal highest-weight representations, as we noted, were the result of a projection of the affine highest-weight representation and correspond to a specific energy level. Energy levels, being understood as the eigenvalues of L_0 , can be used to distinguish these horizontal highest-weight representations and label an infinite tower, where higher L_0 eigenvalues are the result of moving up this tower. One can imagine the affine highest-weight representation as consisting of a tower of these horizontal highest-weight representations, with energy levels climbing up to infinite value.

Like the simple highest-weight representations, which had a Weyl group reflecting the weights into one another, the affine highest-weight representations have an affine Weyl group. Similarly to the simple Weyl group, as applied to the simple highest-weight representations in Section 2.2.2, the affine Weyl group is defined in terms of a set of primitive reflections. Significantly, the affine Weyl group is ∞ -dimensional. An additional reflection element, the primitive affine reflection ω_0 , is the main source of the differences between the simple and affine Weyl groups.

Projections of the affine highest-weight representation onto the horizontal highest-

weight representation also projects with it the ∞ -dimensional affine Weyl group W_{Affine} to the ∞ -dimensional horizontal Weyl group \widehat{W} . Like the simple Weyl group the horizontal Weyl group is generated by primitive reflections around hyperplanes, which are normal to the simple roots. For the projected case we note that we have an additional hyperplane, the ‘affine hyperplane.’ The affine hyperplane is the result of the truncation on the Weyl alcove and is placed along a boundary of the shifted Weyl alcove, defined by the horizontal weights in the Weyl alcove σ , where $(\sigma + \rho) \cdot \theta = N + k$. Shifted Weyl alcove is the Weyl alcove with all weight shifted by the addition of the highest root ρ .

Unlike the other primitive reflections, the affine reflection can be used to move between horizontal highest-weight representations. Explicitly the affine reflection is written as follows:

$$\omega_0(\lambda) = \lambda - \frac{2(\lambda, \rho)}{(\rho, \rho)}\rho + (k + h^\vee)\theta. \quad (4.13)$$

Combining this affine reflection with the horizontal Weyl group the ∞ -dimensional affine Weyl group \widehat{W} is obtained.

Definition 15. *Simple reflections across hyperplanes normal to the simple roots and the affine reflection across the hyperplane defined by the affine wall at level k can be used to generate the ∞ -dimensional horizontal Weyl group \widehat{W} :*

$$\widehat{W} = \langle \omega_0, \omega_1 \dots \omega_{N-1} \rangle. \quad (4.14)$$

4.2 Conformal Field Theory

Quantization of the classical conformal symmetry required the introduction of a central charge into the Witt algebra, forming the Virasoro algebra, in order to preserve unitarity. Centrally extending the Witt algebra results in some drastic changes on

the types of objects that can be considered.

There are two types of fields present in a CFT, the primary fields and the secondary fields. Secondary fields are generated from the primary fields by the action of lowering operators. Lowering operators that act on the primary field will obey the Virasoro algebra in equation (4.6) and can be used to obtain a representation by acting on a state $|h\rangle$ with conformal weight h , which corresponds to the appropriate primary field $|h\rangle = \phi(0)|0\rangle$.

There are many types of CFT with many properties, but those we are concerned with, the WZW models, are rational and have a finite number of primary fields. Though there are a finite number of primary fields, the ∞ -dimensional conformal symmetry results in these primary fields resulting in an infinity of secondary fields.³ A level condition can be imposed on the state and in so doing restricts the number of descendant fields. Level restricts the number of lowering steps that an operator is allowed to induce on a primary field, with additional steps past the level value annihilating the state. For the WZW models, these level defined pieces of the full representation are analogous to horizontal highest-weight sub-representations of the affine Lie group, introduced in Section 4.1.3.

Looking at the states that result from the primary and secondary fields we can talk about unitarity and consider when the states of these fields and their norms satisfy the condition. Central charges that satisfy unitarity can be found by considering the norm of the states acting level by level. As an example those operators at level $k = 3$, and n :

$$L_{-3}|h\rangle, L_{-2}L_{-1}|h\rangle, L_{-1}L_{-2}|h\rangle, L_{-1}^3|h\rangle, \tag{4.15}$$

$$\text{Generally : } L_{-n}|h\rangle, L_{-n+1}L_{-1}|h\rangle, \dots, L_{-1}^n|h\rangle. \tag{4.16}$$

³Secondary fields are also known as descendant fields, since they are obtained by the action of the lowering operators on an appropriate primary field.

Unitarity requires that the inverse of the operators are given by $L_n^\dagger = L_{-n}$. Verma modules are defined at each level as the sum of possible states in equation (4.15) and must satisfy the unitarity condition. Imposing this property and using the Virasoro algebra from equation (4.6) on the norms of the Verma modules in equation (4.15), the possible values of the central charge can be found. These conditions are well known [20] and very important, as they account for different types of CFT models.

- There are no unitary CFTs for $h < 0$ or $c < 0$.
- For $c > 1, h \geq 0$, all Verma modules are unitary and irreducible.
- For $c = 1, h \geq 0$, all Verma modules are unitary, but reducible if $h = \frac{n^2}{4}$ with $n \in \mathbb{N}$.
- For $c \in (0, 1)$, only those with $c = 1 - \frac{6}{m(m+1)}$, $m \in \mathbb{N}_{\geq 2}$ and $h = \frac{((m+1)r-ms)^2-1}{4m(m+1)}$, $r \in 1, 2, \dots, m-1$, $s \in 1, 2, \dots, r$ are unitary and $m = \frac{p}{p-q}$, then $r < p$ and $s < q$ produces unitary, but in general reducible representations.

Values of these central charges impact the type of CFT that is being considered. When $c \in (0, 1)$ the corresponding CFTs are the minimal models, which have been collected in [21]. The Ising model at critical point is an example of a minimal model, and the example considered in Section 4.3.3 occurs when $c = \frac{1}{2}$. When $c = 0$, which effectively removes the central extension, the only unitary CFT has its single field as the vacuum.⁴ Primary fields of the minimal models are accounted for by the Virasoro algebra (4.6).

For the case of $c = 1$ there has been a lot of work done on a variety of models; many of these are collected in [21]. Finally for $c > 1$ there are a huge number of known models [9] and many remain to be found. Among these the Wess-Zumino-Witten (WZW) models are one such class of CFT with $c \geq 1$, for the non-trivial

⁴That is, the only unitary and rational CFT with a Witt algebra is the trivial CFT.

cases. They have a number of very interesting properties in that they are rational, have a Lagrangian formulation, and have a compact Lie group as a target space [6].

For our purposes the most important property of the WZW models is that they are rational CFTs (RCFTs) and that their primary fields can be identified with representations of the affine Lie algebras. As an RCFT, a WZW model has a finite number of primary fields, further the WZW models permit an isomorphism between the primary fields and representations of the affine Lie groups.

Primary conformal fields can be used to label families of fields. These families consist of all secondary fields generated by the application of lowering operators on the primary field that labels the family. Since the number of primary fields is finite, the number of families is also finite. The possible interactions of a theory follow the behaviour of the primary fields. Primary field interactions are found by considering the operator product expansion (OPE) of the two fields and expanding in terms of the displacement between them in order to determine the local behaviour.

4.2.1 Operator Product Expansion

Mathematically, the OPE involves taking the product of local operators and then expanding them out in terms of a parameter that accounts for the ‘distance’ between the combined operators. For CFT the local operators are identified with the primary conformal fields and the expansion parameter is the coordinate distance between the two fields. Values of the level k is fixed by the WZW models, where fields of different levels are not present in the theory. Reminding ourselves that the set of primary fields of the WZW models is isomorphic to the set of representations of an affine Lie group, we can consider the primary fields as labelling representations of the affine Lie group. An affine tensor product of two affine Lie group representations combines their levels for the resultant representation. Affine tensor products change the levels, which suggests that we cannot give an account of the OPE with the affine tensor

product.

Conformal weights can be written as eigenvalues of the Virasoro generator L_0 . We may write the OPE of two primary fields as follows [20]:

$$\phi_\lambda(z, \bar{z})\phi_\mu(w, \bar{w}) = \sum_\nu C_{\lambda,\mu,\nu} z^{(h_\nu - h_\lambda - h_\mu)} \bar{z}^{(\bar{h}_\nu - \bar{h}_\lambda - \bar{h}_\mu)} \phi_\nu(w, \bar{w}). \quad (4.17)$$

The holomorphic and anti-holomorphic, z and \bar{z} respectively, pieces of the primary fields ϕ_p can be separated, but they are left in for the sake of completeness. Conformal weights of the primary fields are given by h_λ, h_μ, h_ν with their anti-holomorphic counterparts marked by \bar{h} .

Of its many properties, the conjectured associativity of the OPE is of particular importance as it is necessary for consistency of the CFT [20]. Associativity in the context of CFT is more commonly referred to as crossing symmetry.⁵ Crossing symmetry indicates that the s - and t -channels of a 4-point correlation function are related to one another by a unitary transformation. Demonstrating the meaning of this condition more clearly, we consider the 4-point correlation function:

$$\langle \phi_\alpha(z_1)\phi_\beta(z_2)\phi_\mu(z_3)\phi_\nu(z_4) \rangle. \quad (4.18)$$

This function can be evaluated either by taking $z_1 \rightarrow z_2$ or by taking $z_1 \rightarrow z_3$.⁶ Associativity of the OPE tells us that the resulting correlation functions must be equivalent, indicating that there must be a unitarity preserving transformation between the two. This results in the standard form of the crossing symmetry [13], pictured in Figure 4.1.

Correlation functions can be broken up into sums of holomorphic and anti-holomorphic

⁵Crossing symmetry is also known as the ‘conformal bootstrap’ or as the ‘consistency condition’ [39].

⁶These two distinct evaluations are equivalent to taking $z_3 \rightarrow z_4$ and $z_2 \rightarrow z_4$ respectively.

functions. These functions are identified as conformal blocks \mathcal{F} and can be used to construct correlation functions of the theory, as they give an account of the interactions between primary fields. Construction of the correlation function from conformal blocks is a standard procedure in CFT. Crossing symmetry is necessary to consider when combining these conformal blocks $\mathcal{F}_{\alpha,\beta}^{\mu,\nu}(p|x)$, so for the 4-point correlation function:

$$\sum_{\sigma} C_{\alpha,\beta,\sigma} C_{\mu,\nu,\sigma} \mathcal{F}_{\alpha,\beta}^{\mu,\nu}(p|x) \overline{\mathcal{F}}_{\alpha,\beta}^{\mu,\nu}(p|\bar{x}) = \sum_{\sigma} C_{\alpha,\mu,\sigma} C_{\beta,\nu,\sigma} \mathcal{F}_{\alpha,\mu}^{\beta,\nu}(p|1-x) \overline{\mathcal{F}}_{\alpha,\mu}^{\beta,\nu}(p|1-\bar{x}). \quad (4.19)$$

This relation is required for crossing symmetry and note that the conformal blocks are distinct, but that the resulting correlation functions are related to one another. Behaviour of the conformal blocks, as building blocks of the theory, is central to the study of CFTs, although they are in general quite complicated to describe explicitly.

As we were able to do with tensor products in the case of angular momentum states, many properties of the interactions of a CFT can be discussed with less information. Doing so motivates the definition of the fusion product, which like the tensor products combines two representations of an algebra and results in a reducible representation.⁷ Decomposition of the reducible representation results in a set of irreps, which are paired with fusion dimensions that indicate how often an irrep appears called the fusion dimensions. The name fusion dimensions is motivated by these objects being equal to the dimensions of the space of conformal blocks. Fusion products are much simpler to compute than the OPE and give use information about the conformal blocks without requiring complete knowledge of them. They provide dimensions rather than complex amplitudes. These advantages make the fusion product and the fusion dimensions (dimensions of the space of conformal blocks) viable simpler alternatives for encoding much of the behaviour of a CFT.

⁷These irreps are each labelled by a primary field in the CFT.

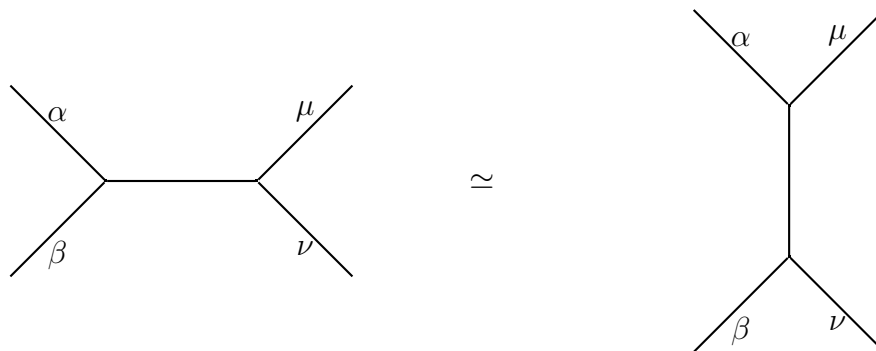


Figure 4.1: Two possible decompositions of the 4-point functions, where the inner edges are summed over and so left unlabelled.

Crossing symmetry can be understood as a special case of the more general Moore-Seiberg duality [33]. Moore-Seiberg duality becomes important when we interpret the n -point correlation functions in terms of trivalent graphs. Trivalent graphs refer to those graphs whose vertices all have 3 edges. These vertices are interpreted based on the labelling of the edges and correspond to the coefficient $C_{\alpha,\beta,\sigma}$, which are coupled to the relevant conformal blocks. In the example for crossing symmetry (see Figure 4.1) we have one inner edge, which is summed over (unlabelled), and four external edges (labelled).

Fusion coefficients $\mathcal{N}_{i,j}^\ell$ can be used to write the fusion product in a similar manner as was done for the tensor products in equation (3.1). Fusion dimensions count the number of times that a primary field ϕ_ℓ appears in the OPE of ϕ_i and ϕ_j . Accounting for the product of primary fields, where k denotes the level of the primary fields being combined, we have:

$$\phi_i \otimes_k \phi_j = \sum_{\ell} \mathcal{N}_{i,j}^\ell \phi_\ell, \quad (4.20)$$

defining the fusion product, denoted by \otimes_k , and its decomposition.

4.2.2 Fusion Dimensions

Equation (4.20), for the fusion product, has a similar form as equation (3.1), for the tensor product. The main difference between the two is the presence of the level, which restricts the possible highest-weights. At infinite level the distinction between tensor and fusion products vanishes, as all highest-weights will appear in the Weyl alcove. Based on this observation that the two operations are identical for large k , it is not overly surprising that the fusion product shares many of the ‘nice’ properties of the tensor product [13].

Fusion dimensions $\mathcal{N}_{\lambda,\sigma}^\mu = {}^{(N,k)}\mathcal{N}_{\lambda,\sigma}^\mu$ depend on group rank N and level k , and indicate the dimension of the space of the relevant conformal block. Suppression of the (N, k) will be used often to avoid an unnecessarily cluttered notation. There is an implied decomposition that will occur when we refer to the fusion product, similar to the abuse of terminology with the tensor product. Fusion dimensions⁸ play the same role for the fusion product as the tensor product multiplicities did for the tensor product. These observations can be used to discern the following properties for the fusion dimensions:

- Identity: there is an identity element given by $\mathcal{N}_{0,\sigma}^\mu = \delta_\sigma^\mu$.
- Commutativity: like the tensor product the order of the fields in the fusion product is irrelevant, which equates $\mathcal{N}_{\lambda,\sigma}^\mu = \mathcal{N}_{\sigma,\lambda}^\mu$.
- Associativity: since dimensions of the spaces of n -point conformal blocks must be consistent this is analogous to the crossing symmetry, $\sum_{\sigma \in P_+^k} \mathcal{N}_{\lambda,\mu}^\sigma \mathcal{N}_{\alpha,\sigma}^\nu =$

⁸These have several names and are also commonly called the Verlinde dimension, fusion numbers, and the 3-point fusion dimensions are commonly called the fusion coefficients.

$\sum_{\sigma \in P_+^k} \mathcal{N}_{\lambda, \alpha}^\sigma \mathcal{N}_{\sigma, \mu}^\nu$, where P_+^k is the Weyl alcove containing all valid highest-weights.

- Non-negativity: the fusion dimensions resulting from the fusion product have values $\mathcal{N}_{\lambda, \mu}^\nu \in \mathbb{Z}_{\geq 0}$.
- Conjugation: since fusion dimensions are non-negative integer valued, $\mathcal{N}_{\lambda, \sigma}^\mu = \mathcal{N}_{\lambda^\dagger, \sigma^\dagger}^{\mu^\dagger}$. On the fields this is equivalent to changing whether they are incoming or outgoing, with Dynkin labels being transposed.

As previously indicated, fusion products provide information about the dimension of the space of conformal blocks and can be used to account for the coefficients appearing in the OPE in a similar manner as the tensor product does for the Clebsch-Gordan coefficients. Fusion dimensions can be indicated by a trivalent graph with vertices representing their relevant 3-point fusion dimensions, which are also known as the fusion coefficients. General fusion products can be written by considering incoming and outgoing fields with raised and lowered indices respectively [13] and contracting over shared fields. CFTs are defined on Riemann surfaces and the conformal blocks are functions on these surfaces. These Riemann surfaces can be degenerated into graphs, which leads to an elegant account of many properties of CFT via Moore-Seiberg duality.

4.3 Moore-Seiberg Duality

How fields combine in a CFT is important data encoded in OPEs and, minimally, in the fusion product. Due to their simplicity to compute, fusion products are often preferable to the more complete OPE and give us sufficient information about interactions in a CFT. In WZW models the fusion products can be understood as the truncation of a tensor product, where the possible states and interactions are restricted by the level.

G. Moore and N. Seiberg [33] introduced a method of looking at multi-point interactions in a way that extends the central concepts of the crossing symmetry. They claim that an n -point, arbitrary genus,⁹ correlation function can be degenerated in many different ways, but these must be equivalent up to unitarity preserving transformation.

Conformal blocks, which are a complete description of the interactions in a theory, can be interpreted as being a Riemann surface with marked points indicating the external fields. Degeneration of a Riemann surface into a trivalent graph and applying Moore-Seiberg duality tells us about required covariances of the conformal blocks. Trivalent graphs resulting from the degeneration of a surface must be related to one another in a unitary way, otherwise conformal blocks with identical topologies would be implied to result in distinct correlation functions, rendering the theory inconsistent.

Those trivalent graphs corresponding to a Riemann surface can be considered as a graph theoretic account of the fusion product. An example decomposition is given in Figure 4.2. Notably, the degenerations are not unique, but according to Moore-Seiberg basis of their spaces of conformal blocks must be related by unitary transformations.

Inner edges of the graph are unlabelled, implying summation over the appropriate indices of the constituent fusion dimensions $\mathcal{N}_{\mu,\lambda}^\nu$. Each vertex corresponds to a fusion dimension, which has its indices labelled based on those edges incident on the relevant vertex. Importantly, the contractions over shared indices are summed over all possible highest weights and indicate an inner edge of the graph. This rule for contracting is important in constructing general formulas for fusion dimensions.

The conformal block on the un-marked torus $T^2 = S^1 \times S^1$ is a particularly fundamental case. The torus is parameterized in terms of the period of a complex

⁹By arbitrary genus we mean that the Riemann surface that the conformal blocks live on are allowed to have holes. Each such hole (or handle) will correspond to a loop in the trivalent graph obtained by degeneration of the surface.

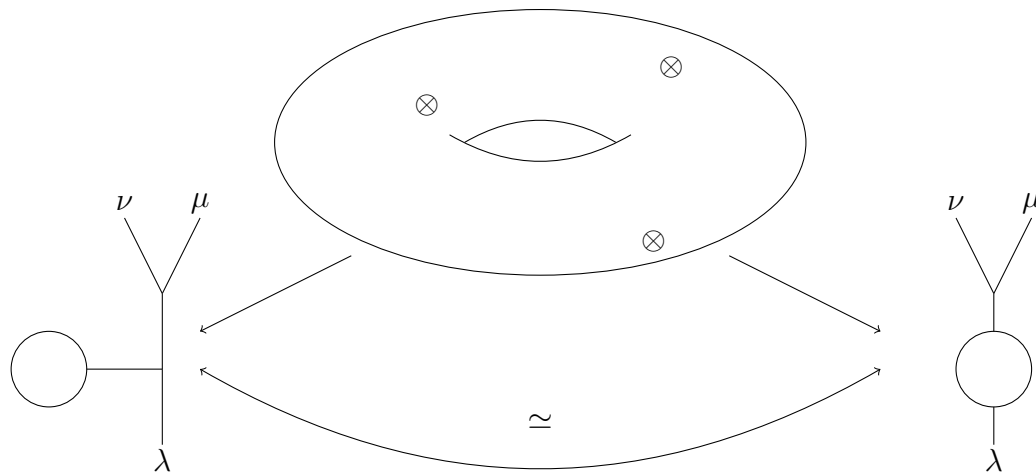


Figure 4.2: A genus-1 surface, in this case the torus, with 3 marked points, corresponding to three external conformal fields, chosen to be λ, μ, ν .

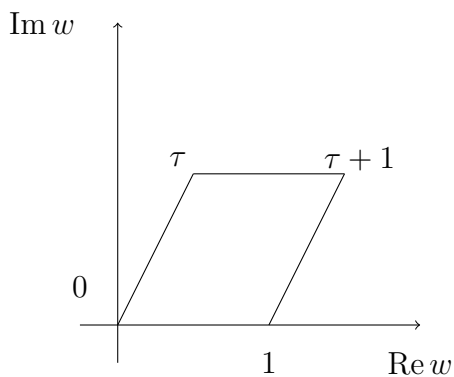


Figure 4.3: Torus complex parameterization in terms of modular parameter τ .

coordinate w on a cylinder. In order more easily account for the behaviour of the torus we introduce the complex parameter τ , which is known as the modular parameter. The behaviour of this parameter is indicated in Figure 4.3.

The conformal block of the torus is a special one, equal to the affine character $\widehat{\text{ch}}_{\widehat{\lambda}}(\tau)$, the character of the affine Lie group of highest weight $\widehat{\lambda}$. Physically it can also be understood as the partition function of the corresponding conformal (affine) tower of states.

For the torus there are several possible degenerations, two of which are illustrated

in Figure 4.4 as being the two cycles. Cycles on the torus are known to be related via the modular transformations. These modular transformations have the following action on the torus parameter τ :

$$T : \tau \rightarrow 1 + \tau, \quad S : \tau \rightarrow -\frac{1}{\tau}. \quad (4.21)$$

Additionally, the modular S and T matrices that correspond to these transformations obey the algebra:

$$S^2 = I, \quad (ST)^3 = I. \quad (4.22)$$

Since these modular transformations relate inequivalent degenerations of the torus to one another, the conformal block identified with the torus must be covariant under the transformation as well. This means that the affine character is covariant under S and T -modular transformations. Acting on the affine character with the modular matrices results in the following:

$$\widehat{\text{ch}}_{\widehat{\lambda}}\left(-\frac{1}{\tau}\right) = \sum_{\sigma \in P_+^k} S_{\lambda, \sigma} \widehat{\text{ch}}_{\widehat{\sigma}}(\tau), \quad (4.23)$$

$$\widehat{\text{ch}}_{\widehat{\lambda}}(\tau + 1) = \sum_{\sigma \in P_+^k} T_{\lambda, \sigma} \widehat{\text{ch}}_{\widehat{\sigma}}(\tau). \quad (4.24)$$

These behaviours were originally noted by Kac-Peterson in [23].

These considerations, which led to the modular symmetry of the affine character, only made use of Moore-Seiberg duality and the identification of the conformal block of the torus with the affine character. Moore-Seiberg duality also implies the crossing condition (4.1), so we conclude that the modular symmetries are a consequence of the consistency of the CFT. From this perspective the S -modular matrices appearance in the Verlinde formula (see Section 4.3.2) is less surprising based on the Moore-Seiberg

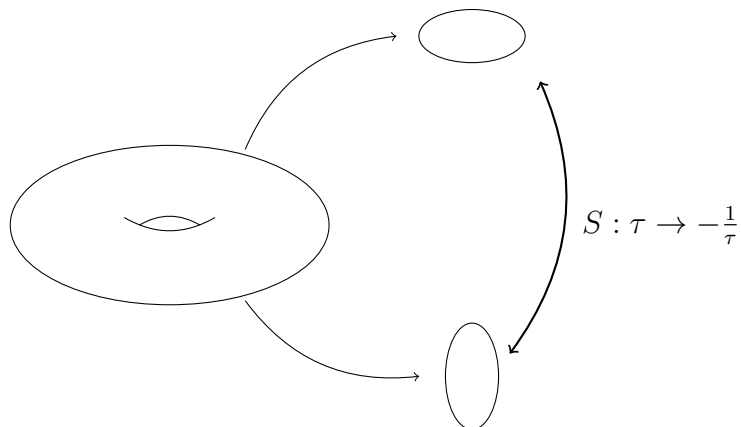


Figure 4.4: The torus and its decomposition into cycles, which are related by the modular transformation S .

picture, where they are fundamental for CFT.

4.3.1 Kac-Peterson Formula

Based on the Moore-Seiberg duality discussion, modular symmetry is a fundamental component of CFT, being arguably necessary for the latter's consistency. Beginning with Moore-Seiberg duality modular symmetries were found to emerge as a necessary consequence. Computing the S -matrices is very difficult in general and requires that we consider their action on the affine characters, see for example the treatment of the Ising model in Section 4.3.3.

Luckily, and curiously, for WZW models Kac and Peterson [23] wrote the S -matrices in a form proportional to the numerator of the Weyl character formula. Consequently, another Kac-Peterson result is:

$$\frac{S_{\lambda,\mu}}{S_{0,\mu}} = \text{ch}_\lambda \left(\frac{-2\pi i}{h^\vee + k} \sigma \right). \quad (4.25)$$

This formula indicates that the S -matrices can be found by a sum over the relevant weights in the horizontal highest-weight representation and shifted Weyl alcove.

Evaluation of the simple Lie character can be done with the Weyl character formula:

$$\text{ch}_\lambda(H) = \frac{1}{\delta} \sum_{\omega \in W} (-1)^{\ell(\omega)} \exp((\lambda + \rho)\omega(H)), \quad (4.26)$$

where H is some weight and $\ell(\omega)$ is the minimum number of primitive reflections within the Weyl group element ω . Subbing equation (4.26) into equation (4.25) we can write the Kac-Peterson formula as:¹⁰

$$\frac{S_{\lambda,\mu}}{S_{0,\mu}} = \sum_{\alpha \in P(\lambda)} \text{mult}_\lambda(\alpha) e^{-\frac{2\pi i}{k+h\nu} \alpha \cdot (\sigma + \rho)}. \quad (4.27)$$

In the next section we will see why the Kac-Peterson relation (4.25) is quite natural, at least in hindsight.

4.3.2 Verlinde Formula

We begin by introducing fusion matrices, whose entries are defined as: $(\mathcal{N}_\lambda)_\sigma^\nu = \mathcal{N}_{\lambda,\sigma}^\nu$. These fusion matrices (\mathcal{N}_λ) have eigenvalues given by $\frac{S_{\lambda,\mu}}{S_{0,\mu}}$; or in terms of simple Lie characters from the Kac-Peterson formula (4.25).

Fusion matrices are diagonalized by the S -modular matrices, which can be used to write down the fusion coefficients, which are the 3-point genus $g = 0$ fusion dimensions. By applying the Kac-Peterson [23] formula in order to write the character in terms of a quotient of the S -modular matrices, leads to the important, and celebrated, Verlinde formula [13]. Fusion coefficients can be computed by the Verlinde formula and are given by:

$$\mathcal{N}_{\mu,\nu}^\lambda = \sum_{\sigma \in P_+^k} S_{\sigma,\mu} S_{\sigma,\nu} \frac{S_{\sigma,\lambda}^*}{S_{\sigma,0}}. \quad (4.28)$$

Sums running over the possible highest-weights contained in the Weyl alcove P_+^k at

¹⁰We are able to make the substitution $h^\vee = N$ when working with $\widehat{SU}(N)$ algebras.

a level k . Conceptually, the Verlinde formula is extremely important, as it accounts for the fusion dimensions in terms of the character and the modular symmetries.

Fusion coefficients consist of two incoming fields and one outgoing field and are the most basic fusion dimension, clarifying why we require our graphs to be trivalent.¹¹ Combinations of two fusion operations can be done by matching incoming and outgoing fields with a sum over the now inner edge. Applying the Verlinde formula (4.28) and the behaviour of the modular matrices (4.22) to combinations of fusion coefficients we can build up more complicated graphs, and relate them back to Riemann surfaces [33]. Moore-Seiberg duality motivates the validity of this constructive process, where two gluings must be related by a unitary transformation, provided that the graphs correspond to topologically equivalent surfaces.¹²

Despite the Verlinde formula providing a method for the computation of fusion dimensions it is non-trivial to apply. Algorithms used for computing the fusion rules are adapted from techniques used for computing tensor product multiplicities and are generally much faster to use than applying the Verlinde formula. Despite their computational advantage, these adapted algorithms do not account for the fusion dimension in a fundamentally affine way. Instead they take advantage of the similarities between the fusion product and the tensor product and apply a truncative property in order to find a result [8, 40]. A combinatorial rule that gives an account of fusion dimensions, without appealing to tensor products, has yet to be found.

To demonstrate the complexity of calculation the fusion dimension we consider the critical Ising model. Over the course of the example the complexity of the calculation should also be noted and provide motivation for wanting an easier method.

¹¹Equivalently, the fusion dimension consists of two outgoing fields and one incoming field, since the fusion dimension is conjugation invariant.

¹²Two surfaces are said to be topologically equivalent when they can be smoothly transformed into the other.

4.3.3 Ising Model Fusion Example

Fusion products are useful in a variety of physical systems due to their connection with CFT. The best known and most successful CFTs is arguably the Ising model [11]. As the simplest non-trivial CFT it is useful to look at how its fusion rules can be computed, following the process in [30]. This derivation will motivate how difficult it is to compute the fusion and demonstrate the power of the modular symmetry. First the modular transformation properties of the characters of the theory will be used to determine the form of the S -modular matrices. The results of the covariant transformation being parachuted in for our use. Once we have the S -matrices, the Verlinde formula can then be used to compute the fusion rules.

Our example under consideration is the minimal model CFT (see Section 4.2) resulting from a central charge $c = 1/2$. This is the Ising model with a vacuum field that denoted as \mathbb{I} or 0 , when written as a subscript, the spin field σ , or $\frac{1}{16}$ as a subscript, and the energy field ϵ , $\frac{1}{2}$ as a subscript.

As a first step we introduce the necessary modular functions in order to write the characters down along with their relevant transformations. Following this we will be able to transform the characters and from there obtain the S -matrix, which will then be used along with the Verlinde formula to compute the fusion rules of the Ising model.

The characters can be written fairly succinctly in terms of Θ -functions and the η -function defined as follows [5] along with their modular property (second column) (with $\tau \in \mathbb{H}$; $q = e^{2\pi i\tau}$):¹³

$$\begin{aligned} \Theta_2(\tau) &= 2q^{\frac{1}{8}} \prod_{n=1}^{\infty} (1 - q^n)(1 + q^n)^2 & \Theta_2(-\frac{1}{\tau}) &= \sqrt{-i\tau} \Theta_4(\tau) \\ \Theta_3(\tau) &= \prod_{n=1}^{\infty} (1 - q^n)(1 + q^{n-\frac{1}{2}})^2 & \Theta_3(-\frac{1}{\tau}) &= \sqrt{-i\tau} \Theta_3(\tau) \\ \Theta_4(\tau) &= \prod_{n=1}^{\infty} (1 - q^n)(1 - q^{n-\frac{1}{2}})^2 & \Theta_4(-\frac{1}{\tau}) &= \sqrt{-i\tau} \Theta_2(\tau) \\ \eta(\tau) &= q^{\frac{1}{24}} \prod_{n=1}^{\infty} (1 - q^n) & \eta(-\frac{1}{\tau}) &= \sqrt{-i\tau} \eta(\tau) \end{aligned}$$

¹³The symbol \mathbb{H} denotes the upper half plane.

Using the transformation properties of the functions we can comment on the transformation of the characters, which can be written in terms of the theta-functions and η -function as:

$$\begin{aligned}\widehat{\text{ch}}_0(\tau) &= \frac{1}{2} \left(\sqrt{\frac{\Theta_3(\tau)}{\eta(\tau)}} + \sqrt{\frac{\Theta_4(\tau)}{\eta(\tau)}} \right) \\ \widehat{\text{ch}}_{\frac{1}{2}}(\tau) &= \frac{1}{2} \left(\sqrt{\frac{\Theta_3(\tau)}{\eta(\tau)}} - \sqrt{\frac{\Theta_4(\tau)}{\eta(\tau)}} \right) \\ \widehat{\text{ch}}_{\frac{1}{16}}(\tau) &= \frac{1}{\sqrt{2}} \sqrt{\frac{\Theta_2(\tau)}{\eta(\tau)}}\end{aligned}$$

Using the modular transformation properties of the characters we obtain the following results by comparison with the transformation properties of the modular functions.

$$\begin{aligned}\widehat{\text{ch}}_0\left(-\frac{1}{\tau}\right) &= \frac{1}{2} \left(\widehat{\text{ch}}_0(\tau) + \widehat{\text{ch}}_{\frac{1}{2}}(\tau) + \sqrt{2}\widehat{\text{ch}}_{\frac{1}{16}}(\tau) \right), \\ \widehat{\text{ch}}_{\frac{1}{2}}\left(-\frac{1}{\tau}\right) &= \frac{1}{2} \left(\widehat{\text{ch}}_0(\tau) + \widehat{\text{ch}}_{\frac{1}{2}}(\tau) - \sqrt{2}\widehat{\text{ch}}_{\frac{1}{16}}(\tau) \right), \\ \widehat{\text{ch}}_{\frac{1}{16}}\left(-\frac{1}{\tau}\right) &= \frac{1}{\sqrt{2}} \left(\widehat{\text{ch}}_0(\tau) - \widehat{\text{ch}}_{\frac{1}{2}}(\tau) \right).\end{aligned}$$

From these results the S -matrix can be read off:

$$S = \begin{pmatrix} \frac{1}{2} & \frac{1}{2} & \frac{1}{\sqrt{2}} \\ \frac{1}{2} & \frac{1}{2} & -\frac{1}{\sqrt{2}} \\ \frac{1}{2} & \frac{1}{2} & 0 \end{pmatrix} \quad (4.29)$$

We now have all the necessary information to compute the fusion dimensions via the Verlinde formula. So we need only carry out the summation over the possible

states.

$$\mathcal{N}_{i,j}^k = \sum_{l=0}^2 \frac{S_{(i,l)} S_{(j,l)} S_{(l,k)}^*}{S_{(l,0)}}$$

Where the indices are the elements of the matrix of the previous result. We have implicitly chosen the ordering $(\mathbb{I}, \epsilon, \sigma) \equiv (0, 1, 2)$ in (4.29). Writing the solution we will identify the fusion dimensions as $(\mathcal{N}_i)_{j,k}$ that is we will choose the i and compute the j, k entries in the matrix.

$$(\mathcal{N}_0)_{jk} = \frac{S_{j0} S_{00} S_{0k}^{-1}}{S_{00}} + \frac{S_{1j} S_{01} S_{1k}^{-1}}{S_{01}} + \frac{S_{j2} S_{02} S_{2k}^{-1}}{S_{02}}$$

Computing all arrangements and noting that the interchange of j and k shouldn't affect the value we find the non-zero elements as being:

$$\begin{aligned} (\mathcal{N}_0)_{00} &= \frac{1}{4} + \frac{1}{2} \cdot \frac{1}{2} + \left(\frac{1}{\sqrt{2}}\right) \cdot \left(\frac{1}{\sqrt{2}}\right) = 1 \\ (\mathcal{N}_0)_{11} &= \frac{1}{4} + \frac{1}{4} + \frac{1}{2} = 1 \\ (\mathcal{N}_0)_{22} &= \frac{1}{2} + \frac{1}{2} + 0 = 1 \end{aligned}$$

$$\mathcal{N}_0 = \begin{pmatrix} 1 & 0 & 0 \\ 0 & 1 & 0 \\ 0 & 0 & 1 \end{pmatrix}$$

This shouldn't be surprising since this is the fusion matrix corresponding to the vacuum field. Looking at the energy (i.e., ϵ) field we find

$$(\mathcal{N}_2)_{jk} = \frac{S_{j0} S_{10} S_{0k}^{-1}}{S_{00}} + \frac{S_{1j} S_{11} S_{1k}^{-1}}{S_{01}} + \frac{S_{j2} S_{12} S_{2k}^{-1}}{S_{02}}$$

Once more we go through all the combinations and find that the non-zero elements

are given by:

$$\begin{aligned}
 (\mathcal{N}_1)_{01} &= \frac{1}{4} + \frac{1}{2} \cdot \frac{1}{2} + \left(\frac{1}{\sqrt{2}}\right) \cdot \left(-\frac{1}{\sqrt{2}}\right) \cdot \left(-\frac{1}{\sqrt{2}}\right) \cdot \sqrt{2} = 1, \\
 (\mathcal{N}_1)_{10} &= (\mathcal{N}_1)_{01} = 1, \\
 (\mathcal{N}_1)_{22} &= \frac{1}{2} + \frac{1}{2} + 0 = 1.
 \end{aligned}$$

$$\mathcal{N}_1 = \begin{pmatrix} 0 & 1 & 0 \\ 1 & 0 & 0 \\ 0 & 0 & 1 \end{pmatrix}$$

And the final fusion rule \mathcal{N}_2 corresponding to the spin field:

$$(\mathcal{N}_2)_{jk} = \frac{S_{j0}S_{20}S_{0k}^{-1}}{S_{00}} + \frac{S_{1j}S_{21}S_{1k}^{-1}}{S_{01}} + \frac{S_{j2}S_{22}S_{2k}^{-1}}{S_{02}}$$

And via the same procedure of summing find that

$$\begin{aligned}
 (\mathcal{N}_2)_{20} &= (\mathcal{N}_2)_{02} = 1, \\
 (\mathcal{N}_2)_{21} &= (\mathcal{N}_2)_{12} = 1.
 \end{aligned}$$

$$\mathcal{N}_2 = \begin{pmatrix} 0 & 0 & 1 \\ 0 & 0 & 1 \\ 1 & 1 & 0 \end{pmatrix}$$

Having obtained all fusion matrices¹⁴ we conclude that the fusion rules are the

¹⁴The components of the fusion matrices are identified as being the, by now familiar, fusion dimensions.

following:

$$\begin{aligned}
 \mathbb{I} \times \mathbb{I} &= \mathbb{I}, & \mathbb{I} \times \epsilon &= \epsilon, \\
 \mathbb{I} \times \sigma &= \sigma, & \epsilon \times \epsilon &= \mathbb{I}, \\
 \epsilon \times \sigma &= \sigma, & \sigma \times \sigma &= \mathbb{I} + \epsilon.
 \end{aligned} \tag{4.30}$$

Even in this simple case, where there are only three fields, the computation was quite lengthy. We saw that the modular transformation property of the characters were required to determine the S -modular matrices and consequently the fusion dimensions. It should be noted that fusion dimensions are non-negative integers in general, but that in this example they were all either 1 or 0 and in general they can be any non-negative integer.

4.3.4 Higher Genus Fusion and the Tadpole

Generalizations of the Verlinde formula (4.28) to arbitrary genus [45] can be done in a variety of ways, but the result is always the same. The general Verlinde formula of an arbitrary genus- g n -point fusion dimension is:

$${}^{(g,N,k)}\mathcal{N}_{\mu_1, \mu_2, \dots, \mu_N} = \sum_{\sigma \in P_+^k} (S_{0,\sigma})^{2g-2} \prod_{i=1}^N \left(\frac{S_{\mu_i, \sigma}}{S_{0,\sigma}} \right). \tag{4.31}$$

The (g, N, k) indicates the genus, the dimension, and the level of the fusion dimension, this notation is often suppressed in practice. Every external edge $\mu_i \in P_+^k$ is labelled by a highest-weight from the Weyl alcove, otherwise the fusion dimension will be identically zero. For $g = 0$ and with 3 conformal fields the fusion coefficient from equation (4.28) is re-obtained, which is a useful check.

Among the higher genus fusion functions there are two that are particularly notable: the genus-1 2-point fusion dimension and the genus-1 1-point fusion dimension.

2-point fusion dimensions looks like a handle operator and can be used in that role [48], inserting a loop within a given edge. The specific gluing needed to obtain the 2-point fusion dimension is illustrated in Figure (4.5) demonstrating that the 2-point fusion dimension can be computed from fusion coefficients. 2-point fusion dimensions are given by the formula:

$${}^{(1,k)}\mathcal{N}_{\mu,\lambda} = \sum_{\substack{\nu \in P_+^k \\ \alpha \in P_+^k}} {}^{(0,k)}\mathcal{N}_{\mu,\alpha} {}^{(0,k)}\mathcal{N}_{\lambda,\nu}. \quad (4.32)$$

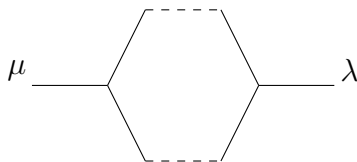


Figure 4.5: A gluing process to obtain the 2-point, genus-1 fusion dimension, where the gluing occurs along the dotted lines.

Genus-1 1-point fusion dimensions, or tadpoles, are immediately noted to have distinct properties compared with other n -point arbitrary genus fusion dimensions. Firstly, tadpoles are not well defined for a standard tensor product, due to the lack of a level restriction that leaves us with an infinite number of highest-weights. Secondly, the tadpole can only be obtained by sewing together two edges of a 3-point fusion dimension, illustrated in Figure 4.6. Thirdly, they are equal to a sum over values of a single, horizontal Lie character:

$$\begin{aligned} \mathcal{T}_\lambda &= \sum_{\mu \in P_+^k} \mathcal{N}_{\lambda\mu}^\mu = \sum_{\mu \in P_+^k} \sum_{\sigma \in P_+^k} \frac{S_{\lambda,\sigma}}{S_{0,\sigma}} S_{\mu,\sigma} S_{\bar{\mu},\sigma}, \\ &= \sum_{\sigma \in P_+^k} \frac{S_{\lambda,\sigma}}{S_{0,\sigma}} = \sum_{\sigma \in P_+^k} \text{ch}_\lambda \left(\frac{2\pi i}{k + h^\vee} \sigma \right). \end{aligned} \quad (4.33)$$

That tadpoles are identified with the horizontal Lie characters suggests that there may be an interpreting of tadpoles as being the sum over something more fundamental

that is present in other fusion dimensions.

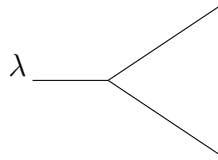


Figure 4.6: The gluing process used to obtain the 1-point genus-1 fusion dimension, or tadpole, where the gluing occurs along the dotted lines.

Our investigation of the tadpoles involved looking at ways that symmetries could be used in order to organize various weights and break up the Verlinde formula into partial sums. These partial sums were examined in the hope that the tadpoles might be written as a sum of non-negative integers. A sum of non-negative integers might point toward some combinatorial atom of the affine tadpole. Such an atom for the tadpole might have held useful insight for a combinatorial rule of more general fusion dimensions.

Chapter 5

Finding Affine Tadpoles

Fusion products can be calculated using several different methods, many of which take advantage of their interpretation as truncated tensor products [40]. Since we were interested in finding a combinatorial argument in terms of manifestly affine objects our study of these truncative methods were cursory. Some attempts were made at using these truncative approaches in order to account for observed properties of the fusion tadpole.

Applying the Kac-Walton algorithm [22, 46, 47] and imposing properties of the tadpole can be used to simplify the calculation. Likewise, we can use the generalized BZ triangles along with additional conditions on them based on relevant tadpole properties. Studying the generalized BZ triangles was fairly fruitful in accounting for observed behaviours, although issues with finding appropriate threshold level constraints for general rank groups, pointed out in [36], prevented more general results from emerging.

In the following section we will be considering horizontal highest-weight representations λ . The weight $\sigma = [\sigma_1, \dots, \sigma_{N-1}]$ are related to the conjugate weight $\bar{\sigma} = [\sigma_{N-1}, \dots, \sigma_1]$ by the reversal of its Dynkin labels. In order to understand how we are thinking of the tadpoles we can write the tadpole in the same form as the fusion product in equation (4.20), where the main difference is that we have an additional sum over the Weyl alcove. Taking the sum over the Weyl alcove we can write the tadpole as:

$$\bigoplus_{\sigma \in P_+^k} R(\sigma) \otimes_k R(\bar{\sigma}) = \bigoplus_{\nu \in P_+^k} \sum_{\sigma \in P_+^k} \mathcal{N}_{\sigma, \bar{\sigma}}^\nu R(\nu) = \bigoplus_{\nu \in P_+^k} \mathcal{T}_\nu R(\nu). \quad (5.1)$$

Beginning in this way, the tadpole for the tensor product is intuitively divergent. This is due to the Weyl chamber P_+ having no upper bound, unlike the Weyl alcove P_+^k whose upper bound forms a polytope. We can introduce a semi-analogous tensor product tadpole by artificially restricting ourselves to the Weyl alcove of the affine

Lie group representation. Doing so we write:

$$\bigoplus_{\sigma \in P_+^k} R(\sigma) \otimes R(\bar{\sigma}) = \bigoplus_{\nu \in P_+} \left(\sum_{\sigma \in P_+^k} C_{\sigma, \bar{\sigma}}^\nu \right) R(\nu), \quad (5.2)$$

where the sum $\sum_{\sigma \in P_+^k} C_{\sigma, \bar{\sigma}}^\nu$ is taken only over the highest-weights on the Weyl alcove. These are interpretable as a partial trace over the simple tensor product multiplicities. Equation (5.2) is defined in terms of a simple tensor product between simple Lie group highest-weight representations, where the sum is an arbitrarily imposed constraint. We introduce this concept in order to argue for the generality of an observed property of the fusion tadpoles (5.37).

5.1 Kac-Walton Algorithm

Weight multiplicities can be used to calculate the tensor product multiplicities resulting from the tensor product of two simple highest-weight representations. This procedure can be generalized to the case of fusion products. Writing the weight multiplicities of a horizontal highest-weight representation as a diagram shifts on the positions of the weights are applied. Following this shift of the weights in the horizontal highest-weight representation the shifted weights are reflected back into the Weyl alcove.¹ This procedure is known as the Racah-Speiser algorithm [35, 43].

Affine Lie groups contain the additional affine reflection element around the affine hyperplane, or affine wall, in addition to the simple Weyl group reflection elements. The affine wall is placed along the weights λ that satisfy $(\lambda + \rho) \cdot \theta = N + k$. Since the weight multiplicities are integers, the Kac-Walton formula gives an integer account of the fusion dimensions. Due to its roots in tensor product calculations makes this explanation unsatisfactory for our goals of writing a manifestly affine account of

¹For tensor product applications, these reflections are applied until the shifted weight moves back into the positive dominant sector, where all Dynkin labels are non-negative integers.

fusion.

The Kac-Walton formula relates fusion coefficients $\mathcal{N}_{\lambda,\mu}^\nu$ to weight multiplicities:

$${}^{(g=0,N,k)}\mathcal{N}_{\lambda,\mu}^\nu = \sum_{\omega \in \widehat{W}} (-1)^{l(\omega)} \text{mult}_\lambda(\omega(\nu + \rho) - \mu - \rho). \quad (5.3)$$

Here \widehat{W} denotes the affine Weyl group and $l(\omega)$ is the length of a reduced decomposition of the affine Weyl element ω . A reduced decomposition is an expression of a Weyl element as a minimal number of primitive reflections.

The form of equation (5.3) implies the following relation between tensor product multiplicities and the fusion coefficient:

$$\mathcal{N}_{\lambda,\mu}^\nu = \sum_{\omega \in \widehat{W}} (-1)^{\ell(\omega)} \mathcal{C}_{\lambda,\mu}^{\omega(\nu+\rho)-\rho}. \quad (5.4)$$

The cancellations in equation (5.4) make the fusion product a truncated tensor product, and provide with a geometric picture of how the truncation occurs. Obtaining the fusion dimension from the formula is done by the application of an algorithm. To calculate all $\mathcal{N}_{\lambda,\mu}^\nu$ for fixed λ, μ the first step is to write down the highest-weight system, which looks like a simple highest-weight representation. Following this, every weight is shifted by the element $\rho = \Lambda^1 + \Lambda^2 + \dots + \Lambda^{N-1}$ for $\widehat{SU}(N)$ $\rho = [1, 1 \dots 1, 1]$ and a weight μ , which is the weight operating on λ . After these two shifts affine Weyl reflection elements are applied on the shifted weights with each reflection flipping the sign of the multiplicity. These reflections are applied until each of the shifted weights are mapped back into the Weyl alcove. Notably, the fact that the sign changes for every primitive reflection implies that all shifted weights along the boundary of the alcove do not contribute to the fusion dimension.

Weyl alcoves are bounded by hyperplanes normal to the simple roots and by the affine wall, which is pushed back as the level k increases. This backward motion of

the affine wall leads to some interesting consequences. Most notably, for the 3-point fusion dimension there will come a level, where the fusion dimension is equal to the corresponding simple Lie algebra tensor product multiplicities. For the case of the tadpole, however, this is not so straightforward. Since the tadpole involves a sum over the Weyl alcove we have to consider the shift due to every weight in the Weyl alcove. Having to shift by every highest-weight element in the Weyl alcove means that we will always have to consider the affine reflection for some of the shifted weights. The required affine component of the tadpoles is unsurprising, since there is no well defined tadpole that naturally emerges from the tensor product alone.²

Since $\mathcal{T}_\lambda = \sum_{\sigma \in P_+^k} \mathcal{N}_{\sigma, \lambda}^\sigma$, the tadpole is the trace of the fusion matrix \mathcal{N}_λ , which have their entries given by the fusion coefficients $\mathcal{N}_{\sigma, \lambda}^\nu$. Fusion matrices treated with the Kac-Walton formula and then traced, by considering equation (5.3), can be used to find a Kac-Walton tadpole formula. These steps are carried out below:

$$\mathcal{T}_\lambda = \sum_{\sigma \in P_+^k} {}^{(g=0, N, k)} \mathcal{N}_{\lambda, \sigma}^\sigma = \sum_{\sigma \in P_+^k} \sum_{\omega \in \hat{W}} (-1)^{l(\omega)} \text{mult}_\lambda((\omega - \mathbb{I}) \cdot (\sigma + \rho)), \quad (5.5)$$

$$= \sum_{\sigma \in P_+^k} {}^{(g=0, N, k)} \mathcal{N}_{\sigma, \bar{\sigma}}^\lambda = \sum_{\sigma \in P_+^k} \sum_{\omega \in \hat{W}} (-1)^{l(\omega)} \text{mult}_\sigma(\omega(\lambda + \rho) - \bar{\sigma} - \rho). \quad (5.6)$$

Unfortunately, the simplification in the weight multiplicities are counteracted by the complexity introduced by the sum over the Weyl alcove. We were not able to find a way of further reducing this Kac-Walton tadpole formula to account for general tadpole properties. The sum over the Weyl alcove in this formula is too unwieldy.

5.2 Berenstein-Zelevinsky Triangles

Berenstein-Zelevinsky triangles (BZ triangles) are a useful combinatorial tool used for computing LR coefficients, which we saw in Section 3.2.3 were equal to the tensor

²The sum over all possible highest-weights for a simple highest-weight representation is clearly divergent.

product multiplicities of $SU(N)$. BZ triangles consist of integer entries, which are used to label a triangle. The origin of the BZ triangle method, like the Kac-Walton formula, is in the computation of tensor product multiplicities. In the original paper [2], Berenstein and Zelevinsky introduced a map between a convex polyhedral cone and the space occupied by the product of the weights. The valid BZ triangles indicate points in this cone and the number of them is equal to its volume.

Valid BZ triangles are written as the linear combination of a set of virtual triangles $\{\mathcal{V}_{i,j}\}$, along with some initial generalized BZ triangle T_0 . This initial BZ triangle must be found by hand, but it is not necessarily unique. Formally, we write the general BZ triangle as the result of a linear combination:

$$T = T_0 + \sum_{\substack{i+j=N-1 \\ i,j \geq 1}} v_{i,j} \mathcal{V}_{i,j} + \sum_h \ell_h \mathcal{L}_{\text{General}}^h, \quad (5.7)$$

with the $\mathcal{L}_{\text{General}}^h$ being the general basis of the triangles under consideration. The coefficients $v_{i,j}$ and ℓ_h are both integers.

The virtual and basis triangles are used to generate all other valid BZ triangles from the initial triangle T_0 with the triangle forms dependent on the group. All valid BZ triangles are required to have non-negative integer entries. All BZ triangles are also constrained by a set of identities, called the hexagon identities: the sum of the two coefficients on the two vertices of an edge of a hexagon must be equal.

The simplest case is that of $SU(2)$, whose entries lay on the triangle corners:

$${}^{SU(2)}T_{\text{General}} = \begin{matrix} & & l_{12} & \\ & & & \\ & m_{12} & & n_{12} \end{matrix}$$

The Dynkin labels of an $SU(2)$ weight are related to the triangle entries by:

$$l_{12} + m_{12} = \nu_1, \quad l_{12} + n_{12} = \mu_1, \quad m_{12} + n_{12} = \lambda_1. \quad (5.8)$$

The corresponding fusion dimension $\mathcal{N}_{\mu,\lambda}^\nu$ is equal to the number of BZ triangles that have non-negative entries, called valid triangles.

BZ triangles can be applied to more general Lie algebras and in this process some new structure emerges. The general BZ triangles are given by the entries:

-

$$\begin{array}{cccc}
 & & & l_{13} \\
 & & m_{12} & n_{23} \\
 {}^{SU(3)}T_{\text{General}} = & & & \\
 & l_{23} & & l_{12} \\
 & m_{13} & n_{12} & m_{23} & n_{13}
 \end{array}$$

For $SU(3)$ valid triangles can be transformed into one another by considering the virtual triangle \mathcal{V} :

$$\mathcal{V} = \begin{array}{cccc}
 & & & 1 \\
 & & -1 & -1 \\
 & -1 & & -1 \\
 1 & -1 & -1 & 1
 \end{array} \tag{5.9}$$

Notably, the number of virtual triangles increases as the group rank increases. In general the virtual triangles are centered on a hexagon and given by:

$$\begin{array}{cccc}
 & & -1 & \\
 -1 & 1 & 1 & -1 \\
 & 1 & & 1 \\
 -1 & 1 & 1 & -1 \\
 & & -1 &
 \end{array} \tag{5.10}$$

With all other virtual triangle entries not appearing in equation (5.10) being zero.

The Dynkin labels correspond to the following triangle entries:

$$\begin{aligned}
 l_{13} + m_{12} &= \nu_1, & l_{23} + m_{13} &= \nu_2, \\
 m_{23} + l_{12} &= \mu_1, & l_{13} + n_{23} &= \mu_2, \\
 m_{13} + n_{12} &= \lambda_1, & m_{23} + n_{13} &= \lambda_2.
 \end{aligned}
 \tag{5.11}$$

There are also sets of equalities that relate certain pairs of entries to other pairs. Called the hexagon identities they are given by the equations:

$$m_{12} + n_{23} = n_{12} + m_{23}, \quad m_{12} + l_{23} = l_{12} + m_{23}, \quad l_{23} + n_{12} = l_{12} + n_{23}. \tag{5.12}$$

These identities occur for every hexagon contained within a BZ triangle. For a given hexagon identity only two of the three resulting identities are linearly independent.

The final BZ triangle that we will be considering is the triangle corresponding to $SU(4)$. For $SU(4)$ the general triangle is given by:

$$\begin{array}{cccccc}
 & & & & & l_{14} \\
 & & & & m_{12} & n_{34} \\
 & & & l_{24} & & l_{13} \\
 {}^{SU(4)}T_{\text{General}} = & & m_{13} & n_{23} & m_{23} & n_{24} \\
 & l_{34} & & l_{23} & & l_{12} \\
 & m_{14} & n_{12} & m_{24} & n_{13} & m_{34} & n_{14}
 \end{array}$$

Notably there are now three hexagons and so three different sets of hexagon identities and three virtual triangles. The virtual triangles can be found by centering the general virtual triangle entries in equation (5.10). And the hexagon identities can be

read off as:

$$\begin{aligned}
m_{13} + n_{23} &= n_{12} + m_{24}, & l_{23} + m_{24} &= m_{13} + l_{34}, & l_{23} + n_{23} &= l_{12} + m_{34}, \\
m_{34} + n_{13} &= m_{23} + n_{24}, & l_{12} + n_{24} &= n_{13} + l_{23}, & l_{12} + m_{34} &= m_{23} + l_{23}, \\
m_{12} + n_{34} &= n_{23} + m_{23}, & l_{13} + n_{34} &= l_{24} + n_{23}, & l_{24} + m_{12} &= l_{13} + n_{23}.
\end{aligned} \tag{5.13}$$

Adapting the BZ triangles to computing fusion dimensions is done by the introduction of a truncative restriction based on the threshold level. These restrictions can be found and are known for the first few ranks, but become increasingly problematic to obtain once the rank+1 $N \geq 3$ [36]. The number of valid generalized BZ triangles equals the fusion dimension. This counting of the valid BZ triangles can also be understood as finding the volume of a discrete polytope [8].

To apply the BZ triangles to fusion, a condition that accounts for the threshold level [1] must be included. Those triangles that satisfy the threshold level condition we call ‘generalized BZ triangles.’ The number of generalized triangles³ found as standard BZ triangles that also meet the threshold level constraint.

Threshold level conditions are non-trivial to calculate. As the rank of the group increases the size of the BZ triangle basis, the number of virtual triangles increase, but the number of conditions on the threshold level increases substantially. Consequently, the number of constraint equations and finding these constraints are the primary obstacle in applying the generalized BZ triangles. It is interesting to note that the generalized BZ triangles can, in principle, be applied to n -point fusion [8].

Like the Kac-Walton formula, the generalized BZ triangle method interprets the fusion dimensions as truncated tensor product multiplicities. The application of the generalized BZ triangles to the computation of tadpoles runs somewhat counter to our

³A general BZ triangle is the general form that a triangle can take, whereas a generalized BZ triangle refers to those BZ triangles relevant to the fusion dimension calculation.

goals of wanting a manifestly affine account of the fusion dimension. However, they were useful as an alternative method of computation. Their utility is in accounting for properties of the tadpoles, which were noted in computer calculation. Application of the generalized BZ triangles to the tadpoles results in a large amount of simplification. Specifically, using that $\sigma_i = \bar{\sigma}_{N-i}$ and identifying each Dynkin labels with the two entries it corresponds to. From the general form of the BZ triangles we know that $\sigma_i = l_{iN} + m_{1(i+1)}$ and $\bar{\sigma}_i = n_{iN} + l_{1(i+1)}$. Then imposing the tadpole condition $\sigma_i = \bar{\sigma}_{N-i}$ we find that we require:

$$n_{(N-i)N} + l_{1(N-i+1)} = l_{iN} + m_{1(i+1)} \quad (5.14)$$

The tadpole for $\widehat{SU}(3)$ permits a particularly simple form of BZ triangle and has a, relatively, simple threshold level condition. It is considered as a first example and a previously obtained general tadpole formula for $N = 3$ re-emerges [8].

Example 9. *Our triangle for $\widehat{SU}(3)$ is identical to the BZ triangle of $SU(3)$ as used in the tensor product. Virtual and basis triangles can be added to a starting triangle to find all valid triangles based on equation (5.15). In the case of the tadpoles the only valid basis triangles will be those that keep the two sides equal $\mathcal{L}_{\text{Loop}} \subset \mathcal{L}_{\text{General}}$. We choose the two upper sides of the tadpole triangle to be the sides we keep equivalent. The appropriate loop triangles for $\widehat{SU}(3)$ are contained in equation (5.16). We have the linear relation for the valid BZ triangles given as:*

$$T = T_0 + v\mathcal{V} + \sum_{i=1}^2 \ell_i \mathcal{L}_{\text{Loop}}. \quad (5.15)$$

For $\widehat{SU}(3)$ the lone virtual triangle \mathcal{V} was noted in equation (5.9). We also have the loop triangles, which are introduced as the tadpole basis. The two loop triangles for

$$\begin{array}{lll}
 0 \leq \lambda_1 + v & 0 \leq (\lambda_1 - \lambda_2) - v & 0 \leq -(\lambda_1 - \lambda_2) - v, \\
 0 \leq (\lambda_1 - \lambda_2) - v + \ell_2 & 0 \leq -v & 0 \leq k - 2\lambda_1 - \ell_1 - \ell_2 - v, \\
 0 \leq k - \lambda_1 - \lambda_2 - \ell_1 - \ell_2 - v & 0 \leq k - \lambda_1 - \lambda_2 - \ell_1 - v & 0 \leq v + \ell_1 \\
 \lambda_2 + v & 0 \leq -v + \ell_2. &
 \end{array}$$

Using these constraints on the summation we can determine the possible values of the coefficients of v, ℓ_1, ℓ_2 corresponding to the generalized BZ triangles. For the special case of $\widehat{SU}(3)$, there is a general formula for any tadpole. Writing the result in terms of the Dynkin labels of λ :

$$\mathcal{T}_\lambda = \frac{1}{2}(\min\{\lambda_1, \lambda_2\} + 1)(k + 1 - \max\{\lambda_1, \lambda_2\})(k + 1 - \lambda_1 - \lambda_2). \quad (5.19)$$

This $\widehat{SU}(3)$ result is well known and suggests that generalized BZ triangles are very applicable to the study of tadpoles and their properties.

Higher rank groups do not permit a general formula in the same form as equation (5.19), however the procedure of constraining the coefficients and then summing over their allowed values remains valid. The constraints were written into a *Mathematica* code and we found that tadpoles for highest-weights in $\widehat{SU}(4)$ could be written rather nicely in many cases. One such example was computed for the adjoint weight $[1, 0, 1]$:

$$\mathcal{T}_\lambda = (k - 1) \frac{(k + 3)(k + 2)(k + 1)}{2!} := (k - 1) \frac{(k + 3)^{\underline{3}}}{2}. \quad (5.20)$$

The second line uses the falling power notation, which is defined by $(N + k)^{\underline{L}} := (N + k)(N + k - 1) \cdots (N + k - L + 1)$ with $(N + k)^{\underline{N+k}} = (N + k)!$. We introduce this notation here in order to write this result in the form suggested by other observations and attempts to explain these observation carried out in Appendix A.1.

The main advantage of the falling power notation is that it is reminiscent of the behaviors of polynomials for integration, but are applicable to summing procedures.

We can define the forward difference of a discrete function $f(x)$ as $\Delta_x(f(x)) = f(x+1) - f(x)$. Falling powers $(a+x)^n$ have the forward difference as $\Delta_x(a+x)^n = (a+x+1)^n - (a+x)^n = (a+x)^{n-1}(a+x+1 - (a+x-n+1)) = n(a+x)^{n-1}$. These falling powers have the particularly useful property of:

$$\sum_{x=a}^A \Delta_x f(x) = f(A+1) - f(a). \quad (5.21)$$

Falling powers have the notable property:

$$\sum_{x=b}^B (a+x)^n = \frac{1}{n+1} \sum_{x=b}^B \Delta_x ((a+x)^{n+1}) = \frac{(B+a+1)^{n+1} - (a+b)^{n+1}}{n+1}. \quad (5.22)$$

The tadpole formula for highest-weights in $\widehat{SU}(3)$ can be written so as to match the notation of (5.20). Taking $\lambda_1 = \lambda_2 = H$ we have the tadpole value:

$${}^{k \geq 2H} \mathcal{T}_{[H,H]} = \frac{1}{2} (H+1)(k+1-H)(k+1-2H), \quad (5.23)$$

$$\mathcal{T}_{[H,H]} = \frac{1}{3!} ((k-H+2)^2(H+1)^1 - (k-H+2)^1(H+1)^2). \quad (5.24)$$

Restricting to a highest-weight of $\widehat{SU}(4)$ that has $\lambda_1 = \lambda_3 = H$ we find a similar equation:

$${}^k \mathcal{T}_{[H,0,H]} = \frac{2}{4!} ((k-H+3)^2(H+2)^2(k-2H+1)), \quad (5.25)$$

$${}^k \mathcal{T}_{[H,0,H]} = \frac{2}{4!} ((k-H+3)^3(H+2)^2 - (k-H+3)^2(H+2)^3). \quad (5.26)$$

For both equations (5.23) and (5.25) we have ${}^{k=2H-1} \mathcal{T}_{[H,0,H]} = 0$ and ${}^{k=2H-1} \mathcal{T}_{[H,H]} = 0$, as expected.

We consider a second worked example for the adjoint weight of $\widehat{SU}(4)$ in order to demonstrate how the difficulty of the computation increases from $\widehat{SU}(3)$ to $\widehat{SU}(4)$.

Example 10. *Considering a generalized BZ triangle for the adjoint highest-weight*

representation, $[1, 0, 1]$, from $\widehat{SU}(4)$. One valid BZ triangle is:

$$T_0 = \begin{array}{cccccc} & & & & & 0 \\ & & & & & 0 & 0 \\ & & & & & 0 & & 0 \\ & & & & & 0 & 0 & 0 & 0 \\ & & & & & 0 & & & 0 \\ & & & & & 1 & 0 & 0 & 0 & 0 & 1 \end{array} . \quad (5.27)$$

For the tadpole we must impose the additional tadpole condition in equation (5.14) on the triangle entries. For $\widehat{SU}(4)$ this result leaves us with three loop triangles:

$$L_1 = \begin{array}{cccccc} & & & & & 1 \\ & & & & & 0 & 0 \\ & & & & & 0 & & 0 \\ & & & & & 0 & 0 & 0 & 0 \\ & & & & & 0 & & & 0 \\ & & & & & 0 & 0 & 0 & 0 & 0 & 0 \end{array} , \quad (5.28)$$

$$L_2 = \begin{array}{cccccc}
 & & & 0 & & \\
 & & & 0 & 0 & \\
 & & 1 & & 1 & \\
 & 0 & 0 & 0 & 0 & \\
 0 & 0 & 0 & 0 & 0 & 0 \\
 & & & & &
 \end{array}, \tag{5.29}$$

$$L_3 = \begin{array}{cccccc}
 & & & 0 & & \\
 & & & 0 & 0 & \\
 & & 0 & & 0 & \\
 & 0 & 0 & 0 & 0 & \\
 1 & & 1 & & 1 & \\
 0 & 0 & 0 & 0 & 0 & 0 \\
 & & & & &
 \end{array} \tag{5.30}$$

From the initial triangle T_0 we can add and subtract virtual triangles, which for this

example yields:

$$T_1 = \begin{array}{cccccc} & & & 0 & & \\ & & & 0 & 0 & \\ & & 0 & & 0 & \\ & 1 & 0 & 0 & 1 & \\ 0 & & 0 & & 0 & \\ 0 & 1 & 0 & 0 & 1 & 0 \end{array}, \quad (5.31)$$

$$T_2 = \begin{array}{cccccc} & & & 0 & & \\ & & & 1 & 1 & \\ & & 0 & & 0 & \\ & 0 & 1 & 1 & 0 & \\ 0 & & 0 & & 0 & \\ 0 & 1 & 0 & 0 & 1 & 0 \end{array}. \quad (5.32)$$

We reduce the triangles found from adding the virtual triangles by subtracting off all loop triangles, we call these our ‘starting triangles.’ The main advantage of reducing to the starting triangles is that it allows us to restrict the coefficients ℓ_i to be non-negative. Applying the loop triangles to the starting triangles, T_0, T_1, T_2 , we will obtain all valid BZ triangles. To obtain the fusion dimension, we also impose the threshold level constraints, thereby removing some of the otherwise valid triangles.

For $\widehat{SU}(4)$ the threshold level constraints are:

$$\begin{aligned}
 k_0 = \max\{ & \lambda_1 + \lambda_2 + \lambda_3 + l_{14}, \mu_1 + \mu_2 + \mu_3 + m_{14}, \\
 & \nu_1 + \nu_2 + \nu_3 + n_{14}, \lambda_1 + \lambda_2 + l_{14} + l_{24} + n_{14}, \\
 & \lambda_2 + \lambda_3 + l_{14} + l_{13} + m_{14}, \mu_1 + \mu_2 + m_{14} + m_{24} + l_{14}, \\
 & \mu_2 + \mu_3 + m_{14} + m_{13} + n_{14}, \nu_1 + \nu_2 + n_{14} + n_{24} + m_{14}, \\
 & \nu_2 + \nu_3 + n_{14} + n_{13} + l_{14}, \\
 & l_{14} + m_{14} + n_{14} + \frac{1}{2}(\lambda_2 + \mu_2 + \nu_2 + l_{23} + m_{23} + n_{23} + 1)\} \quad (5.33)
 \end{aligned}$$

Using the tadpole condition, which requires that the weights of two of the edges be conjugate only results in a moderate simplification. By also applying the assumption that $\lambda_1 = 1 = \lambda_3$ and $\lambda_2 = 0$, the conditions can be substantially reduced. Using that the loop triangle coefficients are ℓ_j and considering the delta functions as accounting for the index of the starting triangles T_i :

$$\begin{aligned}
 k_0 = \max\{ & 2 + \ell_3, 1 + \ell_3 + \ell_2 + \ell_1 + \delta_i^0, \ell_2 + \ell_3 + 2(\delta_i^0 + \delta_i^1) + \delta_i^2, \\
 & 2\delta_i^0 + \delta_i^2 + \ell_1 + \ell_2 + \ell_3, \ell_3 + \ell_2 + 2\delta_i^0 + \delta_i^1 + \frac{1}{2}(\ell_1 + m_{23} + n_{23} + 1)\} \quad (5.34)
 \end{aligned}$$

Interestingly, $(\ell_1 + m_{23} + n_{23})$ is just the sum of the internal labels in the BZ triangle. From here it is straightforward to count the number of allowed triangles for T_0 , T_1 , and T_2 . Taking $k = 3$ we find that T_0 contributes 4, T_1 contributes 5, and T_2 contributes 11. Adding them together we obtain the expected value for the adjoint tadpole at $k = 3$:

$${}^{(k=3)}\mathcal{T}_{[1,0,1]} = 4 + 5 + 11 = 20 \quad (5.35)$$

As this example illustrates the threshold level condition becomes unwieldy very

quickly. This is further complicated by the appearance of affine constraints beyond the constraints introduced by elementary couplings between weights [36]. These affine constraints emerge when $N \geq 3$ and make finding the threshold condition substantially more difficult.

5.2.1 Partial Proof of Equation (5.37)

Investigations of the tadpole resulted in the observation of the following property:

$${}^{(k+jN)}\mathcal{T}_{\lambda+(jN)\Lambda_1} = {}^{(k)}\mathcal{T}_\lambda, \quad (5.36)$$

for certain weights λ . This relationship also works if Λ_1 is replaced with Λ_{N-1} .

Any valid BZ triangle, with the loop coefficient entries being at a minimum non-negative integer value, is given by:

$$T_{\text{Start}} = T_0 + \sum_{i,j \geq 1}^{i+j=N-1} v_{i,j} \mathcal{V}_{i,j} - \sum_k |\ell_k| \mathcal{L}_k.$$

The T_{Start} are valid BZ triangles that will no longer be valid after an additional subtraction of a loop triangle and are called the ‘starting triangles.’ Starting triangles, as used in the example, can be used to build up valid BZ triangles by adding the loop triangles to them. These starting triangles are particularly important for our proof of equation (5.37).

Theorem 1. *For any highest-weight $\lambda = \lambda_1, 0, \dots, 0, \lambda_{N-1}$ with $\lambda_1 \geq \lambda_{N-1}$ of $\widehat{SU}(N)$ with $N = 2, 3, 4$, the tadpole corresponding to the λ obey the following property:*

$${}^{(k)}\mathcal{T}_\lambda = {}^{(k+jN)}\mathcal{T}_{\lambda+(jN)\Lambda_1}. \quad (5.37)$$

Proof. For $\widehat{SU}(3)$ we can use the general formula for the tadpole to demonstrate this property without too much difficulty. The relation follows once we note that the

From the threshold level condition we have the constraints:

$$\begin{aligned}
 k_0 = \max\{ & \lambda_1 + \lambda_2 + \lambda_3 + l_{14}, \mu_1 + \mu_2 + \mu_3 + m_{14}, \nu_1 + \nu_2 + \nu_3 + n_{14}, \\
 & \lambda_1 + \lambda_2 + l_{14} + l_{24} + n_{14}, \lambda_2 + \lambda_3 + l_{14} + l_{13} + m_{14}, \\
 & \mu_1 + \mu_2 + m_{14} + m_{24} + l_{14}, \mu_2 + \mu_3 + m_{14} + m_{13} + n_{14}, \\
 & \nu_1 + \nu_2 + n_{14} + n_{24} + m_{14}, \nu_2 + \nu_3 + n_{14} + n_{13} + l_{14}, \\
 & l_{14} + m_{14} + n_{14} + \frac{1}{2}(\lambda_2 + \mu_2 + \nu_2 + l_{23} + m_{23} + n_{23} + 1)\}, \quad (5.39)
 \end{aligned}$$

and by adding $T_{4\Lambda_1}$ we obtain the shifted constraints:

$$\begin{aligned}
 k_{\lambda+4\Lambda,0} = \max\{ & \lambda_1 + 4 + \lambda_2 + \lambda_3 + l_{14}, \mu_1 + \mu_2 + \mu_3 + m_{14} + 4, \\
 & \lambda_1 + 4 + \lambda_2 + l_{14} + l_{24} + n_{14}, \mu_2 + \mu_3 + m_{14} + m_{13} + 4 + n_{14}, \\
 & l_{14} + m_{14} + n_{14} + \frac{1}{2}(\lambda_2 + \mu_2 + \nu_2 + l_{23} + m_{23} + n_{23} + 1) + \left(\frac{5}{2}\right) + 1. \quad (5.40)
 \end{aligned}$$

Those threshold conditions that do not increase in increments of 4 are:

$$\begin{aligned}
 & \nu_1 + \nu_2 + \nu_3 + n_{14} + 3, \mu_1 + \mu_2 + m_{14} + m_{24} + l_{14} + 3, \nu_1 + \nu_2 + n_{14} + n_{24} + m_{14} + 3, \\
 & \lambda_2 + \lambda_3 + l_{14} + l_{13} + m_{14} + 2, \nu_2 + \nu_3 + n_{14} + n_{13} + l_{14} + 2. \quad (5.41)
 \end{aligned}$$

These incorrectly shifted constraints will be kept in mind and based on the requirement that the number of starting triangles is not changed we will find they are always smaller than the other threshold constraints. Requiring an unchanging

number of starting triangles we require T_λ to have the form:

$$T_\lambda = \begin{array}{cccccc}
 & & & & & 0 \\
 & & & & m_{12} & n_{34} \\
 & & & l_{24} & & l_{13} \\
 T_\lambda = & & m_{13} & n_{23} & 0 & 0 \\
 & l_{34} & & l_{23} & & l_{12} \\
 m_{14} & n_{12} & 0 & 0 & m_{34} & n_{14}
 \end{array} \quad (5.42)$$

We can use the six independent hexagon symmetries of the BZ triangle and the three edge constraints, which emerge from our considering the tadpole. These are:

$$\begin{aligned}
 m_{13} + n_{23} &= n_{12}, & l_{23} &= m_{13} + l_{34}, & l_{23} &= l_{12} + m_{34}, \\
 m_{34} &= 0, & l_{13} &= m_{12} + l_{24}, & n_{23} &= m_{12} + n_{34}, \\
 m_{12} &= n_{34}, & l_{13} &= l_{24} + m_{13}, & l_{34} + m_{14} &= l_{12} + n_{14}.
 \end{aligned} \quad (5.43)$$

Applying these we find that any weight that satisfies these identities must have a starting triangle with coefficients:

$$T_\lambda = \begin{array}{cccccc}
 & & & & & 0 \\
 & & & & m_{12} & m_{12} \\
 & & 0 & & m_{12} & \\
 T_\lambda = & & m_{12} & 2m_{12} & 0 & 0 \\
 & 0 & & m_{12} & & m_{12} \\
 m_{14} & 3m_{12} & 0 & 0 & 0 & n_{14}
 \end{array} . \quad (5.44)$$

These BZ triangles corresponding to a highest-weight $\lambda = [m_{14} + 3m_{12}, 0, n_{14}] = n_{14}[1, 0, 1] + m_{12}[4, 0, 0]$. By considering the threshold level conditions in equation (5.41) on this type of weight, it follows that the constraints are always smaller than

interesting is that we can consider $2\Lambda_2 = [0, 2, 0]$, whose number of starting triangles is the same. By adding $2\Lambda_2 + 2\Lambda_2 = [0, 4, 0]$, which we expect to have three unique starting triangles. These three starting triangles are read off of the work for $2\Lambda_2$ in equation (5.45) resulting in the unique starting triangles:

$$T_{2\Lambda_2,1} + T_{\Lambda_2,1}, \quad T_{2\Lambda_2,1} + T_{2\Lambda_2,2}, \quad T_{2\Lambda_2,2} + T_{2\Lambda_2,2}, \quad (5.47)$$

with addition occurring coefficient in shared triangle positions. Notably, we can observe from the tables that ${}^{(k)}\mathcal{T}_{[0,2,0]} = \left(\frac{3}{2}\right) {}^{(k+2)}\mathcal{T}_{[0,4,0]}$. This is a curious relationship, but not a particularly general one, as far as we could tell.

Motivated by our discussion of how $\Lambda_1 \rightarrow \Lambda_2$ in (5.37) of $\widehat{SU}(4)$ fails to keep the number of starting triangles constant, we can consider the fundamental weight $5\Lambda_2$ of $\widehat{SU}(5)$ and note that it too fails the constant number of starting triangles condition. This analysis is done in a similar vein as equation (5.42), where we want to show that the starting triangle condition will be valid.

A starting triangle for the highest-weight $5\Lambda_2$ can be written as:

$$T_{\Lambda_1} = \begin{array}{cccccccc} & & & & & & & 0 \\ & & & & & & & 1 & 1 \\ & & & & & & & 1 & & 0 \\ & & & & & & & 0 & 0 & 2 & 1 \\ & & & & & & & 0 & & & 2 \\ & & & & & & & 2 & 0 & 0 & 3 & 0 & 0 \\ & & & & & & & 0 & & 0 & & 0 & & 0 \\ & & & & & & & 0 & 0 & 2 & 3 & 0 & 0 & 0 & 0 \end{array} \quad (5.48)$$

which permits the second valid starting triangle:

$$\begin{array}{cccccccc}
 & & & & & & & 0 \\
 & & & & & & 1 & 1 \\
 & & & & & 0 & & 0 \\
 & & & 1 & 1 & 1 & 1 & \\
 T_{\Lambda_1} = & & 1 & & & 1 & & 2 \\
 & & & 1 & 1 & 1 & 2 & 0 & 0 \\
 & & 1 & & 0 & & 1 & & 1 \\
 & 0 & 0 & 2 & 3 & 0 & 0 & 0 & 0
 \end{array} \tag{5.49}$$

For any highest-weight $N\Lambda_i$ the corresponding BZ triangles will permit more than one starting triangle. This can be seen by noting that starting triangles can be envisioned as stacks of lower rank starting triangle of a similar type.

Lemma 1. *For every $N\Lambda_i$, where $i \neq 1, N - 1$, there will be more than one starting triangle.*

Proof. Marking the BZ entries along the base of the triangle as we move up we find hexagons of the form:

$$\begin{array}{ccc}
 0 & & 0 \\
 H & J - H & \\
 0 & & H \\
 J & 0 &
 \end{array} , \quad
 \begin{array}{ccc}
 & & \\
 & J - H & H \\
 H & & 0 \\
 & 0 & J
 \end{array} , \tag{5.50}$$

with $J - H > 0$. Virtual triangles are characterized by a single hexagon of type:

$$\begin{array}{cccc}
 & & -1 & \\
 & -1 & 1 & 1 & -1 \\
 & & 1 & & 1 & . \\
 & -1 & 1 & 1 & -1 \\
 & & -1 & & &
 \end{array} \tag{5.51}$$

Combining a large number of them we can write long virtual triangles with coefficients above and below cancelled by the addition of loop triangles:

$$\begin{array}{cccccccc}
 & & 0 & & & & 0 & \\
 -1 & 1 & 0 & 0 & 0 & 0 & 1 & -1 \\
 & 1 & & 2 & \dots & 2 & & 1 \\
 -1 & 1 & 0 & 0 & 0 & 0 & 1 & -1 \\
 & & 0 & & & & 0 &
 \end{array} \tag{5.52}$$

The hexagons in equation (5.50) appear along a diagonal extending from the initial non-zero coefficients, they will occur along the same horizontal line. Looking at the horizontal above their position we have:

$$\begin{array}{cccccccc}
 & & 0 & & & & 0 & \\
 & J - H - K' & & K' & & u_1 \dots u_i & & K & & J - H - K \\
 K' & & & & 0 & & & 0 & & & K \\
 & 0 & & J - H & & H \dots H & & J - H & & 0 \\
 & & H & & & & & & & H &
 \end{array} \tag{5.53}$$

A BZ triangle with a row of hexagons as described in equation (5.53) can be acted

on by the long root defined in equation (5.52), with non-negative u_i . This situation occurs whenever two hexagons of the type defined by equation (5.50) can be written as in equation (5.53), but this condition is only possible when the highest weight $N\Lambda_i$ has $i \neq 1, N - 1$. \square

Equation (5.2) can be used to write the partial trace of the tensor product multiplicities $\sum_{\sigma \in P_+^k} \mathcal{C}_{\sigma, \bar{\sigma}}^\lambda$ and identified them as being an artificial tensor product tadpole. These partial trace multiplicities are easier to work with, since they have no threshold level conditions. Consequently, whenever the starting triangles are unchanged the partial trace multiplicity will obey a similar property as in equation (5.37). A tensor product tadpole $\sum_{\sigma \in P_+^k} \mathcal{C}_{\sigma, \bar{\sigma}}^\lambda := {}^{(k)}\mathcal{C}^\lambda$ is defined over the Weyl alcove at a level k . These tensor product tadpoles can be related back to the fusion tadpoles by:

$${}^{(k)}\mathcal{T}_\lambda = \sum_{\omega \in \widehat{W}} (-1)^{\ell(\omega)} {}^{(k)}\mathcal{C}_{\omega \cdot \lambda} \tag{5.54}$$

Theorem 2. *For a weight λ whose transform $\lambda + (j \cdot N)\Lambda_i$, with $i = 1, N - 1$, has the same number of starting triangles then the tensor product tadpoles are related by:*

$${}^{(k)}\mathcal{C}^\lambda = {}^{(k+j(N-1))}\mathcal{C}^{\lambda+(jN)\Lambda_i} \tag{5.55}$$

Proof. A proof of this relation is performed by finding the starting triangles for each of the fundamental weights of the BZ triangles. From lemma 1 we know that the highest-weights $N\Lambda_i$ with $i \neq 1, N - 1$ fail our requirement of a unique starting triangle. So we need consider only $N\Lambda_1$ and $N\Lambda_{N-1}$. Since these are related to one another via conjugation we can without loss of generality we can consider $N\Lambda_1$ alone.

We begin with the claim that the highest-weight $N\Lambda_1$ for any $\widehat{SU}(N)$ has a BZ triangle given as:

$$T_{N\Lambda_1} = \begin{array}{cccccccc}
 & & & & & & & 0 \\
 & & & & & & 1 & 1 \\
 & & & & & 0 & & 1 \\
 & & & 1 & & 2 & 0 & 0 \\
 & & & \dots & & & & \dots \\
 & & & & 0 & & & 1 \\
 & & 1 & & N-2 & 0 & 0 & 0 & 0 \\
 & 0 & & & 1 & \dots & 1 & & 1 \\
 1 & N-1 & 0 & 0 & 0 & 0 & 0 & 0 & 0
 \end{array} .$$

The proof of this claim follows from an induction argument, which uses that the BZ triangle contains BZ triangles of $(N - j)\Lambda_1$, for $j \leq N - 2$.

We note that the sum of the coefficients on the two top sides are $N - 1$ and the bottom has a sum of N . Loop triangles are the only valid basis and so it follows that the number of triangles that can be formed at $k + N - 1$ for the highest-weight $\lambda + N\Lambda_1$ are equal to those formed by the highest-weight λ at level k . \square

5.3 Verlinde Formula and Symmetric Polynomials

We were interested in investigating possible explanations of the fusion dimension that were both combinatorial and naturally affine. As a fundamentally affine result, the Verlinde formula provides the most natural starting point for this analysis. The Verlinde formula can be broken up into partial sums based on symmetries of the highest-weight representations that are summed over in the calculation. Analysis of these partial sums were carried out (see Section 6.1) in the hopes of finding a combinatorial atom of the fusion tadpole.

Applying the Verlinde formula requires choosing a fusion dimension to calculate. Due to their relative simplicity and their fundamentally affine nature, we considered calculation of the tadpoles via the Verlinde formula. It is possible to build up a

similar object to the tadpole for tensor products via a partial trace. The tensor product tadpole is the result of this partial trace and is motivated by the level k selecting out the Weyl alcove $P_+^k \subset P_+$ (5.2), but are not an obviously natural object. Treating an affine object, with a manifestly affine equation it was suspected that this should provide a window into some underlying structure.

Combining the Verlinde formula (4.28) with the Kac-Peterson relation (4.25), the tadpoles can be written in terms of roots of unity. These roots of unity have degrees written in terms of bilinear products of weights in the horizontal highest-weight representation and Weyl alcove and the level k and the dual-Coxeter number h^\vee :

$$\mathcal{T}_\lambda = \sum_{\sigma \in P_+^k} \mathcal{N}_{\lambda, \sigma}^\sigma = \sum_{\sigma \in P_+^k} \sum_{\alpha \in P(\lambda)} \text{mult}_\lambda(\alpha) \exp \left\{ \frac{2\pi i}{k + h^\vee} \alpha \cdot (\sigma + \rho) \right\}. \quad (5.56)$$

This form of the Verlinde formula expresses tadpoles as sums of complex numbers, but we would like a way to write them in terms of non-negative integers. Fusion coefficients ${}^{(k)}\mathcal{N}_{\mu, \lambda}^\nu$ are known to be non-negative-integer-valued, but a combinatorial and fundamentally affine description has yet to emerge. Based on our knowledge of the tensor product multiplicities a combinatorial account of fusion is still expected to be possible.

Tadpoles calculated from these roots of unity considerations were compiled into tables for a variety of group ranks and highest-weight representations in Appendix B.1. Attacking these sums head on, computing sums in a brute force manner, did not result in any obvious simplifications. Instead of strong-arming the Verlinde formula, we attempted to rewrite the formula in order to remove some of the more complicated pieces. We use the notation

$$\sigma^\alpha := e^{\frac{2\pi i}{k+N} \alpha \cdot (\sigma + \rho)}, \quad (5.57)$$

where we have dropped the fraction in the exponent.

Then the tadpole Verlinde formula becomes:

$$\mathcal{T}_\lambda = \sum_{\sigma \in P_+^k} \sum_{\alpha \in P(\lambda)} \text{mult}_\lambda(\alpha) \sigma^\alpha = \sum_{\alpha \in P(\lambda)} \text{mult}_\lambda(\alpha) \sum_{\sigma \in P_+^k} \sigma^\alpha. \quad (5.58)$$

We can break up the horizontal highest-weight representations into Weyl orbits and pull the weight multiplicity out from one of the sums. Written as:

$$\mathcal{T}_\lambda = \sum_{\beta \in P(\lambda)/W} \text{mult}_\lambda(\beta) \left(\sum_{\alpha \in W(\beta)} \sum_{\sigma \in P_+^k} \sigma^\alpha \right), \quad (5.59)$$

where the brackets should be noted as containing a level dependent sum.

Tadpoles can also be written, via the Schur-Weyl duality [38], in terms of Kostka numbers and symmetric polynomials. Reminding ourselves that we can jump between Dynkin label and partition notation for the weights, via the transformation in equation (3.8), we introduce the Schur polynomials.

Definition 16. *Schur polynomials are a basis of the symmetric polynomials and given by the sum over SSYT filling of a tableau $T(\lambda)$:*

$$s_{(\lambda)}(X) = \sum_{\text{SSYT}(\lambda, \mu)} X^T = \sum_T X_1^{\mu(1)} X_2^{\mu(2)} \dots X_{N-1}^{\mu(N-1)} X_N^{\mu(N)}, \quad (5.60)$$

where the sum is taken over all valid SSYT with content (μ) and shape λ .

Schur polynomial correspondence with the tadpoles, in the case of $\widehat{SU}(N)$, is done by the a relationship between the S -modular matrix and the Schur polynomials:

$$\frac{S_{\lambda, \sigma}}{S_{0, \sigma}} = s_\lambda(X(\sigma)),$$

$$\mathcal{T}_\lambda = \sum_{\sigma \in P_+^k} s_\lambda(X(\sigma)). \quad (5.61)$$

Schur polynomials have been treated with Weyl orbits in the past to understand weight multiplicities. This pushed us in the direction pursued in Appendix A.1. We use a different basis for the symmetric polynomials, called the symmetric monomials, in order to treat the tadpole in a piece-wise way.

Definition 17. *Like the Schur polynomials, the symmetric monomials form a basis of the symmetric polynomials. They are invariant under operations of the symmetric group S_N . Let L be the length of the partition $(\lambda) = (\lambda_{(1)}, \dots, \lambda_{(L)})$ and $(\lambda) \vdash jN$. Then the symmetric monomials take the form:*

$$M_\lambda(\sigma) = \sum_{s \in S_N} \sigma_{s(1)}^{\lambda_{(1)}} \cdots \sigma_{s(L)}^{\lambda_{(L)}}, \quad (5.62)$$

where $X_j^{\lambda_i}(\sigma) := \sigma_j^{\lambda_i}$.

Rewriting the tadpoles in terms of symmetric polynomials provides us with powerful combinatorial techniques [29]. Interpreting the symmetric polynomials as forming a fusion ring also lets us talk about fusion using fundamentally combinatorial objects.

The isomorphism between the symmetric group and the horizontal Weyl group for $\widehat{SU}(N)$ indicates that the symmetric monomials are invariant under the horizontal Weyl group action. So we label the symmetric monomials by the dominant weights from the corresponding highest-weight representation. This lets us reproduce the situation of equation (5.59), where the symmetric monomials select out the appropriate horizontal Weyl orbits. By replacing the weight multiplicity with the corresponding Kostka number we write:

$$\mathcal{T}_\lambda = \sum_{(\mu) \preceq (\lambda)} K_{(\lambda),(\mu)} \sum_{\sigma \in P_+^k} M_\mu(\sigma). \quad (5.63)$$

By equation (3.8) we can rewrite the weights as partitions and vice-versa. This allows us to consider the Verlinde formula in terms of symmetric polynomials and monomials.

The question of how the sum over the Weyl alcove in a different light.

This observation is central to our investigation in Section A.1 and is an attempt to simplify the sum over the roots of unity into an easily computed form. Symmetric monomial decomposition behaviour, given by equation (A.7), along with the fusion ideals in the symmetric polynomials [40], are the tools we use to simplify the sums via some constraint procedures. Fusion ideals are interesting in that their imposition results in an isomorphism between the behaviour of symmetric polynomials and the fusion product. They are, for $\widehat{SU}(N)$, defined as [19]:

$$s_{(1^N)}(\sigma) = M_{(1^N)}(\sigma) = 1, \quad \sum_{\sigma \in P_+^k} M_{\mu'}(\sigma) = 0, \quad (5.64)$$

where μ' is not a partition of jN for some positive integer j . The ideals are known and have been applied to fusion in the past, but this is their first application to tadpoles and the dominant weight sums.

Our work in Appendix A.1 focuses on adding constraints to the monomials through the ideals. With this procedure we are able to reduce the sums into easily computable forms for certain weights, although the method is still largely conjectural. Since it was based on intuition and several arguably sound, but unproven, assumptions the results were not proven. Despite their conjectural nature the formulas replicated the table values produced in Appendix B.1 for a variety of highest-weights and group ranks.

Chapter 6

Experimental Investigations of the Affine Tadpole

The calculations of the tadpoles in the previous chapter provided some insight, but were based on tensor product methods. They could not provide the hoped for expression of the tadpole in terms of non-negative-integer-valued quantities.

We turn to the Verlinde formula (4.31), whose affine pedigree is indisputable. With $N = 1$, $g = 1$ (4.31) gives:

$$\mathcal{T}_\lambda = \sum_{\sigma \in P_+^k} \frac{S_{\lambda, \sigma}}{S_{0, \sigma}}. \quad (6.1)$$

This is a sum over a discrete set of values of the simple Lie characters.

We can also understand the tadpoles resulting from the joining of two legs of a 3-point fusion, see Figure 4.6. This consideration lets us write the one point fusion product as:

$$\bigoplus_{\sigma \in P_+^k} R(\sigma) \otimes_k R(\bar{\sigma}) = \bigoplus_{\lambda \in P_+^k} \mathcal{T}_\lambda R(\lambda), \quad (6.2)$$

which can be understood as a sum of a specific form of fusion product. Consideration of the tadpole in this form also suggests that $\overline{\mathcal{T}}_\lambda = \mathcal{T}_\lambda$, which follows from $\mathcal{N}_{\mu, \lambda}^\nu = \mathcal{N}_{\mu, \bar{\lambda}}^{\bar{\nu}}$.

The action of the simple current symmetry can be used to restrict the types of highest-weights that need to be considered to those appearing in the root lattice.¹ The S -modular matrices can be acted on with simple current operators $r \in \mathcal{R}$ and introduce a phase shift as $S_{r(\lambda), \sigma} = \exp(2\pi i \lambda \cdot r(\Lambda^0)) S_{\lambda, \sigma}$. This, when combined with the definition of the tadpole results in:

$$\begin{aligned} \mathcal{T}_\lambda &= \sum_{\sigma \in P_+^k} \frac{S_{\lambda, \sigma}}{S_{0, \sigma}} = \sum_{r(\sigma) \in P_+^k} \frac{S_{\lambda, r(\sigma)}}{S_{0, r(\sigma)}}, \\ \mathcal{T}_\lambda &= \sum_{\sigma \in P_+^k} \exp(2\pi i \lambda \cdot r(\Lambda^0)) \frac{S_{\lambda, \sigma}}{S_{0, \sigma}} = \exp(2\pi i \lambda \cdot r(\Lambda^0)) \mathcal{T}_\lambda. \end{aligned} \quad (6.3)$$

¹The root lattice contains all dominant weights that can be expressed as integer combinations of simple roots.

This implies that $\exp(2\pi i\lambda \cdot r(\Lambda^0)) = 1$, which is only possible when λ is in the root lattice or that $\mathcal{T}_\lambda = 0$.

In order to find a sum of non-negative integers that provide a manifestly affine account of the fusion dimension we will consider the symmetries of the tadpole. These symmetries are used to break up the tadpoles into partial sums that are then analyzed. The hope is to find a partial sum that has the non-negative-integer property and that this would lead to the identification of a combinatorial atom. Symmetries of the tadpoles can be categorized into those that affect the horizontal projection of the highest-weight representation, and those acting on the Weyl alcove highest weights.

By taking the correct partial sum it was hoped that we might find a hint that would point toward a combinatorial rule for fusion dimensions. A method of writing the tadpoles as a sum of non-negative integers might lead to an understanding of them in Lie theoretic terms. We did not find such a result, but did notice a number of curious relations. Furthermore, we observed two near misses of the partial sums that let us write the tadpoles as sums of integer values, albeit sometimes negative integers.

The rearrangements of sums in the Verlinde formula were done by hand and the partial sums were computed using *Mathematica*. We made use of the *LieART* package [7] to generate horizontal projections of the affine highest-weight representation and used our own algorithm for to construct the Weyl alcove and another to break up the tadpole.

6.1 Breaking Up the Sums

We begin from the general Verlinde formula (4.31), with $N = 1$ and $g = 1$, since we are considering the tadpole. With Kac-Peterson relation (4.27) we are able to rewrite

the tadpole as:

$$\mathcal{T}_\lambda = \sum_{\sigma \in P_+^k} \sum_{\alpha \in P(\lambda)} \text{mult}_\lambda(\alpha) \exp \left\{ \frac{2\pi i}{k+N} \alpha \cdot (\sigma + \rho) \right\}. \quad (6.4)$$

The substitution for the dual Coxeter number $h^\vee = N$ for $\widehat{SU}(N)$ having been made.

6.1.1 No Sum Taken in (6.4)

As an initial check we look at the roots of unity without any sum taken, we have:

$$\sum_{\alpha \in P(\lambda)} \sum_{\sigma \in P_+^k} \left\{ \text{mult}_\lambda(\alpha) \exp \left\{ \frac{2\pi i}{k+h^\vee} \alpha \cdot (\sigma + \rho) \right\} \right\} = \sum_{\alpha \in P(\lambda)} \sum_{\sigma \in P_+^k} \Theta_\lambda(\sigma, \alpha). \quad (6.5)$$

Θ_λ was, unsurprisingly, found to yield complex values.

6.1.2 Sum Over the Weyl Alcove

We consider now the next simplest case, the sum over the Weyl alcove P_+^k . Reordering equation (6.4) we obtain:

$$\sum_{\alpha \in P(\lambda)} \text{mult}_\lambda(\alpha) \left\{ \sum_{\sigma \in P_+^k} \exp \left(\frac{2\pi i}{k+h^\vee} \alpha \cdot (\sigma + \rho) \right) \right\} = \sum_{\alpha \in P(\lambda)} \text{mult}_\lambda(\alpha) \Sigma_\lambda(\alpha), \quad (6.6)$$

and find that $\Sigma_\lambda(\alpha) \in \mathbb{C}$.

6.1.3 Sum Over the Projected Highest-Weight Representation

Summing over $P(\lambda)$ amounts to a reversal of the summing order of equation (6.6):

$$\sum_{\sigma \in P_+^k} \left\{ \sum_{\alpha \in P(\lambda)} \text{mult}_\lambda(\alpha) \exp \left(\frac{2\pi i}{k+h^\vee} \alpha \cdot (\sigma + \rho) \right) \right\} = \sum_{\sigma \in P_+^k} \mathcal{P}_\lambda(\sigma). \quad (6.7)$$

Looking at the values taken by $\mathcal{P}_\lambda(\sigma)$ we find that $\mathcal{P}_\lambda(\sigma) \in \mathbb{C}$.

6.1.4 Simple Currents of the Group

Having looked at the three simplest possibilities, we now consider some more involved methods of breaking up the sums. The simple currents are an affine symmetry that have no analog in the simple Lie groups [12] and sorts the highest-weight elements in the Weyl alcove into appropriate orbits. Simple current orbits change based on the level, but are fairly easily computed.

The form of an affine weight is: $\hat{\lambda} = [k - \sum_i \lambda_i; \lambda_1, \dots, \lambda_{N-1}]$. The action of the simple-current operator $r \in \mathcal{R} \simeq \mathbb{Z}_N$, is to permute the Dynkin labels cyclically:

$$r\left([k - \sum_i \lambda_i^{N-1}; \lambda_1, \dots, \lambda_{N-1}]\right) \rightarrow [\lambda_{N-1}; k - \sum_i \lambda_{i=1}^{N-2}; \lambda_1, \dots, \lambda_{N-2}] \quad (6.8)$$

Taking the sum over the simple current orbits we have:

$$\sum_{\mu \in P_+^k/\mathcal{R}} \left\{ \sum_{\sigma \in R(\mu)} \sum_{\alpha \in P(\lambda)} \text{mult}_\lambda(\alpha) \exp\left(\frac{2\pi i}{k+h^\vee} \alpha \cdot (\sigma + \rho)\right) \right\} = \sum_{\mu \in P_+^k/\mathcal{R}} \text{SC}_\lambda(\mu). \quad (6.9)$$

We observe that $\text{SC}_\lambda(\mu) \in \mathbb{C}$.

6.1.5 Galois Symmetries

The Galois symmetry of the affine fusion is the next property we exploit. Galois symmetry relates primitive roots of unity to one another. So for an M -th primitive root of unity that is the zero of a polynomial with rational coefficients then so is a different primitive M -th root of unity. For the affine fusion the Galois symmetry relates two $M = (k + N)N$ -th primitive roots of unity that correspond to certain weights in the Weyl alcove. The Galois transformation is found by introducing an integer a , coprime to M .² The condition for the Galois transformation of a weight σ

²Equivalently, the coprime condition is $\text{gcd}(a, (k + N)N) = 1$.

is:

$$a(\sigma + \rho) = \omega([a\sigma] + \rho), \quad a\omega(\sigma + \rho) - \rho = [a\sigma]. \quad (6.10)$$

With $\sigma, a\sigma \in P_+^k$ and $\omega \in \widehat{W}$.

The Weyl alcove is broken up into Galois orbits [15]. This results in a rational scaling factor being introduced into our sum, added in order to prevent over or under counting. Applying the Galois symmetry we can break the sum up into the following triple summation, writing the whole Galois group as Gal. Similarly, $\text{Gal}(\sigma)$ corresponds to the Galois group orbit of the weight σ . We write:

$$\begin{aligned} \mathcal{T}_\lambda &= \sum_{\alpha \in P(\lambda)} \text{mult}_\lambda(\alpha) \sum_{\sigma' \in P_+^k/\text{Gal}} \frac{|\text{Gal}(\sigma')|}{|\text{Gal}|} \sum_{\sigma \in \text{Gal}(\sigma')} \exp\left(\frac{2\pi i}{k+h^\vee} \alpha \cdot (\sigma + \rho)\right), \\ &= \sum_{\sigma' \in P_+^k/\text{Gal}} \frac{|\text{Gal}(\sigma')|}{|\text{Gal}|} \left\{ \sum_{\alpha \in P(\lambda)} \text{mult}_\lambda(\alpha) \sum_{\sigma \in \text{Gal}(\sigma')} \exp\left(\frac{2\pi i}{k+h^\vee} \alpha \cdot (\sigma + \rho)\right) \right\}, \\ &= \sum_{\sigma' \in P_+^k/\text{Gal}} \frac{|\text{Gal}(\sigma')|}{|\text{Gal}|} \mathcal{G}_\lambda(\sigma'). \end{aligned} \quad (6.11)$$

These computations are time consuming and, like the simple currents, must be redone for every level. This complication limits the size of the tadpoles that we could analyze. Despite this difficulty in computation, the sums were observed to be integer-valued for groups $\widehat{SU}(3)$ and $\widehat{SU}(4)$.

$$\mathcal{G}_\lambda(\sigma') \in \mathbb{Z} \quad (6.12)$$

6.1.6 Dominant Weight Sums

Horizontal Weyl orbits were used to break up the horizontal highest-weight representation $R(\lambda)$. These Weyl orbits were labelled by dominant weights.³ Significantly the Weyl orbits have no dependence on the level of the affine highest-weight representation.

We write $P(\lambda)/W$ to denote the set of dominant weights that index the unique Weyl orbits:

$$\sum_{\beta \in P(\lambda)/W} \text{mult}_\lambda(\beta) \left\{ \sum_{\alpha \in W\beta} \sum_{\sigma \in P_+^k} \exp\left(\frac{2\pi i}{k+h^\vee} \alpha \cdot (\sigma + \rho)\right) \right\} = \sum_{\beta \in P(\lambda)/W} \text{mult}_\lambda(\beta) \mathcal{E}_\lambda(\beta). \quad (6.13)$$

For $\widehat{SU}(N)$ this corresponds to the sum over a basis of symmetric monomials, as was suggested in Section 5.3. The results of our computations are strictly integer-valued. However, as for the Galois orbits, these ‘dominant weight sums’ give negative integer values as well as positive ones.

There is a large amount of structure apparent in the tables of the dominant weight sums, most notably they appear to behave like polynomials in the level. This was a particularly surprising observation, particularly since it appears to be robust and was observed for many weights at a variety of group ranks. Furthermore, it is consistent with the results obtained via the generalized BZ triangle approach in equation (5.25). The consistency between tadpole values and those predicted by the dominant weight sum was also checked for other tadpole values, particularly the $\widehat{SU}(5)$ tadpoles in Table B.3. This check was done by pairing the predicted dominant weight sum polynomial with the relevant dominant weight multiplicity, which produced polynomial formulas for the tadpoles and motivated several conjectures (see Section 6.3). We

³Recall that the horizontal Weyl group is the Weyl group of the horizontal Lie subgroup.

attempt to understand these observations in Appendix A.1.

6.1.7 Dominant Weights and Simple Current Symmetries

Having observed that the dominant weight sums were integer valued, we consider them in conjunction with the simple current symmetries. The resulting sums are the \mathcal{WSC}_λ in:

$$\begin{aligned} {}^{(k)}\mathcal{T}_\lambda &= \sum_{\mu \in P_+^k/\mathcal{R}} \sum_{\beta \in P(\lambda)/W} \left\{ \sum_{\sigma \in R(\mu)} \sum_{\alpha \in W\beta} \text{mult}_\lambda(\alpha) \exp\left(\frac{2\pi i}{k+h^\vee} \alpha \cdot (\sigma + \rho)\right) \right\} \\ &= \sum_{\mu \in P_+^k/\mathcal{R}} \mathcal{WSC}_\lambda(\mu, \beta). \end{aligned} \quad (6.14)$$

Unfortunately, the $\mathcal{WSC}_\lambda(\mu, \beta)$ are complex valued.

6.1.8 Dominant Weights and Galois Symmetries

Given that both dominant weight sums and the sums over Galois orbits resulted in integers, we combine both methods of breaking up the sum. This results in two sums having to be taken out the front, but the resulting objects are more fine than either the Galois orbits or the dominant weight sums on their own. For this reason these objects were considered prime candidates for being the combinatorial atom. The resulting sums are the \mathcal{GW}_λ in:

$${}^{(k)}\mathcal{T}_\lambda = \sum_{\substack{\alpha \in P(\lambda)/W \\ \sigma' \in P_+^k/\text{Gal}}} \text{mult}_\lambda(\alpha) \frac{|\text{Gal}(\sigma')|}{|\text{Gal}|} \left\{ \sum_{\substack{\beta \in W\alpha \\ \sigma \in \text{Gal}(\sigma')}} \exp\left(\frac{2\pi i}{k+h^\vee} \beta \cdot (\sigma + \rho)\right) \right\} \quad (6.15)$$

$$= \sum_{\substack{\alpha \in P(\lambda)/W \\ \sigma' \in P_+^k/\text{Gal}}} \text{mult}_\lambda(\alpha) \frac{|\text{Gal}(\sigma')|}{|\text{Gal}|} \mathcal{GW}_\lambda(\alpha, \sigma'). \quad (6.16)$$

Like the previous mixture of partial sums, the $\mathcal{GW}_\lambda(\alpha, \sigma')$ resulted in complex values.

6.2 Observed Properties of the Dominant Weight Sums

A number of curious observations were made about the behaviour of the dominant weight sums $\mathcal{E}_\lambda(k)$ in equation (6.13).

The dominant weight sums were uniquely specified by a dominant weight and level. Weight multiplicities were separated from the dominant weight sum, leaving them defined independent of a highest-weight representation. Once we have an dominant weight sum, indexed by a dominant weight, it can be used for the calculation of any tadpole whose highest weight representation contains the dominant weight.

Dominant weight sums have a trivial case corresponding to the zero weight $\lambda = [0, 0, \dots, 0] \equiv (1^N)$ and can be easily computed. Doing so we can observe that the tadpole:

$$\begin{aligned} \mathcal{T}_{[0, \dots, 0]} &= \sum_{\sigma \in P_+^k} \mathcal{E}_{[0, \dots, 0] = (1^N)}(\sigma), \\ &= |P_+^k| = \binom{k + N - 1}{N - 1}, \\ \mathcal{T}_{(1^N)} &= \frac{(k + N - 1)(k + N - 2) \dots (k + 1)}{(N - 1)!} := \frac{(k + N - 1)^{N-1}}{(N - 1)!}. \end{aligned} \quad (6.17)$$

The value of the null tadpole is a trivial and well-known result, but notable in that it is polynomial in the level k .

From the tables of Appendix B.2 one can find polynomials that coincide with the reported values. These polynomials have their degree strictly bounded by the value of the group rank:⁴

$$\deg(\mathcal{E}_\lambda(k)) < N - 1. \quad (6.18)$$

⁴This is important since it indicates that we are not finding an arbitrary degree polynomial and ‘over-fitting’ our results.

In the tables the dominant weight sums were observed to be strictly increasing, strictly decreasing, or constant for increasing level k . The degree of the dominant weight sum seems to be related to whether it is increasing or decreasing.⁵

Curiously, the number of integers needed to specify the dual Dynkin labels and the degree of proposed polynomial in k fitting the dominant weight sum were observed to be related. The number of unique integers needed to specify the dual Dynkin labels are used to define the ‘root rank.’

Definition 18. *Dual Dynkin labels are notated a^i , and can be used to write a weight as $\lambda = a^1\alpha_1 + \dots + a^{N-1}\alpha_{N-1}$, where α_i is the i^{th} simple root. Take the minimum set of unique integer coefficients needed to specify the dual Dynkin labels of a highest weight to be:*

$$A = \{a^i | a^i \neq a^j \text{ with } i < j \text{ and } a^i \neq 0\}. \quad (6.19)$$

The root rank is defined as the number of elements in this set $|A|$.

Our experimental observation is that the degree of the polynomial in k that fits the dominant weight sums is given by:

$$\deg(\mathcal{E}_\lambda(k)) = (N - 1) - |A| \quad (6.20)$$

There is a special case for the null weight, which has $|A| = 0$, corresponding to the dominant weight sum with the maximum degree: $N - 1$. All other weights have at least 1 entry in A and a maximum of $N - 1$ entries in A . Root rank examples are given below in order to make this observed behaviour explicit.

Example 11. $\lambda = [N, 0, 0, 0 \dots 0]$ corresponds to a root representation of $\lambda = (N -$

⁵When the polynomial is constant the maximum degree of the fitted polynomial determines the sign of the constant values. The degree appears to dictate the sign of all the polynomials at first glance, however upon closer inspection several exceptions, such as the weight $[3, 2, 1, 0]$ in Table B.8, emerge.

$(-)^{ A }$	$\deg(\mathcal{E}_\lambda)$	$ A $
(+)	$N - 1$	0
(-)	$N - 2$	1
(+)	$N - 3$	2
...
$(-)^{N-1}$	0	$N - 1$

Table 6.1: Root rank seems to indicate the degree of the polynomial of the dominant weight sum and whether it is increasing or decreasing.

$1)\alpha_1 + (N-2)\alpha_2 + \dots + 2\alpha_{N-2} + \alpha_{N-1}$, which has the set of $A = \{a_i\} = \{1, 2, 3, \dots, N-1\}$ so $|A| = N-1$. Using this value for the root rank we find the degree of the polynomial to be $\deg(\mathcal{E}_{[N,0,\dots,0]}) = N - 1 - (N - 1) = 0$. A degree of zero indicating that the dominant weight sum is constant, which is supported by observation.

Example 12. $\lambda = [H, 0, 0, \dots, 0, 0, H]$ has the root representation $\lambda = H\alpha_1 + H\alpha_2 + \dots + H\alpha_{N-2} + H\alpha_{N-1}$ so in this case $\{a_i\} = \{H\}$ and so $|A| = 1$. Using this root rank gives the degree as $\deg(\mathcal{E}_{[H,0,\dots,0,H]}) = N - 1 - 1 = N - 2$. This result agrees with the proposed polynomial equations and matches the tabulated values.

Root rank was also observed to correspond to whether the dominant weight sum was increasing or decreasing. To indicate whether the polynomial is increasing (+) or decreasing (-), $\deg(\mathcal{E}_\lambda)$ is the degree of the polynomial, and the $|A|$ is root rank. The last entry in Table 6.1 is constant and so either positive- or negative-valued, equalling the sign of $(-)^{N-1}$.

Table 6.1 makes a strong case for an emergent structure here, which, to our knowledge, has not been previously explored or observed in the literature.

The polynomial nature of the dominant weight sums is strongly supported by our experimental observations. These observations led to several conjectured formulas for the dominant weight sums, equation (A.19), which were then used to conjecture equations for certain classes of tadpoles. In both cases, the equations reproduced the tabulated values without over-parameterization. These dominant weight sums, if they

exist, can be classified so as to be re-used for different highest-weight representations. We report many dominant weight sum values in our tables in Appendix B.2.⁶

6.3 Formulas and Conjectures for the Affine Tadpole

From the tabulated results for the tadpoles we conjecture several formulas. They agree with polynomials produced by generalized BZ triangle analysis, where applicable. The conjectured formula for the adjoint tadpole in equation (6.21) has a particularly simple form.

Conjecture 1. *For any adjoint highest-weight $\lambda = [1, 0, \dots, 0, 1]$, the tadpole is given by a polynomial in the level k ,*

$${}^{(N,k)}\mathcal{T}_{[1,0,\dots,0,1]} = (k-1) \frac{(k+N-2)^{N-2}}{(N-1)!}. \quad (6.21)$$

Based on the work done in Appendix A.1 and studying the produced tables in Appendices B.1 and B.2 motivated the tadpole conjectures. Multiplicities computed via the Kostka coefficients were used with conjectures about the forms of dominant weight sums, found in Appendix A.1, to suggest forms of the conjectures.

We were able to conjecture a general-level arbitrary-dimension formula for any tadpole for a weight with threshold level $k_0 = 2$, as given by equation (7.4).

There are two obstacles to computing a general formula for a tadpole of a given highest weight: computation of the Kostka coefficient and calculating the dominant weight sum.

Demonstrating the process we used to determine a suggested form we consider

⁶The dominant weight sums are explored further in Appendix A.1.

several example and use the dominant weight sums to obtain the results.

$$\mathcal{T}_{(2,2,1^{N-4})} = \mathcal{T}_{[0,1,0,\dots,0,1,0]} = \mathcal{E}_{(2,2,1^{N-4})} + (N-3)\mathcal{E}_{(2,1^{N-2})} + \frac{(N)(N-3)}{2}\mathcal{E}_{(1^N)} \quad (6.22)$$

$$= \frac{N(N-3)}{2} \cdot \frac{(k+N-3)^{N-3}}{(N-1)!} (k^2 - k) \quad (6.23)$$

$$\mathcal{T}_{[2,0,\dots,0,1,0]} = \mathcal{E}_{(3,1^{N-3})} + \mathcal{E}_{(2,2,1^{N-4})} + (N-2)\mathcal{E}_{(2,1^{N-2})} + \frac{(N-1)(N-2)}{2}\mathcal{E}_{(1^N)} \quad (6.24)$$

$$= \frac{1}{2}(k-2)(k-1) \frac{(k+N-3)^{N-3}}{(N-3)!} \quad (6.25)$$

The dominant weight sums are those given by the conjectured equation (A.19), reducing these computations to elementary algebra.

The following polynomials give the tadpole value for an arbitrary level k and group rank $N-1$; only the form of the tadpole weight is fixed.

$$\mathcal{T}_{2,1^{N-2}} = (k-1) \frac{(k+N-2)^{N-2}}{(N-2)!}, \quad (6.26)$$

$$\mathcal{T}_{3,1^{N-3}} = \frac{1}{2}(k-2)(k-1) \frac{(k+N-3)^{N-3}}{(N-3)!}, \quad (6.27)$$

$$\mathcal{T}_{4,1^{N-4}} = \left(\frac{(k-1)^3}{3!} \right) \frac{(k+N-4)^{N-4}}{(N-4)!}. \quad (6.28)$$

These culminate in the following conjecture, dependant on the validity of our assumptions on the form of the dominant weight sums.

Conjecture 2. *Given a highest-weight whose shape yields a hook Young tableau, which we call a hook partition, then the corresponding tadpole can be written as:*

$$\mathcal{T}_{(H,1^{N-H})} = \frac{(k-1)^{H-1}}{(H-1)!} \frac{(k+N-H)^{N-H}}{(N-H)!} \quad (6.29)$$

Using the conjectured results for dominant weight sums (A.19) we can also write

the following tadpole values, which were checked against tabulated values. In order to compute these tadpoles we take advantage of the general Kostka number formula (A.29) to account for weight multiplicities. We find:

$$\mathcal{T}_{2,2,1^{N-4}} = \frac{N(N-3)}{2} (k^2 - k) \frac{(k+N-3)^{N-3}}{(N-1)!}, \quad (6.30)$$

$$\mathcal{T}_{(2^3,1^{N-6})} = \frac{N(N-5)}{3!} k(k^2 - 1) \frac{(k+N-4)^{N-4}}{(N-2)!}, \quad (6.31)$$

$$\mathcal{T}_{(2^4,1^{N-8})} = \frac{N(N-7)}{4!} (k+2)^4 \frac{(k+N-5)^{N-5}}{(N-3)!}, \quad (6.32)$$

and we observe an emerging pattern, which leads to a conjecture about threshold level $k_0 = 2$ highest-weight tadpoles.

Conjecture 3. *Given a weight with threshold level $k_0 = 2$ its partition will be of the form $(2^L, 1^{N-2L})$ and the tadpole can be calculated by the polynomial*

$$\mathcal{T}_{(2^L,1^{N-2L})} = \frac{(N-2L+1)N}{L!} (k-2+L)^L \frac{(k+N-1-L)^{N-1-L}}{(N+1-L)!} \quad (6.33)$$

We also have a conjectured result for the adjoint-multiple weights, proven for $N = 2, 3, 4$ via computer calculation with generalized BZ triangles.

Conjecture 4. *Considering a tadpole whose highest-weight is a multiple of the adjoint highest eight. Then the following polynomial in the level k gives the tadpole values:*

$$\mathcal{T}_{[L,0,\dots,0,L]} = \mathcal{T}_{(2L,L^{N-2})} = (k-2L+1) \frac{(k+N-L-1)^{N-2} (L+N-2)^{N-2}}{(N-1)!(N-2)!}. \quad (6.34)$$

Combining two of our four conjectures (6.34) and (6.29) results in a general conjecture for tadpoles with both classes of highest-weight.

Conjecture 5. *The value of the tadpole for a partition of the form (MH, M^{N-H}) is:*

$$\mathcal{T}_{(MH, M^{N-H})} = \frac{(k - 2M + 1)^{H-1}}{(H - 1)!} \frac{(k + N - H - M + 1)^{N-H}}{(N - H + 1)} \frac{(M + N - H)^{N-H}}{(N - H)!}. \quad (6.35)$$

It should be noted that this result agrees with the known form of the tadpole values for $SU(2)$, which are given by:

$$\mathcal{T}_{2M} = (k - 2M + 1) \quad (6.36)$$

Finally, we conclude with an additional note about a symmetry of the tadpole, which was considered, with proof, in Section 5.2.1.

Theorem 3. *For any highest-weight $\lambda = [\lambda_1, 0, \dots, 0, \lambda_{N-1}]$ with $\lambda_1 \geq \lambda_{N-1}$ of $\widehat{SU}(N)$ with $N = 2, 3, 4$, the tadpole corresponding to the λ obey the following property:*

$${}^{(k)}\mathcal{T}_\lambda = {}^{(k+jN)}\mathcal{T}_{\lambda+(jN)\Lambda_1}. \quad (6.37)$$

The proof of this theorem in Section 5.2.1 involved several steps. Firstly, we demonstrated that the fundamental weight $N\Lambda_1$ had a unique starting BZ triangle. The importance of the first step is that for the counting to be identical in general the number of starting triangles for λ and $\lambda + N\Lambda_1$ should be equal. If $N\Lambda_1$ has more than 1 starting triangle it is not hard to see that $\lambda + N\Lambda_1$ will have an increased number of starting triangles relative to λ . Secondly, we considered the possible forms that λ could take in order to satisfy the condition of a constant number of starting triangles. This consideration of the valid forms of λ , led to a restriction of λ to the form $\lambda = [\lambda_1, 0, \dots, 0, \lambda_{N-1}]$ with $\lambda_1 \geq \lambda_{N-1}$. The third and final step consisted of looking at the threshold level conditions introduced by the generalized BZ triangles.

This final consideration resulted in the conclusion that the threshold level condition is shifted by $k_0 \rightarrow k_0 + N$ for $N = 2, 3, 4$. This shift in the threshold level, combined with the constant number starting triangles concludes the proof of the theorem.

More generally we suggest that this condition may extend to certain other weights, but note that Λ_i with $i \neq 1, N-1$ will not satisfy this condition as proven in Lemma 1. We were able to demonstrate that for a relaxed threshold condition on the generalized BZ triangles one obtains a similar relationship between the partial trace or tensor product tadpoles in Theorem 2.

An explanation for our conjectured polynomial formulas proved to be difficult to find. Methods used to acquire them in Appendix A.1 did provide a partial account, but it was somewhat ad hoc. In addition, the root rank does not play an obvious role in the conjectured formula. A more complete interpretation of the dominant weight sums would be expected to include the root rank. Such an account of the dominant weight sums in terms of the root rank (defined in equation (6.19)) was beyond the scope of this thesis.

Chapter 7

Conclusion and Conjectures

The Verlinde formula provides a description of affine fusion in terms of S -modular matrices, which for the WZW models can be rewritten in terms of horizontal Lie character and weight systems. Symmetries of the Verlinde formula can be used to break up the general Verlinde formula (4.28) into partial sums. Notably, tadpoles are accounted for by the Verlinde formula in a particularly simple way: as a sum over discrete simple Lie group characters. Partial sums of the tadpole were investigated in the hopes of finding a manifestly affine method for computing the fusion dimension.

Although the Verlinde formula provides an affine account of the fusion dimensions, it is neither combinatorial or manifestly non-negative-integer valued. We were interested in finding a way to rewrite the Verlinde formula in terms of non-negative-integers. Being able to rewrite the Verlinde formula in that way might provide a hint about a manifestly affine combinatorial interpretation of the fusion dimensions. This combinatorial interpretation is not known, but has been long sought after.

Arguably, the simplest fusion dimension is the genus-1 1-point fusion dimension or tadpole, so named using terminology from Feynman diagrams in QFT [4]. Simplicity of the tadpoles was considered to be advantageous in looking for a way to rewrite the Verlinde formula and allowed us to efficiently investigate partial sums based on symmetries of the highest-weight representations, the dominant Weyl alcove, and the modular S -matrix. These symmetries were used to break up and re-order the sums in a search for a way of writing the Verlinde formula as a sum over non-negative integers. Such a sum might suggest a direction for a possible combinatorial account of the tadpole in terms of some affine Lie theoretic quantity. A combinatorial explanation of the tadpole would likely provide insight for a similar combinatorial explanation of more general fusion dimensions.

Algorithms used to calculate tensor product multiplicities can be adapted to compute the fusion dimensions, but these resulting descriptions involve cancellations due

to the appearance of both positive and negative contributions. They also lack the manifestly affine nature we believe is natural and likely necessary. While lacking a fundamentally affine underpinning, these algorithms were leveraged in order to account for special cases of some properties of the tadpoles seen in the tables of Appendix B.1. These adapted algorithms were looked at in Sections 5.1 and 5.2. Generalized BZ triangles allowed us to prove several conjectures for the fusion dimensions of highest-weight representations of groups $\widehat{SU}(N)$ with $N \leq 4$, such as equations (5.37), (A.38), and the equations (5.23) and (5.25). Unfortunately, the substantial difficulty of finding threshold level constraints for larger values of N limits the utility of the generalized BZ triangle method to a small set of group ranks.

Interpreting the tadpole in terms of fundamentally affine objects requires that we start with a fundamentally affine account of the fusion dimension. The Verlinde formula gives just such an account. Tadpoles were chosen since, like the Verlinde formula, they are most natural in the affine Lie group scenario, further they substantially simplified the Verlinde formula.

The Verlinde formula, even in its simplified tadpole form, involves sums over roots of unity, which are in general complex valued. This contrasts with the known to non-negative-integer values of the fusion dimensions. Adjusted tensor product multiplicity algorithms do provide an integer account for fusion, but they are not affine in their origins. The Kac-Walton formula expressed the fusion dimension in a manifestly integer manner, although it is not completely non-negative. The depth rule can be used to provide a manifestly non-negative account of the fusion, although it is quite difficult to implement. Both of these techniques, however, are based on adapted tensor product algorithms and are of limited use in obtaining a manifestly affine account of fusion.

Partial sums of the Verlinde formula were written based on symmetries present in the horizontal weight system and Weyl alcove of an affine highest-weight repre-

sentation. A study of the possible combinations of these symmetries, in Section 6.1, indicated that both the sum over Galois orbits (6.11), and the dominant weight sums (defined in equation (6.13)) gave the tadpoles as a sum over integer values. Other summation procedures were all found to contribute complex values, including the mixed Galois/dominant weight sum of equation (6.15).

Galois orbits are the result of a particularly interesting symmetry of the affine Lie groups [15] and are not present for the simple Lie groups. Galois orbits were defined as consisting of those weights on the Weyl alcove, at a given level k , who were related to one another via Galois transformation. Level dependence of the Galois symmetry made the computation of these orbits fairly complicated, since they had to be re-computed at every level. This difficulty in computation limited the size of the tables we were able to produce for the Galois orbit sums compared to tables produced for the dominant weight sums.

Galois orbits were found to break up the Verlinde formula, in Section 6.1.5, as:

$${}^{(k)}\mathcal{T}_\lambda = \sum_{\sigma \in P_+^k/\text{Gal}} \frac{|\text{Gal}(\sigma)|}{|\text{Gal}|} \mathcal{G}_\lambda(\sigma). \quad (7.1)$$

These Galois orbit sums $\mathcal{G}_\lambda(\sigma)$ were observed to be integer valued, however they did not have a clear pattern to them unlike dominant weight sums, also integer valued.

Dominant weight sums resulted from sums taken over Weyl orbits of the horizontal weight system of the highest-weight representation and the Weyl alcove of highest weights. The horizontal Weyl group, sans the affine reflection, could be used to break up the horizontal weight system into weights related by Weyl group reflections. These sets of weights are labelled by a dominant weight contained in the set and are referred to as the Weyl orbits, which is also defined in Section 2.2.2. Breaking up the tadpole

into dominant weight sums we wrote:

$${}^{(k)}\mathcal{T}_\lambda = \sum_{\mu \in P(\lambda)/W} \text{mult}_\lambda(\mu) \mathcal{E}_\mu(k). \quad (7.2)$$

All the dominant weight sums $\mathcal{E}_\mu(k)$ we computed were integer-valued and their sets of values had a lot of structure. In particular, their values could be described by polynomials in the level k , whose degree was inversely related to the root rank of equation (6.19). Furthermore, the dominant weight sums were found to be either strictly increasing, strictly decreasing, or constant. These observed behaviours are noted in the Table 6.1.

Based the observed polynomial behaviour of the values of dominant weight sums we conjectured that the tadpoles themselves were quasi-polynomial in the level k . With this claim in mind we were able to conjecture equations that yielded the tadpole values in Section 6.3. As previously mentioned, proofs were found for special cases with $N \leq 4$ by using the generalized BZ triangles in section 5.2.

In Appendix A.1 we attempt to give an account for the appearance of the polynomial behaviour in the dominant weight sums. These considerations culminate in the conjectured formulas for hook-type partitions (A.37), adjoint multiple (A.38), and all weights with threshold level $k_0 = 2$ (A.36). These equations are also collected in Section 6.3, with the motivation and insight behind them being based on considerations given the dominant weight sums. Requirement of consistency between the hook-type and adjoint multiple conjectures resulted in an additional conjecture for multiples of hook-type highest-weights in equation (A.39).

General polynomials of dominant weight sums that were labelled by partitions of jN with $j > 1$ were problematic for all but a handful of special cases. The general formulas for the polynomials of dominant weight sums agreed with all tabulated values, which is strong evidence that the dominant weight sums, as we propose them,

Source of Index	Summed Terms	Domain of Values
pHWR	$\mathcal{P}(\mu_i)$	\mathbf{C}
WA	$\text{ch}_\lambda(\sigma_i)$	\mathbf{C}
WA+pHWR	$\mathcal{WSC}_\lambda(\mu_i, \sigma_i)$	\mathbf{C}
WA+pHWR	$\mathcal{GW}_{\mu_i}(\sigma_i)$	\mathbf{C}
WA	$\mathcal{G}_\lambda(\sigma_i)$	\mathbf{Z}
pHWR	$\mathcal{E}(\mu_i)$	\mathbf{Z}

Table 7.1: Results of the various methods of partial sums used to break up the Verlinde formula.

are correct. A more constructive definition of the dominant weight sums may provide a more general method for their computation and provide a window into computing the tadpole. A more complete explanation of these polynomials may also indicate why they contribute either strictly increasing, decreasing, or constant values to the tadpoles.

The results of the partial sum decompositions of the Verlinde formula are collected in Table 7.1. Sums are taken over either the horizontal weight system of the affine highest-weight representation, denoted as pHWR, or from the Weyl alcove of highest-weights, denoted WA. The weights μ_i denote weight elements of the horizontal projection of an affine highest-weight representation and the σ_i denote those highest-weight elements in the Weyl alcove.

The Verlinde formula does not seem to know about the Moore–Seiberg duality, although this duality is central to the CFTs. Fusion coefficients are the central object in the Moore–Seiberg picture, but from the general Verlinde formula (4.31) alone there is no reason to expect the fusion coefficients to be the most fundamental object. Tadpoles were considered due to their simplicity and the fact that we expect that a combinatorial atom for the fusion coefficients would also be an atom for the tadpoles.

Recent work on combinatorial interpretations of fusion dimensions, in particular the Morse rules on the cylindrical-skew-SSYT [34], have found some success. Their

work with these objects gives an account of the fusion coefficients for a reasonable class of highest-weights. Attempts at re-applying their results to the tadpoles were not straightforward. Our attempts at doing so reduced to the idea of tadpoles as the trace of the fusion coefficient, which might be the route to take for future searches for the combinatorial atom of affine fusion.

Although we did not find a non-negative-integer sum for the tadpole, we did observe many ways to write them in terms of integers. In addition, we observed a surprising amount of structure underlying the dominant weight sums. From these observations we were able to write down several general formulas, which culminated in a set of conjectures, which we repeat here. A full explanation of these results is beyond the scope of this thesis, but a first attempt at an explanation is made in Appendix A.1.

Given a multiple of a hook-type partition (MH, M^{N-H}) the tadpole value is given by the polynomial:

$$\mathcal{T}_{(MH, M^{N-H})} = \frac{(k - 2M + 1)^{H-1}}{(H - 1)!} \frac{(k + N - H - M + 1)^{N-H}}{(N - H + 1)} \frac{(M + N - H)^{N-H}}{(N - H)!}. \quad (7.3)$$

Any weight with a threshold level $k_0 = 2$, will have a partition of the form $(2^L, 1^{N-2L})$ and the tadpole of such a weight will be equal to:

$${}^{(k)}\mathcal{T}_{(2^L, 1^{N-2L})} = \frac{(N - 2L + 1)N}{L!} (k - 2 + L)^L \frac{(k + N - 1 - L)^{N-1-L}}{(N - 1 - L)!}. \quad (7.4)$$

We also noticed an unexplained additional symmetry of the tadpole. Adding fundamental weights $\Lambda_1 = [1, 0, \dots, 0]$ or $\Lambda_{N-1} = [0, 0, \dots, 0, 1]$ to a highest-weight λ we have $\lambda + (jN)\Lambda_1 = [\lambda_1 + jN, \lambda_2, \dots, \lambda_{N-1}]$, where $j \in \mathbb{Z}_{\geq 0}$. When the highest-weight λ has the appropriate form we have that the two tadpoles \mathcal{T}_λ and $\mathcal{T}_{\lambda+(jN)\Lambda_1}$

are related by:

$${}^{(N,k+jN)}\mathcal{T}_{[\mu_1+jN,0,\dots,\mu_{N-1}]} = {}^{(N,k)}\mathcal{T}_{[\mu_1,0,\dots,\mu_{N-1}]}.$$
 (7.5)

This relation was only valid for $SU(4)$ when $\lambda = [\lambda_1, 0, \lambda_3]$ and $\lambda_1 \geq \lambda_3$. We suspect that this will hold for higher-rank weights μ under the similar condition of $\mu = [\mu_1, 0, \dots, 0, \mu_{N-1}]$, when $\mu_1 \geq \sum_{i=2}^{N-1} \mu_i$. We were able to show this theorem was valid for $N \leq 4$ via generalized BZ triangles. An additional argument was made for this condition hold for tensor product tadpoles, which use a relaxed threshold level condition on the valid generalized BZ triangles, to argue for this theorems possible validity at larger N in Section 5.2.1.

Our observations of partial sums of the Verlinde formula introduce a number of questions:

- Why do the dominant weight sums result in values that appear to be polynomial in the level k ?
- Are the tadpoles quasi-polynomial in all cases?
- Can the dominant weight sums be generalized for use in computing the fusion coefficients?
- Can we account for the negativity of some of the dominant weight sums?
- Is there a counting argument that reproduces the conjectured dominant weight sums, possibly by considering a polytope volume argument?

Answering this final question, may end up affirming our suspicion that the tadpole provides a window to a non-negative, manifestly affine account of the fusion dimension. Such a combinatorial argument would avoid much of the complexity of the Verlinde formula. Interpretation of the dominant weight sums as polytope volumes

was considered, although a method for treating them in this way remains unclear. It should be noted that much of the difficulty of a polytope interpretation of the dominant weight sums stem from their behaviour when considering highest-weights corresponding to partitions $(\lambda) \vdash jN$ with $j > 1$.

We found that there was no standard method for breaking the Verlinde formula up into non-negative-integers. Over the course of the search for combinatorial atoms we did find a number of interesting results. Both dominant weight sums and the Galois orbit sums were found to be integer valued, which has not to our knowledge been previously seen in the literature. More surprisingly, we found that there were polynomials in the level k that reproduced our tabled values. We also introduced the idea of a root rank, which appeared to be closely related to these polynomials in the level k that reproduced the dominant weight sum's behaviour. We gave a partial account of these polynomials and used this account to produce several conjectured equations for tadpole corresponding to several classes of highest-weights.

Bibliography

- [1] L. Bégin, A. N. Kirillov, P. Mathieu, M.A. Walton. *Berenstein Zelevinsky Triangles, Elementary Couplings and Fusion Rules*, Lett. Math. Phys. 28, 257, (1993).
- [2] A.D. Berenstein, A.V. Zelevinsky, *Triple Multiplicities for $sl(r+1)$ and the Spectrum of the Exterior Algebra of the Adjoint Representation*, Journal of Algebraic Combinatorics 1, 7, (1992).
- [3] Bourbaki, *Lie Groups and Lie Algebras*, Chapters 4-6, Springer-Verlag (2002).
- [4] S. Coleman, S. L. Glashow, *Departures from the Eightfold Way: Theory of Strong Interaction Symmetry Breakdown*, Phys. Rev. 134 B, 671, (1964).
- [5] C. J. Efthimiou, D. A. Spector, *A Collection of Exercises in Two-Dimensional Physics Part I*, arXiv:hep-th/0003190v1, (2000).
- [6] G. Felder, K. Gawedzki, A. Kupianen, *Spectra of Wess-Zumino-Witten Models with Arbitrary Simple Groups*, Commun. Math. Phys. 117, 127, (1988).
- [7] R. Feger, T. W. Kephart, *LieART - A Mathematica Application of Lie Algebras and Representation Theory*, arXiv: 1206.6379v2 [math-ph], (2014).
- [8] G. Flynn, J. Rasmussen, M. Tahic, M. A. Walton, *Higher-genus $su(N)$ Fusion Multiplicities as Polytope Volumes*, J. Phys. A, Math. Gen. 35, 10129, (2002).
- [9] P. Di Francesco, P. Mathieu, D. Sénéchal, *Conformal Field Theory*, Springer, (1996).
- [10] E. Frenkel, *Affine Kac-Moody Algebras, Integrable Systems and Their Deformations*, arXiv:math/0305216 [math.QA], (2003).
- [11] S. Friedli and Y. Velenik, *Equilibrium Statistical Mechanics of Classical Lattice Systems: A Concrete Introduction, Preliminary Draft, Chapter 3*, www.unige.ch/math/folks/velenik/smbook, (2014).
- [12] J. Fuchs, *Affine Lie Algebras and Quantum Groups*, Cambridge University Press, (1995).
- [13] J. Fuchs, *Fusion Rules in Conformal Field Theory*, Fortsch. Phys. 42, 1, (1993).
- [14] W. Fulton, J. Harris, *Representation Theory: A First Course*, Springer, (1991).

-
- [15] T. Gannon, M. A. Walton, *On Fusion Algebras and Modular Matrices*, Commun. Math. Phys. 206, 1, (1999).
- [16] M. Gell-Mann, *A Schematic Model of Baryons and Mesons*, Phys. Lett. 8, 214, (1964).
- [17] H. Georgi, *Lie Algebras in Particle Physics, Second Edition*, Westview Press, (1999).
- [18] H. Georgi, *Introduction to Representation Theory and Lie Groups for Physicists*, Westview Press, (1999).
- [19] F. M. Goodman, H. Wenzl, *Littlewood-Richardson Coefficients for Hecke Algebras at Roots of Unity*, Advances in Mathematics, 82, 244, (1990).
- [20] P. Ginsparg, *Applied Conformal Field Theory*, in Fields, Strings and Critical Phenomena, (Les Houches, Session XLIX, 1988) ed. by E. Brézin and J. Zinn Justin, (1989).
- [21] C. Itzykson, H. Saleur and J.B. Zuber, *Conformal Invariance and Applications to Statistical Mechanics*, World Scientific Pub Co. Inc., (1988).
- [22] V.G. Kac, *Infinite Dimensional Lie Algebras*, Third Edition, Cambridge University Press, (1990).
- [23] V.G. Kac, D.H. Peterson, *Infinite-Dimensional Lie Algebras, Theta Functions and Modular Forms*, Adv. Math. 53, 125, (1984).
- [24] V. G. Kac, D. H. Peterson, *Affine Lie Algebras and Hecke Modular Forms*, Bull. Amer. Math. Soc. (N.S.) 3, 3, 1057, (1980).
- [25] K. Koike, I. Terada, *Young-Diagrammatic Methods for the Representation Theory of the Classical Groups of Type B_n , C_n , D_n* , Journal of Algebra, 107, 2, 466, (1987).
- [26] P. Hersh, C. Lenart, *Combinatorial Constructions of Weight Bases: The Gelfand-Tsetlin Basis*, The Electronic Journal of Combinatorics, Volume: 17, Issue: 1, Research Paper R33 (2010).
- [27] T. Lam, L. Lapointe, J. Morse, A. Schilling, M. Shimozono, M. Zabrocki, *k -Schur Functions and Affine Schubert Calculus*, arXiv:1301.3569v2 [math.CO], (2013).
- [28] P. Littelmann, *A Generalization of the Littlewood-Richardson Rule*, Journal of Algebra 130, 328, (1990).
- [29] I. G. Macdonald, *Symmetric Functions and Hall Polynomials*, Oxford Science Publishing, (1995).
- [30] S. Mayer, *Fusion Rules and the Verlinde Formula*, Proseminar Conformal Field Theory and String Theory, (2013).

-
- [31] I. Markina, A. Vasilév, *Virasoro algebra and dynamics in the space of univalent functions*, in *Five Lectures in Complex Analysis*, Contemp. Math., 525, 85, (2010).
- [32] G. Moore and N. Seiberg, *Polynomial Equations for Rational Conformal Field Theories*, Phys. Lett. B212, 451, (1988).
- [33] G. Moore and N. Seiberg, *Classical and Quantum Conformal Field Theory*, Commun. Math. Phys 123, 177, (1989).
- [34] J. Morse and A. Schilling, *A Combinatorial Formula for Fusion Coefficients*, DMTCS proc AR, 735, (2012).
- [35] G. Racah, *Lecture on Lie Groups. In Group Theoretical Concepts and Methods in Elementary Particle Physics (Lectures Istanbul Summer School Theoret. Phys., 1962)* (1964).
- [36] J. Rasmussen, M. A. Walton, *Purely Affine Elementary $su(N)$ Fusions*, Mod. Phys. Lett. A17, 1249, (2002).
- [37] E. Rassart, *Geometric Approaches to Computing Kostka Numbers and Littlewood-Richardson Coefficients*, Doctoral Thesis MIT (2004).
- [38] R. Howe, *Perspectives on Invariant Theory: Schur Duality, Multiplicity-Free Actions and Beyond*, in *The Schur lectures* (1992) (Tel Aviv), Israel Math. Conf. Proc., 8, Bar-Ilan Univ., Ramat Gan, 1, (1995).
- [39] S. Rychkov, *EPFL Lecture on Conformal Field Theory in $D \geq 3$ Dimensions*, Lecture notes prepared with the help of G. Karanana, (2012).
- [40] O. Saldarriaga, *Type A Fusion Rules*, Revista Integracion, Escuela de Matematicas, Volume 27, No. 2, (2009).
- [41] M. Schottenloher, *A Mathematical Introduction to Conformal Field Theory*, Lect. Notes. Phys. 759, (2008).
- [42] J. Serre, *Linear Representations of Finite Groups*, Springer (1977).
- [43] D. Speiser, *Theory of Compact Lie Groups and Some Applications to Elementary Particle Physics*, in *Group Theoretical Concepts and Methods in Elementary Particle Physics (Lectures Istanbul Summer School Theoret. Phys., Gordon and Breach, 201, (1964)*.
- [44] H. Sugawara, *A Field Theory of Currents*, Phys. Rev. 170, 1659, (1968).
- [45] E. Verlinde, *Fusion Rules and Modular Transformations in 2d Conformal Field Theory*, Nucl. Phys. B300, 360, (1988).
- [46] M. A. Walton, *Algorithm for WZW Fusion Rules: a Proof*, Phys. Lett. B241, 365, (1990).

- [47] M. A. Walton, *Fusion Rules in Wess-Zumino-Witten Models*, Nucl. Phys. B, 240, 777, (1990).
- [48] M. A. Walton, *Hopping in the Phase Model to a Non-Commutative Verlinde Formula for Affine Fusion*, J. Phys.: Conf. Series 474, (2013).
- [49] Y. Zhao, *Young Tableaux and the Representations of the Symmetric Group*, The Harvard College Mathematics Review, 2, 33, (2008).

Appendix A

Exploring the Dominant Weight Sums

In Section 6.1.6 we saw that the dominant weight sums $\mathcal{E}_\alpha(k)$ were integer valued (also see Appendix B.2) and that they were polynomial in the level k . These properties were very curious and necessitated some additional consideration. Alcove Weyl sums appear to give results that can be expressed as polynomials in the level. These polynomials can be relatively easy to obtain and have a great deal of structure (see Section 6.2), which suggests that there is something useful here.

An attempt at giving an account of the dominant weight sums and their observed behaviour in this section. Our claims depend on the assumption that imposing ideals constrain the possible highest-weights that are summed over. This assumption is not completely understood, but with it we were able to obtain equation (A.19) and note that they agreed with our tables in Appendix B.1. Difficulty in applying this technique to partitions with a sum of parts greater than the group dimension N was thought to be the result of accidentally overcounting constraints.

In Section 5.3 we wrote the tadpoles as a sum over symmetric monomials $M_\alpha(\sigma)$. A sum taken over the Weyl alcove of the symmetric monomials was later defined as being the dominant weight sums. Taking α to be a dominant weight of some highest-weight representation, and k to be the level of the representation:

$$\mathcal{E}_\alpha(k) := \sum_{\sigma \in P_+^k} M_\alpha(\sigma). \quad (\text{A.1})$$

Alcove Weyl sums have no dependence on the highest-weight λ , useful since a single computation will be valid for any highest-weight representation. Calculating the tadpoles requires that the dominant weight sums be recombined with their relevant weight multiplicities of the dominant weight they correspond to. For our notation we will often suppress the dominant weight sum as implicitly reliant on the level k . All weights considered in this section will be in their partition form unless otherwise indicated, due to the relative simplicity that they can be used to express the dominant weight sums.

A.1 Working with the Dominant Weight Sums

The simplest highest-weight is the zero weight, where the roots of unity in the Verlinde formula are 1 for every weight letting us compute the tadpole outright. Sums over 1 count the dimension of the Weyl alcove:¹

$$\mathcal{T}_{(1^N)} = \frac{(k + N - 1)^{N-1}}{(N - 1)!} := \sum_{\kappa \in P_+^k} 1 = \frac{(k + N - 1)(k + N - 2) \dots (k + 1)}{(N - 1)!}. \quad (\text{A.2})$$

We make use of the falling power notation, whose main advantage is that it is reminiscent of the behaviors of polynomials for integration, but for applicable to summing procedures. We can define the forward difference of a discrete function $f(x)$

¹We use the falling power notation so as to be reminiscent of polynomial behaviour in calculus.

as $\Delta_x(f(x)) = f(x+1) - f(x)$. Falling powers $(a+x)^n$ have the forward difference as $\Delta_x(a+x)^n = (a+x+1)^n - (a+x)^n = (a+x)^{n-1}(a+x+1 - (a+x-n+1)) = n(a+x)^{n-1}$. These falling powers have the particularly useful property of:

$$\sum_{x=a}^A \Delta_x f(x) = f(A+1) - f(a). \quad (\text{A.3})$$

Falling powers have the notable property:

$$\sum_{x=b}^B (a+x)^n = \frac{1}{n+1} \sum_{x=b}^B \Delta_x ((a+x)^{n+1}) = \frac{(B+a+1)^{n+1} - (a+b)^{n+1}}{n+1}. \quad (\text{A.4})$$

The zero weight is particularly special in that its Schur polynomial is equal to the symmetric monomial, both of which are equal to 1. Letting us conclude that the value of the dominant weight sum is simply the same as the tadpole value calculated.

$$\mathcal{T}_{(1^N)} = \sum_{\sigma \in P_+^k} s_{(1^N)}(\sigma) = \sum_{\sigma \in P_+^k} M_{(1^N)}(\sigma) = \mathcal{E}_{(1^N)} \quad (\text{A.5})$$

Taking the fusion ideals [40] there is a map between the space of symmetric polynomials and the fusion ring, where the fusion dimension acts like a basis. Such a relation is achieved by imposing a set of ideals on the space of symmetric polynomials for $\widehat{SU}(N)$ we have the following:

$$s_{(1^N)}(\sigma) = M_{(1^N)}(\sigma) = 1, \quad \sum_{\sigma \in P_+^k} M_{\mu'}(\sigma) = 0. \quad (\text{A.6})$$

For the ideal $|(\mu')| \neq jN$, where $j \in \mathbb{Z}_{\geq 0}$ and N is the group dimension. These two ideals account for the noted behaviour of the zero weight and for the tadpole vanishing when the weight is not in the co-root lattice, i.e., the condition on μ' .

Along with these ideals the symmetric monomial have their own decomposition rules into other symmetric monomials. The general decomposition rule for symmetric monomials is given by:

$$\begin{aligned} M_{\lambda_1, \dots, \lambda_L} &= M_{\lambda_1, \dots, \lambda_{i-1}, j, \lambda_{i+1}, \dots, \lambda_L} M_{\lambda_i - j} - M_{\lambda_1 + \lambda_i - j, \dots, \lambda_{i-1}, j, \lambda_{i+1}, \dots, \lambda_L}^- \\ &\quad - M_{\lambda_1, \lambda_2 + \lambda_i - j, \dots, \lambda_{i-1}, j, \lambda_{i+1}, \dots, \lambda_L}^- \cdots - M_{\lambda_1, \lambda_2, \dots, \lambda_{i-1} + \lambda_i - j, j, \lambda_{i+1}, \dots, \lambda_L}^- \\ &\quad - M_{\lambda_1, \lambda_2, \dots, \lambda_{i-1}, j, \lambda_{i+1} + \lambda_i - j, \dots, \lambda_L}^- \cdots \\ &\quad - M_{\lambda_1, \lambda_2, \dots, \lambda_{i-1}, j, \lambda_{i+1}, \dots, \lambda_L + \lambda_i - j} - M_{\lambda_1, \lambda_2, \dots, \lambda_{i-1}, j, \lambda_{i+1}, \dots, \lambda_L, \lambda_i - j}. \end{aligned} \quad (\text{A.7})$$

This decomposition permits us to decompose difficult to sum symmetric monomials into those we already know how to compute. For example, we can consider the decomposition of the dominant weight sum $\mathcal{E}_{(2, 1^{N-2})}$:

$$\mathcal{E}_{(2, 1^{N-2})} = \left(\sum M_{(1)} M_{(1^{N-1})} \right) - N \mathcal{E}_{(1^N)}. \quad (\text{A.8})$$

The N appearing due to the number of ways that it is possible to add the partition (1) to (1^{N-1}) in order to get (1^N) .

The difficulty introduced by the decomposition of the dominant weight sums is in evaluating the sum of products of the symmetric monomials. In order to start building up how these values behave we find the form of $\mathcal{E}_{(H,1^{N-H})}$.

Conjecture 6. *Given a partition of shape $(H, 1^{N-H})$, which we call hook partitions, we can write the polynomial corresponding to the dominant weight sum as:*

$$\mathcal{E}_{(H,1^{N-H})} = (-1)^{H-1} N \frac{(k + N - H)^{N-H}}{(N - H)!} \quad (\text{A.9})$$

Proof. We make heavy use of the ideals from equation (A.6) in this proof. Dominant weight sums can be written as:

$$\begin{aligned} \mathcal{E}_{(H,1^{N-H})} &= \sum_{\sigma \in P_+^k} (\sigma_1^H \sigma_2 \dots \sigma_{N-H} + \text{Permutations}, \\ &= \sum_{\sigma \in P_+^k} \sigma_1 \sigma_2 \dots \sigma_{N-H} (\sigma_1^{H-1} + \dots + \sigma_{N-H}^{H-1}) + \text{Permutations}. \end{aligned} \quad (\text{A.10})$$

We can use the ideal, $M_{1N} = 1$, to transform $\sigma_1 \sigma_2 \dots \sigma_{N-H}$ to $\sigma_{N-H+1}^{-1} \dots \sigma_N^{-1}$ at the cost of introducing a fix on the products denoted with $\delta_{1,2,\dots,N-H}^{N-H+1,\dots,N}$. Doing so we can rewrite equation (A.10) as:

$$\begin{aligned} \mathcal{E}_{(H,1^{N-H})} &= \left(\sum_{\sigma_1} \sigma_1^{H-1} + \dots + \sum_{\sigma_{N-H}} \sigma_{N-H}^{H-1} \right) \sum_{\sigma \in P^{k,N-1}} \sigma_{N-H+1}^{-1} \dots \sigma_N^{-1} \delta_{1,2,\dots,N-H}^{N-H+1,\dots,N} + \dots, \\ &= - \sum_{\sigma \in P^{k,N}} \delta_{1,2,\dots,N-H}^{N-H+1,\dots,N} (\sigma_{N-H+1}^{H-1} + \dots + \sigma_{N-H}^{H-1}) \sigma_{N-H+1}^{-1} \dots \sigma_N^{-1} + \dots, \\ &= \sum_{\sigma \in P^{k,N-1}} (\sigma_{N-H+1}^{H-2} + \dots + \sigma_{N-H+1}^{H-2}) \sigma_1 \dots \sigma_{N-H+1} + \text{Permutations}. \end{aligned} \quad (\text{A.11})$$

This procedure reduces the rank of the sum piece by piece until we are left with the following N pieces:

$$\begin{aligned} \mathcal{E}_{(H,1^{N-H})} &= (-1)^{H-2} \left(\sum_{\sigma_1} \sigma_1 + \dots + \sum_{\sigma_{N-1}} \sigma_{N-1}^{H-2} \right) \sum_{\sigma \in P^{k,N-H+2}} \delta_{1,2,\dots,N-1}^N \sigma_N^{-1} + \dots, \\ &= N(-1)^{H-1} \sum_{\sigma \in P^{k,N-H+1}} 1 = (-1)^{H-1} N \frac{(k + N - H)^{N-H}}{(N - H)!}. \end{aligned} \quad (\text{A.12})$$

□

There are a number of corollaries that follow this conjecture. Firstly the identification of a partition type we call ‘symmetrized’ in analogy with the physical interpretations of $SU(3)$ states and they are identified as partitions with a single part

(N).

Corollary 1. *Given a symmetrized partition (N) with some group dimension N , then the Weyl alcove sum is constant and specified as:*

$$\mathcal{E}_{(N)} = (-1)^{N+1}N \quad (\text{A.13})$$

With these dominant weight sum values we can determine the sum of a product of certain monomials. With the hook dominant weight sums obey equation (A.9) and using the decomposition rules (A.7) we can find the following rule for the symmetric monomials.

Corollary 2. *When a symmetrized partition monomial is multiplied by a monomial with partition (1^M), where $M < N$, with N being the dimension of the group. Then we can write:*

$$\sum_{\sigma \in P_+^k} M_{(N-M)} M_{1^M} = (-1)^{(N-M+1)} N k \frac{(k+M-1)^{M-1}}{(M-1)!} = (-1)^{N-M+1} k \frac{N}{M} \mathcal{E}_{(1^M)}. \quad (\text{A.14})$$

Proof. The decomposition rules can be written as:

$$\sum_{\sigma \in P_+^k} M_{(N-M)} M_{1^M} = \sum_{\sigma \in P_+^k} (M_{(N-M, 1^M)} + M_{(N-M+1, 1^{M-1})}).$$

Subbing in equation (A.9) for these decompositions we obtain the conjectured result:

$$\begin{aligned} \sum_{\sigma \in P_+^k} M_{(N-M)} M_{1^M} &= (-1)^{N-M+1} N \frac{(k+N-(N-M+1))^{N-(N-M+1)}}{(N-(N-M))!} ((k+M)-M), \\ &= (-1)^{N-M+1} N k \frac{(k+N-(N-M+1))^{N-(N-M+1)}}{(N-(N-M))!}, \\ &= (-1)^{N-M+1} \frac{N}{M} k \frac{(k+N-(N-M+1))^{N-(N-M+1)}}{N-(N-M+1)!}, \\ &= (-1)^{N-M+1} k \frac{N}{M} \mathcal{E}_{(1^M)}. \end{aligned} \quad (\text{A.15})$$

□

This previous result motivates another conjecture based on the fact that we did not use any special properties of the (1^M) partition to conclude the above. One can also go through a similar derivation for partitions that have 2 parts greater than 1 in order to observe the following result for many cases.

Conjecture 7. *When we take the sum over the Weyl alcove of two symmetric monomials with at least one being symmetrized then we have the following dominant weight*

sum value that results:

$$\sum_{\sigma \in P_+^k} M_{(H)} M_\mu = (-1)^{H+1} k \frac{N}{L} \mathcal{E}_{(\mu_{(1)}, \dots, \mu_{(L)})}. \quad (\text{A.16})$$

We can find more general product identities, which are useful when considering specific forms of dominant weight sums. This can be done by the application of equations (A.9) and (A.16) leading to the following conjecture.

Conjecture 8. *For a pair of symmetric monomials $M_{(H-1,1)} M_{(1^{N-H})}$ the Weyl alcove sum value corresponding to this product is written as:*

$$\begin{aligned} \sum_{\sigma \in P_+^k} M_{(H,L-1)} M_{(1^{N-H-L+1})} &= (-1)^{H+L+1} N \left((k+1) \frac{(k+N-H-L)^{N-H-L+1}}{(N-H-L+1)!} \right), \\ &= \frac{N}{(H+L-1)(N-H-L+1)} k \mathcal{E}_{(H,L-1)} \mathcal{E}_{(1^{N-H-L+1})}. \end{aligned} \quad (\text{A.17})$$

Proof. We consider the possible decompositions of the product:

$$\begin{aligned} \sum_{\sigma \in P_+^k} M_{H,L-1} M_{1^{N-L-H+1}} &= \sum_{\sigma \in P_+^k} (M_H M_{L-1} - M_{H+L-1}) M_{1^{N-L-H+1}}, \\ &= \sum_{\sigma \in P_+^k} (M_H M_{(L-1,1^{N-L-H+1})} + M_H M_{(L,1^{N-L-H})} - M_{H+L-1} M_{1^{N-L-H+1}}), \\ &= (-1)^{H+L+1} N (k+1) k \frac{(k+N-H-L)^{k+N-H-L}}{(k+N-H-L+1)!}, \\ &= \frac{N}{(H+L-1)(N-H-L+1)} k \mathcal{E}_{(H,L-1)} \mathcal{E}_{(1^{N-H-L+1})}. \end{aligned} \quad (\text{A.18})$$

□

A.1.1 General Dominant Weight Sums

Motivated by the fact that the form of μ shouldn't affect the evaluation, we attempt to classify the dominant weight sums. Equation (A.16) follows from equation (A.9) and we can find more general formulas. Beginning by analyzing a partition of the form $(\mu) = (\mu_{(1)}, 2, 1^{N-\mu_{(1)}-2})$, with $\mu_{(1)} \geq 2$. Our procedure assumes that $\mu_{(1)} \neq \mu_{(2)}$, but the equality is easily dealt with by dividing everything by 2, which accounts for the degeneracy in the decomposition.²

These decompositions and the conjectured equation (A.16) can be used to conjecture a formula for more general dominant weight sums.

²More generally for a partition with L identical parts the corresponding dominant weight sum will be divided by L , which corrects the overcounting of the decomposition procedure.

Conjecture 9. For some partition with unique parts $\mu_{(i)}$ and total partition form $(\mu) = (\mu_{(1)}, \mu_{(2)}, \dots, \mu_{(L)}, 1^{N - \sum_{i=1}^L \mu_{(i)}})$ there is a corresponding dominant weight sum formula in k :

$$\mathcal{E}_{(\mu_{(1)}, \dots, \mu_{(L)}, 1^{N - \sum_{i=1}^L \mu_{(i)}})} = (-1)^{\sum_{i=1}^L \mu_{(i)} + L} \frac{(k + N - \sum_{i=1}^L \mu_{(i)} + L - 1)^{N - \sum_{i=1}^L \mu_{(i)} + L - 1}}{(N - (\sum_{i=1}^L \mu_{(i)}))!}. \quad (\text{A.19})$$

Proof. This proof requires that equation (A.16) be valid. This proof will be done via induction arguments in order to build up more general sets of equations concluding with claimed result. This formula is valid for any dominant weight sum corresponding to a partition of the group dimension N .

We begin by considering the case of two non-unitary parts of a partition. Using equation (A.7) we can break up the dominant weight sum $\mathcal{E}_{(\mu_{(1)}, \mu_{(2)}, 1^{N - \mu_{(1)} - \mu_{(2)}})}$ into sub-monomials. The base case is taken as $\mu_{(2)} = 2$:

$$\begin{aligned} \mathcal{E}_{(\mu_{(1)}, \mu_{(2)}, 1^{N - \mu_{(1)} - \mu_{(2)}})} &= \sum M_{(\mu_{(1)}, 2, 1^{N - \mu_{(1)} - 2})}, \\ &= \sum (M_{(\mu_{(1)}, 1^{N - 1 - \mu_{(1)}})} - M_{(\mu_{(1)} + 1, 1^{N - \mu_{(1)} - 1})} - \\ &\quad - (N - \mu_{(1)}) M_{(\mu_{(1)}, 1^{N - \mu_{(1)}})}). \end{aligned}$$

With the results of equation (A.9) and using the multiplication rule (A.16) one finds:

$$\begin{aligned} \mathcal{E}_\mu &= (-1)^{\mu_1 + 1} N \left(k \frac{(k + N - 1 - \mu_1)^{N - 1 - \mu_1}}{(N - 1 - \mu_1)!} \right) + \\ &\quad + (-1)^{\mu_1 + 1} N \left(\frac{(k + N - \mu_1 - 1)^{N - \mu_1 - 1}}{(N - \mu_1 - 1)!} - \frac{(k + N - \mu_1)^{N - \mu_1}}{(N - \mu_1)!} \right), \\ &= (-1)^{\mu_1 + 2 - 1} N \frac{(k + N - \mu_1 - 1)^{N - \mu_1 - 1}}{(N - \mu_1 - 1)!} (k + 1 - (k + N - \mu_1)), \\ &= (-1)^{\mu_1 + 2} N \frac{(k + N - \mu_1 - 1)^{N - \mu_1 - 1}}{(N - \mu_1 - 2)!}. \end{aligned} \quad (\text{A.20})$$

This resulting form proves the base case and we can consider a general form for a partition given by $\mu = (\mu_1, \mu_2, 1^{N - \mu_1 - \mu_2})$ with $\mu_1 \neq \mu_2$. Looking at the base case we propose the induction hypothesis:

$$\mathcal{E}_{(\mu_1, \mu_2 - 1, 1^{N - \mu_1 - \mu_2 + 1})} = (-1)^{\mu_1 + \mu_2 + 1} N \frac{(k + N - 1 - \mu_1 - (\mu_2 - 1) + 2)^{N - \mu_1 - \mu_2 + 2}}{(N - \mu_1 - (\mu_2 - 1))!}. \quad (\text{A.21})$$

To prove the N th case we look at the $\mu = (\mu_1, \mu_2, 1^{N - \mu_1 - \mu_2})$ partition and its

resulting sub-monomials:

$$\begin{aligned} \mathcal{E}_{(\mu_1, \mu_2, 1^{N-\mu_1-\mu_2})} &= \sum (M_{\mu_2-1} M_{(\mu_1, 1^{N-\mu_2+1-\mu_1})} - \\ &\quad - M_{(\mu_1+\mu_2-1, 1^{N-\mu_1-\mu_2+1})} - M_{(\mu_1, \mu_2-1, 1^{N-\mu_1-\mu_2+1})}). \end{aligned}$$

Subbing in our identities and applying our induction hypothesis A.21 and working through the algebra:

$$(-1)^{\mu_1+\mu_2-1} N \left(\frac{(k+N-\mu_2+1-\mu_1)^{N-\mu_1-\mu_2+1}}{(N-\mu_1-\mu_2+1)!} \right) ((k+1) - (k+N-\mu_1-\mu_2+2)).$$

After some algebra and pulling out an overall negative we reobtain a formula in the same form as equation (A.21). Concluding that the summed monomial for partitions of the form $\mu = (\mu_1, \mu_2, 1^{N-\mu_1-\mu_2})$ is given by:

$$\mathcal{E}_{(\mu_1, \mu_2, 1^{N-\mu_1-\mu_2})} = (-1)^{\mu_1+\mu_2} N \frac{(k+N-\mu_1-\mu_2+1)^{N-\mu_1-\mu_2+1}}{(N-\mu_1-\mu_2)!}. \quad (\text{A.22})$$

Equation (A.22) is taken as the base case for a general dominant weight sum corresponding to a partition with L parts not equal to 1. So we propose a second induction hypothesis for a partition of the form $\mu = (\mu_1, \mu_2, \dots, \mu_L, 1^{N-\sum \mu_i})$. We have the necessary condition on μ that $\sum_i \mu_i \leq N$ with equality when there are no trailing 1's in the partition.

We assume our induction hypothesis, that a summed monomial $\mathcal{E}_{(\mu_1, \dots, \mu_L, 1^{N-L})}$ has the form:

$$\mathcal{E}_{(\mu_1, \dots, \mu_L, 1^{N-\sum_i \mu_i})} = (-1)^{\sum_{i=1}^L \mu_i + L} \frac{(k+N - \sum_{i=1}^L \mu_i + L - 1)^{N-\sum_{i=1}^L \mu_i + L - 1}}{(N - \sum_{i=1}^L \mu_i)!}. \quad (\text{A.23})$$

Where it is noted that A.23 coincides with equation A.22 at the appropriate values as required. Like in the case for two parts of the partition not equal to 1, we consider the dominant weight sum $\mathcal{E}_{(\mu_1, \dots, \mu_{L-1}, 2, 1^{N-\sum_i \mu_i-2})}$. Acting on the dominant weight sum we again decompose it by equation (A.7):

$$\begin{aligned} \mathcal{E}_{(\mu_1, \dots, \mu_L, 2, 1^{N-\sum_i \mu_i-2})} &= \sum (M_1 M_{(\mu_1, \dots, \mu_L, 1, 1^{N-\sum_i \mu_i-2})} - M_{(\mu_1+1, \dots, \mu_L, 1, 1^{N-\sum_i \mu_i-2})} - \dots, \\ &\quad - M_{(\mu_1, \dots, \mu_L+1, 1, 1^{N-\sum_i \mu_i-2})} - (N - \sum_{i=1}^L \mu_i) M_{(\mu_1, \dots, \mu_L, 1^{N-\sum_i \mu_i})}). \end{aligned}$$

Each of these terms are known and in fact it is known from looking at the symmetries between μ_i in equation (A.23) that all the dominant weight sums with parts $\mu_i + 1$ will be equal. Substituting this into the decomposition we have for

$$(\mu) = (\mu_1, \dots, \mu_L, 2, 1^{N - \sum_i^L \mu_i - 2}):$$

$$\begin{aligned} \mathcal{E}_{(\mu)} &= (-1)^{\sum_i^L \mu_i + 2 + L - 1} N \left(\frac{(k + N - \sum_{i=1}^L \mu_i + L - 2)^{N - \sum_{i=1}^L \mu_i + L - 2}}{(N - \sum_{i=1}^L \mu_i - 1)!} (k + L) \right), \\ &\quad - (-1)^{\sum_i^L \mu_i + 2 + L - 1} N \left(\frac{(k + N - \sum_{i=1}^L \mu_i + L - 1)^{N - \sum_i^L \mu_i + L - 1}}{(N - \sum_i^L \mu_i - 1)!} \right). \end{aligned}$$

After simplifying this yields the expected result (noting that $\sum_i^L \mu_i + 2 = \sum_i^{L+1} \mu_{(i)}$) we retrieve the induction hypothesis for the $L + 1$ th case.

$$\mathcal{E}_{(\mu)} = (-1)^{\sum_i^{L+1} \mu_i + L + 1} \frac{(k + N - \sum_{i=1}^{L+1} \mu_i + (L + 1) - 1)^{N - \sum_{i=1}^{L+1} \mu_i + (L+1) - 1}}{(N - (\sum_{i=1}^L \mu_i + 2))!} \quad (\text{A.24})$$

The final step is analogous to what was done for (A.22) and is an exercise in algebra. \square

We can rewrite the conjectured equation (A.19) in terms of Dynkin labels instead of partitions. Equation (3.8) indicates how to do so³ and has the result:

$$\begin{aligned} \mathcal{E}_{(\mu)} &= \mathcal{E}_{(\lambda_1, \dots, \lambda_{N-1})_\Lambda}, \\ &= (-1)^{\sum_i^{N-1} (j \cdot \lambda_j) - N + 1} \frac{(k + 2N - \sum_i^{N-1} (j \cdot \lambda_j) - N - 1)^{2N - \sum_i^{N-1} (j \cdot \lambda_j) - 1}}{(2N - \sum_i^{N-1} (j \cdot \lambda_j) - L)!}. \end{aligned} \quad (\text{A.25})$$

This Dynkin label notation is fairly obtuse compared to the partition notation and doesn't offer any obvious interpretational benefits so the partition notation is preferable.

A.2 Dominant Weight Sums and Tadpole Calculations

As an example of the utility of these techniques we can apply the conjectured general form (A.19) to the tadpoles. Several tadpoles are explicitly computed below. Multiplicities, particularly those used in the conjectured forms, were computed by looking at certain cases of the Kostka number. We remind ourselves, that for $SU(N)$ the Kostka numbers correspond to weight multiplicities.

Using equation (A.9) and the form of the multiplicity for the adjoint multiplicities we can find the adjoint tadpole fairly simply:

$$\begin{aligned} \mathcal{T}_{(21^{N-2})} &= (N - 1) \mathcal{E}_{1^N}(k) + \mathcal{E}_{(2, 1^{N-2})}(k) \\ &= (N - 1) \frac{(k + N - 1)^{(N-1)}}{(N - 1)!} - N \frac{(k + N - 2)^{(N-2)}}{(N - 2)!}. \end{aligned}$$

³Given by $\mu_i = \sum_i^{N-1} \lambda_i$

This result applies to all dimensions and levels, which given the difficulty involved in computing these objects via traditional methods [1] is fairly shocking. We note that applying these methods to solving more general types of tadpoles was not so easy, due to the complexity of obtaining the multiplicities and in decomposing the dominant weight sums appropriately.

In principle we can find a general level, arbitrary dimension formula for any tadpole that consists of weights whose partitions is a class described by the conjectured equation (A.19). So for all weights corresponding to partitions of the group dimension N one can find their tadpole. One can push slightly outside this restriction, by considering special cases with a dominant weight being a multiple of a dominant weight corresponding to a known dominant weight sums. Dominant weight sums labelled by dominant weights that are multiples of another were observed to be identical to the non-multiple dominant weight sum, provided that both λ and $j\lambda$ were in the Weyl alcove. This affords us the useful relation

$$\mathcal{E}_{j\lambda}(k) = \mathcal{E}_\lambda(k), \quad (\text{A.26})$$

when $\lambda \in P_+^k$ and $j\lambda \in P_+^k$. This relation is consistent with all of our tabled examples. One might be able to understand this by interpreting the components of the symmetric monomials as $(N+k)$ -th roots of unity.

For computing the general formulas of a tadpole there are two obstacles. We must know the form of the dominant weight sum and we must compute the Kostka number. Kostka numbers are fairly easy to compute, although there is no general closed form solution for them. The most difficult part then is the computing of the dominant weight sum. From equation (A.19) we have determined a fairly respectable class of the alcove Wey sums and can apply them below:

$$\begin{aligned} \mathcal{T}_{(2,2,1^{N-4})} = \mathcal{T}_{[0,1,0,\dots,0,1,0]} &= \mathcal{E}_{(2,2,1^{N-4})} + (N-3)\mathcal{E}_{(2,1^{N-2})} + \frac{(N)(N-3)}{2}\mathcal{E}_{(1^N)} \\ &= \frac{N(N-3)}{2} \cdot \frac{(k+N-3)^{N-3}}{(N-1)!} (k^2 - k) \end{aligned} \quad (\text{A.27})$$

$$\begin{aligned} \mathcal{T}_{(3,1^{N-3})} = \mathcal{T}_{[2,0,\dots,0,1,0]} &= \mathcal{E}_{(3,1^{N-3})} + \mathcal{E}_{(2,2,1^{N-4})} + (N-2)\mathcal{E}_{(2,1^{N-2})} + \\ &\quad + \frac{(N-1)(N-2)}{2}\mathcal{E}_{(1^N)}, \\ &= \frac{1}{2}(k-2)(k-1) \frac{(k+N-3)^{N-3}}{(N-3)!} \end{aligned} \quad (\text{A.28})$$

We can write a general forms of the Kostka number corresponding to a shape $(H, 1^{N-H})$ partitions and those with threshold level $k_0 = 2$ respectively. Kostka numbers for weights with threshold level $k_0 = 2$ can be found via the following

summation:

$$K_{(2^L, 1^{M-2L}), (1^M)} = \sum_{J_1=L}^{M-L} \sum_{J_2=L-1}^{J_1} \cdots \sum_{J_{L-1}=2}^{J_{L-2}} (J_{L-1}). \quad (\text{A.29})$$

Where M is the sum of the parts of the partition. Making use of this equation one can write any threshold level 2 tadpole as a polynomial by making use of the dominant weight sum results.

Collecting these results we can write the following results, which give formulas for tadpoles with a specific class of highest weight. The following polynomials give the tadpole value for an arbitrary level and group dimension being fixed only by the form of the weight that indexes them. This weight λ is the highest weight of the tadpole system.

$$\mathcal{T}_{2,1^{N-2}} = (k-1) \frac{(k+N-2)^{N-2}}{(N-2)!} \quad (\text{A.30})$$

$$\mathcal{T}_{3,1^{N-3}} = \frac{1}{2}(k-2)(k-1) \frac{(k+N-3)^{N-3}}{(N-3)!} \quad (\text{A.31})$$

$$\mathcal{T}_{4,1^{N-4}} = \left(\frac{(k-1)^3}{3!} \right) \frac{(k+N-4)^{N-4}}{(N-4)!} \quad (\text{A.32})$$

Making use of the conjectured result for Weyl alcove sums (A.19) the following tadpole values were obtained and found to agree with tabulated values.

$$\mathcal{T}_{2,2,1^{N-4}} = \frac{N(N-3)}{2} (k^2 - k) \frac{(k+N-3)^{N-3}}{(N-1)!} \quad (\text{A.33})$$

$$\mathcal{T}_{(2^3, 1^{N-6})} = \frac{N(N-5)}{3!} k(k^2 - 1) \frac{(k+N-4)^{N-4}}{(N-2)!} \quad (\text{A.34})$$

$$\mathcal{T}_{(2^4, 1^{N-8})} = \frac{N(N-7)}{4!} (k+2)^4 \frac{(k+N-5)^{N-5}}{(N-3)!} \quad (\text{A.35})$$

Looking at the form of the threshold $k_0 = 2$ highest weights we introduce the following conjecture. Using a computer algorithm this conjecture was checked and could be obtained by combining the Kostka numbers (A.29) with the appropriate dominant weight sums (A.19).

Conjecture 10. *Given a weight with threshold level $k_0 = 2$ its partition will be of the form $(2^L, 1^{N-2L})$ and the tadpole can be calculated by the polynomial*

$$\mathcal{T}_{(2^L, 1^{N-2L})} = \frac{(N-2L+1)N}{L!} (k-2+L)^L \frac{(k+N-1-L)^{N-1-L}}{(N-1-L)!} \quad (\text{A.36})$$

Similarly to the previous conjecture we can combine the Kostka numbers with the hook dominant weight sums (A.9) to obtain a conjecture for hook tadpoles.

Conjecture 11. *Given a highest weight of a hook partition then the corresponding*

tadpole can be written as:

$$\mathcal{T}_{(H,1^{N-H})} = \frac{(k-1)^{H-1} (k+N-H)^{N-H}}{(H-1)! (N-H)!}. \quad (\text{A.37})$$

We conclude with two conjectured formula obtained from consideration of the tadpole tables, whose form is motivated by the previous conjectures.

Conjecture 12. *There is another conjecture about highest weights that are adjoint-multiples once again in a simple polynomial form. This of course reducing to the derived adjoint tadpole when $L = 1$ as the formula must.*

$$\begin{aligned} \mathcal{T}_{[L,0,\dots,0,L]} &= (k-2L+1) \frac{(k+N-L-1)^{N-2} (L+N-2)^{N-2}}{(N-1)! (N-2)!}, \\ \mathcal{T}_{(2L,L^{N-2})} &= (k-2L+1) \frac{(k+N-L-1)^{N-2} (L+N-2)^{N-2}}{(N-1)! (N-2)!}. \end{aligned} \quad (\text{A.38})$$

Combining the conjectured equations (A.38) and (A.37) and making them consistent results in the following tadpole formula.

Conjecture 13. *Given some partition of the form (MH, M^{N-H}) the tadpole value can be found by evaluating the polynomial.*

$$\mathcal{T}_{(MH,M^{N-H})} = \frac{(k-2M+1)^{H-1} (k+N-H-M+1)^{N-H} (M+N-H)^{N-H}}{(H-1)! (N-H+1) (N-H)!} \quad (\text{A.39})$$

Appendix B
Tables of Tadpoles

B.1 Computed Values for Tadpoles \mathcal{T}_λ of Equation (5.56)

Each of these tables were computed using the general Verlinde formula for the tadpole, that is equation (4.31) with $g = 1$ and $N = 1$. Combined with the Kac-Peterson formula (4.25) this reduces to equation (5.56), which is reprinted below:

$$\mathcal{T}_\lambda = \sum_{\sigma \in P_+^k} \sum_{\alpha \in P(\lambda)} \text{mult}_\lambda(\alpha) \exp\left(\frac{2\pi i}{k+h^\vee} \alpha \cdot (\sigma + \rho)\right).$$

One can use this relation to obtain a general formula for the $SU(2)$ formula directly, which is known, and given as:

$$\mathcal{T}_{2M} = (k - 2M + 1). \tag{B.1}$$

level k	[0, 0]	[1, 1]	[3, 0]	[2, 2]	[4, 1]	[6, 0]	[3, 3]	[5, 2]
0	1							
1	3							
2	6	3						
3	10	8	1					
4	15	15	3	6				
5	21	24	6	15	3			
6	28	35	10	27	8	1	10	
7	36	48	15	42	15	3	24	6
8	45	63	21	60	24	6	42	15
9	55	80	28	81	35	10	64	27
10	66	99	36	105	48	15	90	42
11	78	120	45	132	63	21	120	60
12	91	143	55	162	80	28	154	81
13	105	168	66	195	99	36	192	105
14	120	195	78	231	120	45	234	132
15	136	223	91	270	143	55	280	162
16	153	255	105	312	168	66	330	195

Table B.1: $SU(3)$ Tadpole Values \mathcal{T}_λ

level k	[0, 0, 0]	[1, 0, 1]	[0, 2, 0]	[2, 1, 0]	[2, 0, 2]	[4, 0, 0]	[1, 2, 1]	[3, 1, 1]	[0, 4, 0]	[5, 0, 1]
0	1									
1	4									
2	10	6	2							
3	20	20	8	4						
4	35	45	20	15	20	1	13		3	
5	53	84	40	36	60	4	44	20	12	
6	84	140	70	70	126	10	100	64	30	6
7	120	216	112	120	224	20	188	140	60	20
8	165	315	168	189	360	35	315	256	105	45
9	220	440	240	280	540	53	488	420	168	84
10	286	594	330	396	770	84	714	640	252	140
11	364	780	440	540	1056	120	1000	924	360	216
12	455	1001	572	715	1404	165	1353	1280	495	315
13	560	1260	728	924	1820	220	1780	1716	660	440
14	680	1560	910	1170	2310	286	2288	2240	858	594
15	816	1904	1120	1456	2880	364	2884	2860	1092	780
16	969	2295	1360	1785	3536	455	3575	3584	1365	1001
17	1140	2736	1632	2160	4284	560	4368	4420	1680	1260
18	1330	3230	1938	2584	5130	680	5270	5376	2040	1560

Table B.2: $SU(4)$ Tadpole Values \mathcal{T}_λ

level k	[0, 0, 0, 0]	[1, 0, 0, 1]	[0, 1, 1, 0]	[2, 0, 1, 0]	[1, 2, 0, 0]	[1, 1, 1, 1]	[3, 1, 0, 0]	[3, 0, 1, 1]	[2, 2, 0, 1]
0	1								
1	5								
2	15	10	5						
3	35	40	25	10	5				
4	70	105	75	45	25	55	5		
5	126	224	175	126	75	224	24	75	51
6	210	420	350	280	175	595	70	280	205
7	330	720	630	540	350	1280	160	700	540
8	495	1155	1050	945	630	2415	315	1440	1155
9	715	1760	1650	1540	1050	4160	560	2625	2170
10	1001	2574	2575	2376	1650	6699	924	4400	3726
11	1365	3640	3575	3510	2575	10240	1440	6930	5985
12	1820	5005	5005	5005	3575	15015	2145	10400	9130
13	2380	6720	6825	6930	5005	21280	3080	15015	13365
14	3060	8840	9100	9360	6825	29315	4290	21000	18915
15	3876	11424	11900	12376	9100	39424	5824	28600	26026
16	4845	14535	15300	16065	11900	51935	7735	38080	34965
17	5985	18240	19380	20520	15300	67200	10080	49725	46020
18	7315	22610	24225	25840	19380	85595	12920	63840	59500

Table B.3: $SU(5)$ Tadpole Values \mathcal{T}_λ

B.2 Dominant Weight Sums \mathcal{E}_λ of Equation (6.13)

Selected values of the dominant weight sums, computed with equation (6.13). The defining equation is reprinted below for convenience:

$$\mathcal{E}_\beta(k) := \sum_{\alpha \in W\beta} \sum_{\sigma \in P_+^k} \exp\left(\frac{2\pi i}{k+h^\vee} \alpha \cdot (\sigma + \rho)\right).$$

level k	[0, 0]	[1, 1]	[3, 0]	[2, 2]	[4, 1]	[6, 0]	[3, 3]	[5, 2]
0	1							
1	3							
2	6	-9						
3	10	-12	3					
4	15	-15	3	-15				
5	21	-18	3	-18	6			
6	28	-21	3	-21	6	3		
7	36	-24	3	-24	6	3	-24	6
8	45	-27	3	-27	6	3	-27	6
9	55	-30	3	-30	6	3	-30	6
10	66	-33	3	-33	6	3	-33	6
11	78	-36	3	-36	6	3	-36	6
12	91	-39	3	-39	6	3	-39	6
13	105	-42	3	-42	6	3	-42	6
14	120	-45	3	-45	6	3	-45	6
15	136	-48	3	-48	6	3	-48	6
16	153	-51	3	-51	6	3	-51	6

Table B.4: $SU(3)$ Dominant Weight Sums \mathcal{E}_λ

level k	[0, 0, 0]	[1, 0, 1]	[0, 2, 0]	[2, 1, 0]	[2, 0, 2]	[4, 0, 0]	[1, 2, 1]	[3, 1, 1]	[0, 4, 0]	[5, 0, 1]
0	1									
1	4									
2	10	-24	6							
3	20	-40	8	16						
4	35	-60	10	20	-60	-4	8	48	10	
5	53	-84	12	24	-84	-4	12	56	12	
6	84	-112	14	28	-112	-4	16	64	14	-12
7	120	-144	16	32	-144	-4	20	72	16	-12
8	165	-180	18	36	-180	-4	24	80	18	-12
9	220	-220	20	40	-220	-4	28	88	20	-12
10	286	-264	22	44	-264	-4	32	96	22	-12
11	364	-312	24	48	-312	-4	36	104	24	-12
12	455	-364	26	52	-364	-4	40	112	26	-12
13	560	-420	28	56	-420	-4	44	120	28	-12
14	680	-480	30	60	-480	-4	48	128	30	-12
15	816	-544	32	64	-544	-4	52	136	32	-12

Table B.5: $SU(4)$ Dominant Weight Sums \mathcal{E}_λ

level k	[0, 6, 0]	[3, 0, 3]	[2, 2, 2]	[3, 3, 1]	[4, 2, 0]	[1, 4, 1]	[6, 1, 0]	[4, 1, 2]	[2, 3, 0]	[8, 0, 0]
5									-12	
6	18	-112	16		28	20			-12	
7	20	-144	20	-24	32	24	-12	64	-12	
8	22	-180	24	-24	36	28	-12	72	-12	-4
9	24	-220	28	-24	40	32	-12	80	-12	-4
10	26	-264	32	-24	44	36	-12	88	-12	-4
11	28	-312	36	-24	48	40	-12	96	-12	-4
12	30	-364	40	-24	52	44	-12	104	-12	-4
13	32	-420	44	-24	56	48	-12	112	-12	-4
14	34	-480	48	-24	60	52	-12	120	-12	-4
15	36	-544	52	-24	64	56	-12	128	-12	-4
16	38	-612	56	-24	68	60	-12	136	-12	-4

Table B.6: $SU(4)$ Dominant Weight Sums \mathcal{E}_λ Cont'd

level k	[0, 0, 0, 0]	[1, 0, 0, 1]	[0, 1, 1, 0]	[2, 0, 1, 0]	[1, 2, 0, 0]	[1, 1, 1, 1]	[3, 1, 0, 0]	[3, 0, 1, 1]	[2, 2, 0, 1]	[2, 0, 0, 2]
0	1									
1	5									
2	15	-50	30							
3	35	-100	50	50	-20					
4	70	-175	75	75	-25	75	-25			-175
5	126	-280	105	105	-30	120	-30	210	-40	-280
6	210	-420	140	140	-35	175	-35	280	-50	-420
7	330	-600	180	180	-40	240	-40	360	-60	-600
8	495	-825	225	225	-45	315	-45	450	-70	-825
9	715	-1100	275	275	-50	400	-50	550	-80	-1100
10	1001	-1430	330	330	-55	495	-55	660	-90	-1430

Table B.7: $SU(5)$ Dominant Weight Sums \mathcal{E}_λ

level k	[5, 0, 0, 0]	[0, 2, 2, 0]	[3, 0, 0, 3]	[2, 1, 2, 0]	[4, 1, 0, 1]	[4, 0, 2, 0]	[2, 1, 1, 2]	[6, 0, 0, 1]	[1, 3, 1, 0]	[3, 2, 1, 0]
4		75								
5	5	105		-90					-40	
6	5	140	-420	-105	-105	140	175		-50	5
7	5	180	-600	-120	-120	180	240	20	-60	0
8	5	225	-825	-135	-135	225	315	20	-70	-5
9	5	275	-1100	-150	-150	275	400	20	-80	-10
10	5	330	-1430	-165	-165	330	495	20	-90	-15
level k	[5, 1, 1, 0]	[3, 2, 0, 2]	[4, 0, 0, 4]	[5, 1, 0, 2]	[3, 1, 2, 1]	[5, 0, 2, 1]	[3, 1, 1, 3]	[1, 2, 2, 1]	[5, 0, 1, 3]	[5, 0, 0, 5]
6								175		
7	-120	-60			-120			240		
8	-135	-70	-825	-135	-135	450	315	315		
9	-150	-80	-1100	-150	-150	550	400	400	550	
10	-165	-90	-1430	-165	-165	660	495	495	660	-1430

Table B.8: $SU(5)$ Dominant Weight Sums \mathcal{E}_λ Cont'd

level k	[0, 0, 0, 0, 0]	[1, 0, 0, 0, 1]	[0, 1, 0, 1, 0]	[0, 0, 2, 0, 0]	[1, 1, 1, 0, 0]	[2, 0, 0, 1, 0]	[3, 0, 1, 0, 0]	[1, 1, 0, 1, 1]	[3, 0, 0, 1, 1]
0	1								
1	6								
2	21	-90	90	-12					
3	56	-210	180	-20	-120	120			
4	126	-420	315	-30	-180	210	-90	360	
5	252	-756	504	-42	-252	336	-126	630	672
6	462	-1260	756	-56	-336	504	-168	1008	1008
7	792	-1980	1080	-72	-432	720	-216	1512	1440
8	1287	-2970	1485	-90	-540	990	-270	2160	1980
9	2002	-4290	1980	-110	-660	1320	-330	2970	2640
10	3003	-6006	2574	-132	-792	1716	-396	3960	3432

Table B.9: $SU(6)$ Dominant Weight Sums \mathcal{E}_λ

k	$[1, 0, 0, 0, 0, 1]$	$[01, 0, 0, 1, 0]$	$[0, 0, 1, 1, 0, 0]$	$[0, 2, 1, 0, 0, 0]$	$[1, 0, 2, 0, 0, 0]$	$[1, 1, 0, 1, 0, 0]$	$[2, 0, 0, 0, 1, 0]$	$[0, 1, 1, 1, 1, 0]$
2	-147	210	-70					
3	-392	490	-140	70	70	-420	245	
4	-882	980	-245	105	105	-735	490	-280
5	-1764	1764	-392	147	147	-1176	882	-504
6	-3234	2940	-588	196	196	-1764	1470	-833
7	-5544	4620	-840	252	252	-2520	2310	-1288
8	-9009	6930	-1155	315	315	-3465	3465	-1890
9	-14014	10010	-1540	385	385	-4620	5005	-2660
10	-21021	14014	-2002	462	462	-6006	7007	-3619
11	-30576	19110	-2548	546	546	-7644	9555	-4788
12	-43316	25480	-3185	637	637	-9555	12740	-6188
13	-59976	33320	-3920	735	735	-11760	16660	-7840
14	-81396	42840	-4760	840	840	-14280	21420	-9765
15	-108528	54264	-5712	952	952	-17136	27132	-11984

Table B.10: $SU(7)$ Dominant Weight Sums \mathcal{E}_λ 1/4

k	[0, 2, 0, 1, 0, 1]	[1, 3, 0, 0, 0, 0]	[1, 0, 1, 1, 0, 1]	[2, 1, 1, 0, 0, 0]	[1, 1, 0, 0, 1, 1]	[3, 0, 0, 1, 0, 0]	[2, 0, 0, 0, 0, 2]	[1, 2, 0, 1, 1, 0]
4	-525	-35	105	210	1225	-245	-882	
5	-882	-42	0	294	2352	-392	-1764	-1764
6	-1372	-49	-196	392	4116	-588	-3234	-2744
7	-2016	-56	-504	504	6720	-840	-5544	-4032
8	-2835	-63	-945	630	10395	-1155	-9009	-5670
9	-3850	-70	-1540	770	15400	-1540	-14014	-7700
10	-5082	-77	-2310	924	22022	-2002	-21021	-10164
11	-6552	-84	-3276	1092	30576	-2548	-30576	-13104
12	-8281	-91	-4459	1274	41405	-3185	-43316	-16562
13	-10290	-98	-5880	1470	54880	-3920	-59976	-20580
14	-12600	-105	-7560	1680	71400	-4760	-81396	-25200
15	-15232	-112	-9520	1904	91392	-5712	-108528	-30464

Table B.11: $SU(7)$ Dominant Weight Sums \mathcal{E}_λ 2/4

k	[2, 1, 0, 0, 2, 0]	[2, 0, 2, 0, 0, 1]	[2, 1, 0, 1, 0, 1]	[3, 2, 0, 0, 0, 0]	[4, 0, 1, 0, 0, 0]	[3, 0, 0, 0, 1, 1]	[1, 2, 0, 0, 2, 1]
5	-1176	84	-1764	-42	147	1764	
6	-1764	147	-2744	-49	196	2940	4116
7	-2520	224	-4032	-56	252	4620	6720
8	-3465	315	-5670	-63	315	6930	10395
9	-4620	420	-7700	-70	385	10010	15400
10	-6006	539	-10164	-77	462	14014	22022
11	-7644	672	-13104	-84	546	19110	30576
12	-9555	819	-16562	-91	637	25480	41405
13	-11760	980	-20580	-98	735	33320	54880
14	-14280	1155	-25200	-105	840	42840	71400
15	-17136	1344	-30464	-112	952	54264	91392

Table B.12: $SU(7)$ Dominant Weight Sums \mathcal{E}_λ 3/4

k	[0, 2, 0, 0, 2, 0]	[0, 2, 1, 0, 0, 1]	[2, 0, 1, 1, 1, 0]	[1, 2, 1, 0, 0, 1]	[2, 0, 1, 1, 0, 2]	[3, 1, 1, 0, 0, 1]	[3, 1, 0, 1, 1, 0]
4	980	35					
5	1764	84	1260	672			
6	2940	147	1715	931	-833	931	-196
7	4620	224	2240	1232	-1288	1232	-504
8	6930	315	2835	1575	-1890	1575	-945
9	10010	420	3500	1960	-2660	1960	-1540
10	14014	539	4235	2387	-3619	2387	-2310
11	19110	672	5040	2856	-4788	2856	-3276
12	25480	819	5915	3367	-6188	3367	-4459
13	33320	980	6860	3920	-7840	3920	-5880
14	42840	1155	7875	4515	-9765	4515	-7560
15	54264	1344	8960	5152	-11984	5152	-9520

Table B.13: $SU(7)$ Dominant Weight Sums \mathcal{E}_λ 4/4

B.3 Galois Orbit Sums $\mathcal{G}_\lambda(\sigma)$ of Equation (6.11)

Below are the tables of some selected Galois orbit sums. When a table entry is left blank this is due to the dominant weight not being a label of the Galois orbit. This is noted as being distinct from those entries that are zero, which indicate that the dominant weight is valid, but contributes nothing to the tadpole.

$\sigma \in P_+^k$	$k = 2$	$k = 3$	$k = 4$	$k = 5$
000	4	3	12	6
010	-1	3	2	3
100	0	4	16	24
002	4	2	2	12
020			-2	
101	-1			
012		2		0
111			-1	
030			6	
003		6		
102			0	
022			2	0
004			12	12
040				3
103			2	6
013				6
005				12

Table B.14: $SU(4)$ Galois orbit sums $\mathcal{G}_{[1,0,1]}(\sigma)$ of the tadpole $\mathcal{T}_{[1,0,1]}$

$\sigma \in P_+^k$	$k = 2$	$k = 3$	$k = 4$	$k = 5$
000	2	4	8	9
010	1	4	4	3
001	-4	-4	0	0
002	2	-2	-4	0
020			4	
101	1			
012				-2
111			0	
030				9
003		8		
102				-4
022			-4	-2
004			8	0
040				3
103			4	
013				6
005				18

 Table B.15: $SU(4)$ Galois orbit sums $\mathcal{G}_{[0,2,0]}(\sigma)$ of the tadpole $\mathcal{T}_{[0,2,0]}$

$\sigma \in P_+^k$	$k = 3$	$k = 4$	$k = 5$
000	2	12	9
010	2	-2	0
001	-2	0	0
002	-1	-2	0
020		-2	
101			
012	-1		0
111		1	
030			9
003	4		
102			0
022		-2	0
004		12	0
040			0
103		-2	
013			0
005			18

 Table B.16: $SU(4)$ Galois orbit sums $\mathcal{G}_{[2,1,0]}(\sigma)$ of the tadpole $\mathcal{T}_{[2,1,0]}$